The Dissertation Committee for Eri Takematsu Certifies that this is the approved version of the following Dissertation:

Transmembrane Stem Cell Factor Protein Therapeutics Enhance Revascularization in Ischemia without Mast Cell Activation

Committee:

Aaron B. Baker, Supervisor

Andrew K. Dunn

David W. Terreson

Jeanne C. Stachowiak

Laura J. Suggs

Transmembrane Stem Cell Factor Protein Therapeutics Enhance Revascularization in Ischemia without Mast Cell Activation

by

Eri Takematsu

Dissertation

Presented to the Faculty of the Graduate School of

The University of Texas at Austin

in Partial Fulfillment

of the Requirements

for the Degree of

Doctor of Philosophy

The University of Texas at Austin

May 2020

Dedication

To My Family and Friends

Acknowledgements

First, I would like to thank my mother and father for raising and supporting me to be who I am now. My mom had an especially huge influence on me pursuing my Ph.D. Since I was a child, she always told me that working as a researcher is fun since you can work on whatever you like to pursue. Though she sometimes looks exhausted by grading exams for 400 students, she looks happy and content when she interacts with her students and works on her research. Since then, I have wished to become a Ph.D. so that I can pursue something I like. I also want to thank my grandparents for always caring and being by my side no matter what happens. They are the main reason why I chose to study biomedical engineering. I hope in the future, the rate of cardiovascular disease and diabetes will reduce, and less people suffer from these conditions.

I would like to thank a lot of people who have contributed directly or indirectly towards my Ph.D. degree and my life. Please excuse me if I forget to mention your name explicitly. I really do appreciate your presence in my life.

When I was in Seinan-Gakuin high school, I really hated math (now I am okay with it). I appreciate my math teacher, Mr. Shiiba, who did not give up on me learning math and still cared for me long after I graduated from high school. During my study in high school, I found Chemistry interesting, so I majored in applied chemistry at Tokyo University of Science (TUS). I appreciated the study abroad program supported by TUS at University of California at Davis during my junior year. Without this program, I would not even think about coming to the U.S. for a Ph.D. In Davis, I met many important friends in my life. Yusuke, Trina, Alvin, and Manabe-sensei were graduate students at Davis at that time and taught me chemistry and how to enjoy my life in the U.S. They were super smart, hard workers, and also experts at enjoying their life. They inspired me to pursue my graduate degree in the U.S. Among them, special thanks go to Yusuke, who has been the greatest supporter in my life. I also appreciate Moe and Tomoe who always hung out with me in Davis, and still hung out with me even 10 years after we left Davis. I

would also like to thank Asuka, Alex, Zhao, and Teru for remotely supporting me during my Ph.D. study.

During my study for a master's degree at Tokyo Institute of Technology (TiTech), I met many great mentors. I really appreciate Dr. Matsushita who was my PI. He not only guided my thesis, but he taught me essential interpersonal skills as well. I especially thank him for supporting me during my difficult time even after I graduated from TiTech. He is the most warm-hearted professor ever. I also thank Dr. Ohuchi who was my PI during my summer internship at University of Washington (UW). He gave me an opportunity to work as a graduate student in the U.S. I appreciate his continuous support even after I left UW. I thank Dr. Ikoma who provided me a lot of guidance on my master's thesis and kept supporting me during my Ph.D. I also met many wonderful friends during my master's study. Shiina-chan, Azu, Arrietty, Nabe-chan, Miya, and Chimo-san, who supported me remotely even after we graduated from Titech.

During my Ph.D. study, I was supported by many friends. I especially want to thank Hieu, who is always by my side and provides me advice and mental support throughout my Ph.D. Without her, I would not have been able to finish my Ph.D. I would also like to thank Yao, Kameel, Chungmin, and Ryota for being great companions and sharing happiness and sadness with me. I also want to thank all of my Karate, badminton, climbing, flag football and running friends who share joy and keep me in good shape. I also thank Reika, Shuqi, and Moy for providing me with great advice and mentorship.

Most importantly, I want to thank Dr. Aaron Baker who guided me through my entire Ph.D. I really appreciate that he persistently taught biomedical engineering to me as someone who was not too familiar with this field initially. I will not forget his patience and kindness. I really admire his wisdom and creativity, and wish to be a scientist like him in my future. I also want to thank all the Baker lab members for helping my daily research and making my lab life fun. Special thanks go to Drew and Kayla who have been going through this journey together from the beginning. Thank you to Jason, Moy, Adrianne, Vicky, Anthony, and Almu for kindly teaching and mentoring me. I want to thank Nikita, Lei, Daniel, Ki, Miles, and especially Austin for entertaining my daily life

in the lab. Without them, I would not have been able to enjoy my life in the lab. I must acknowledge a significant contribution of my undergrad students, Marjan, Jeff, AJ, Aditya, Po-Chih, Sophia, and Sanjana. Special thanks go to Jeff and Po-Chih who have been working with me for four years even on weekends and in the nighttime.

Lastly, I would like to acknowledge my dissertation committees, Dr. Stachowiak, Dr. Suggs, Dr. Dun and Dr. Terreson, for providing guidance, advice and feedback on my dissertation. I would like to especially thank Dr. Stachowiak for providing advice on my mechanistic study, and Dr. Terreson for providing me an opportunity to observe his work at the hospital. I also want to thank Ms. Arasappan for RNA sequencing analysis, Dr. Sherman for Cryo-EM imaging, and Dr. Mukhopadhyay for helping with colocalization analysis. Again, I would like to thank everyone who has contributed directly or indirectly towards my Ph.D. degree and my life.

Abstract

Transmembrane Stem Cell Factor Protein Therapeutics Enhance Revascularization in Ischemia without Mast Cell Activation

Eri Takematsu, Ph.D.

The University of Texas at Austin, 2020

Supervisor: Aaron B. Baker

Diabetes mellitus affects approximately 350 million people worldwide, leading to the death of about 4.6 million people per year. As a complication of diabetes, 30-40 percent of patients age 50 and older develop peripheral artery disease (PAD). The current standard of care treatments for PAD includes surgical revascularization with bypass grafting or percutaneous interventions. However, these interventions cannot be performed in a significant portion of patients, and many do not respond to these therapies. An alternative approach for treating PAD is to use proteins to stimulate the body to create new vasculature, thus restoring blood flow through its own regenerative processes. Stem cell factor (SCF) is a cytokine that acts through the receptor tyrosine kinase c-Kit to regulate hematopoiesis and has been a candidate protein for treating PAD. Clinical use of soluble SCF would be highly beneficial but has been limited due to toxicity related to mast cell activation. SCF also exists in a transmembrane form that has differential activity from soluble SCF and has not been explored as a therapeutic agent. To explore the transmembrane SCF (tmSCF) as a therapeutic we created formulations of tmSCF embedded in proteoliposomes or in lipid nanodiscs. Mouse models of anaphylaxis and ischemia revealed the tmSCF-based therapies did not activate mast cells and were effective in improving the recovery from ischemia in both wild type and diabetic mice.

We also found that the formulation of the lipid nanocarrier to deliver tmSCF altered the biological response and trophism of the tmSCF-based treatments. Proteoliposomal tmSCF preferentially acted on mature endothelial cells to induce angiogenesis while tmSCF nanodiscs had greater activity in inducing stem cell mobilization from the bone marrow and recruitment to ischemic sites. A mechanistic analysis of the effects of the treatments on mast cells, mature endothelial cells and endothelial progenitor cells, revealed that the nanocarriers altered the relative utilization of clathrin- versus caveolin-mediated uptake pathways of c-Kit in response to the treatments. Overall, our studies support tmSCF-based therapies can provide therapeutic benefits without off-target effects on mast cells and that lipid nanocarriers can be used to tailor the properties of membrane protein-based therapeutics.

Table of Contents

List of Tables

List of Figures

Chapter 1: Introduction

1.1 MOTIVATION

Diabetes mellitus affects approximately 350 million people worldwide, leading to the death of about 4.6 million people per year[1,2]. As a complication of diabetes, 30 to 40 percent of patients age 50 and older develop peripheral artery disease (PAD)[3]. Severe PAD increases the risk of non-healing ulcers, pain from intermittent claudication and limb amputation. There are several reports stating that diabetic patients possess altered gene expression, which may be a causal factor for severe PAD conditions. An understanding of the changes in gene expression in the skin of diabetic patients may provide insight into the processes and mechanisms that precede the formation of non-healing ulcers. In the first half of this thesis, I investigated the genome wide changes in gene expression in skin between patients with type 2 diabetes and non-diabetic patients using next generation sequencing. I compared the gene expression in skin samples taken from 27 patients (13 with type 2 diabetes and 14 non-diabetic). This information may be useful in identifying the causal factors and potential therapeutic targets for the prevention and treatment of diabetic related diseases.

The current standard of care treatments for PAD includes surgical revascularization with bypass grafting or percutaneous interventions such as angioplasty, stenting and atherectomy. However, these interventions cannot be performed in a significant portion of patients, and many do not respond to these therapies[4]. An alternative approach for treating ischemic disease is to stimulate the body to create new vasculature, thus restoring blood flow through its own regenerative processes. Several approaches have been attempted including the delivery of progenitor cells[5,6], viral vectors to express growth factor/angiogenic transcription factor genes[7-10] or through the delivery of growth factors[11-13]. While cell therapy is labor-intensive and gene therapy has safety issues, protein therapeutics such as growth factor treatments have potential advantages from delivery and safety perspectives[6].

One potential therapeutic protein for treating ischemic disease is stem cell factor (SCF), which signals through the c-Kit receptor (CD117)[14]. One endogenous SCF isoform (SCF248) is initially a transmembrane protein that contains an enzyme cleavable domain allowing its release as soluble SCF (SCF163)[15]. In addition to its well-known role in hematopoiesis, SCF also

induces angiogenesis, enhances recovery from stroke and improves recovery after myocardial infarction[16-18]. In many studies, SCF has a synergetic effect with granulocyte colony-stimulating factor (G-CSF) to enhance angiogenesis and neurogenesis after stroke in animal studies[17,19,20]. Several clinical trials demonstrated increased peripheral blood progenitor cell mobilization after co-stimulation with SCF and G-CSF (Filgrastim)[21,22]. While SCF has therapeutic potential, clinical studies found that patients injected with SCF had mast cell degranulation leading to the formation of a wheal and flare response[23]. The examination of these injection site reactions by transmission electron microscopy demonstrated extensive degranulation of dermal mast cells[23]. Moreover, Johnsen et al. reported in a phase II clinical study that 13% of the patients who received the combination therapy of SCF and G-CSF suffered from intense allergic episodes, including in some cases fever and rigor. Furthermore, 3% of the patients experienced hepatic failure[24]. Based on these and other findings, researchers concluded that a phase III trial of treatments using soluble SCF were inadvisable [24].

The shorter isoform of SCF (SCF220), lacking a cleavable domain at exon 6, is known as a tmSCF. Transmembrane SCF is found in the stromal cells of the bone marrow where it functions to support the proliferation and survival of progenitor cells[25]. Soluble and transmembrane SCF differ in terms of their ability to activate the c-Kit receptor, induce cellular responses and ability to promote adhesion between hematopoietic stem cells and extracellular matrix[14,26]. Several reports have further demonstrated that tmSCF caused more prolonged activation of the c-Kit receptor[27] and induced longer term proliferation of $CD34^+$ hematopoietic cells in comparison to soluble SCF[28]. Most importantly, it is possible that tmSCF may not cause mast cell activation.

In the second half of this study, I developed therapeutics based on tmSCF embedded in lipid nanocarriers. I found that tmSCF-based therapies do not induce mast cell activation in mice, in contrast to soluble SCF. Trafficking studies demonstrated that mast cells mainly use clathrin-mediated endocytosis to uptake SCF, while they use both clathrin- and caveolin-mediated endocytosis to uptake tmSCF therapies. I further found that tmSCF nanodiscs and

proteoliposomes enhanced the recovery of wild type and ob/ob mice following the induction of hind limb ischemia. Mechanistic studies suggest that proteoliposomal formulation enhances angiogenic activity of endothelial cells while nanodisc formulation enhances the mobilization of endothelial progenitor cells, thus contributing to the recovery from ischemia. Overall, our tmSCF-based protein therapies suggest safe potential therapeutics for PAD to diabetic patients who have reduced response to growth factor therapy.

1.2 DISSERTATION ROADMAP

The motivation behind this dissertation and the comprehensive summary of the thesis research are introduced in Chapter 1. A brief background and prior work are discussed in Chapter 2. Chapter 3 describes the gene expression changes in skin from patients with type 2 diabetes to identify the causal factors and potential therapeutic targets for the prevention and treatment of diabetic related disease. The development of tmSCF-based therapies and their functional examination are described in chapter 4, where I conducted Evan's blue dye extravasation, hind limb ischemia studies on WT type and ob/ob mice, and EPC mobilization study. Chapter 5 describes the mechanistic studies on SCF and tmSCF-based therapies to decipher endocytosis mechanisms behind the SCF and tmSCF-based therapy. Protein uptake kinetics, signaling, and endocytosis studies on three different cell types including mast cell, EPCs, and endothelial cells were conducted. Chapter 6 concludes the dissertation and presents future research directions.

Chapter 2: Background

2.1 Type 2 Diabetes and non-healing ulcers

Diabetes mellitus affects approximately 350 million people, leading to the death of about 4.6 million people in the world[2,29]. Diabetic patients have abnormal pancreatic function which leads to glucose insensitivity and deficiency of insulin hormone. A host of other problems accompany diabetes including to heart disease, stroke, hypertension, hypercholesterolemia, neuropathy, nephropathy, chronic kidney disease, peripheral vascular disease, non-alcoholic fatty liver, periodontal disease, erectile dysfunction, loss of hearing, depression, and pregnancy complications[30].

Diabetes leads to a disturbance of the blood vessel wall through promotion of vascular inflammation and endothelial cell dysfunction[31,32]. These abnormalities increase the severity of vascular disease in diabetic patients[33]. A major complication of diabetes is the formation of non-healing ulcers. Patients with type 2 diabetes are prone to the development of non-healing ulcers, particularly on the lower limbs[34]. These non-healing ulcers are a major factor in the cost of treating diabetes. It is estimated that non-healing ulcers add 9-13 billion dollars to the overall annual cost of treating diabetes in the United States alone[35]. A wide variety of treatments have been explored to heal or prevent these ulcers from forming[36]. However, the majority of these treatments have been found to either be ineffective in clinical trials or have limited benefits in a subset of patients[37].

2.2 Peripheral Artery Disease and its current standard care

As a complication of diabetes, 30 to 40 percent of patients age 50 and older develop peripheral artery disease (PAD)[3]. Severe PAD increases the risk of non-healing ulcers, pain from intermittent claudication and worst case for limb amputation. Current standard cares of PAD include physical therapy, medication, and surgical revascularization. The goals of PAD therapy depend on the severity of the disease. For all patients with PAD, reducing the risk of cardiovascular morbidity and mortality is the primary concern. For patients with intermittent claudication, improving functional status is an additional goal. Finally, for patients with critical limb ischemia, preventing leg amputation, restoring mobility, and reducing mortality are of

paramount concern. Depending on the population and the goal, different treatment choices should be discussed.

Exercise

Patients with intermittent claudication have been treated for their leg symptoms with medical therapy, lifestyle modification, and exercise programs because of the low overall risk of limb-threatening ischemia. In patients with claudication, a supervised exercise program is recommended to improve functional status and quality of life and to reduce leg symptoms. Exercise will increase the nitric oxide synthase activity and prostacyclin to improve endothelial function. Exercise also reduces free radicals, helping to reduce inflammation. Exercise also upregulates VEGF, leading to a possible angiogenesis[38].

Medication

Cilostazol has been shown to significantly improve maximal walking distance[39] and is, therefore, considered a Class I therapy in the ACC/AHA practice guidelines[40]. Cilostazol increases blood flow to the limbs both by preventing blood clots and by widening the blood vessels. Common side effects of this medication include headache and diarrhea. An alternative medication to cilostazol is pentoxifylline, which rarely has side effects though occasionally patients complain of nausea and diarrhea. However, a previous study comparing cilostazol, pentoxifylline, and placebo found cilostazol to be superior by improving maximal walking distance by 24 weeks while pentoxifylline was not different from placebo[39].

Surgery[41]

Once patients develop severe symptoms, surgical intervention should be considered. Multiple strategies for revascularization include surgery, angioplasty (cryoplasty, drug-coated, cutting, and standard angioplasty balloons are available for use in peripheral arteries), stenting (self-expanding and balloon-expandable stents are available, but drug-eluting stents are not currently approved for treating peripheral arteries in the United States), and atherectomy (laser, directional, orbital, and rotational atherectomy devices are approved for use in the United States). During my hospital visit thanks to the courtesy of Dr. Terreson, I had a chance to observe an atherectomy surgery on a PVD patient. A surgeon used a magnetic navigation system (MNS) to

enable the precise control of catheter[42] (**Figure 2.1**). The tip of the catheter for MNS is softer than conventional catheter tips. Moreover, a surgeon can control the catheter head very precisely (can move by 1mm and 1°). Thanks to these technological advancements, more hospitals started to use MNS, and a growing number of PVD cases were treated by MNS.

2.3 NON-INVASIVE THERAPY FOR PERIPHERAL VASCULAR DISEASE

Though angioplasty, stenting or grafting are the current standard care for PAD, these revascularization methods are invasive to blood vessels, sometimes causing re-occlusion of blood vessels called restenosis. An alternative approach for treating ischemic disease is to stimulate the body to create new vasculatures to restore blood flow through its own regenerative processes. Several approaches have been tried, which includes the delivery of progenitor cells[5,6], viral vectors to express growth factor/angiogenic transcription factor genes[7-10] or through the delivery of growth factors[11-13]. While cell therapy is labor-intensive and gene therapy has safety issues, protein therapeutics such as growth factor treatments have potential advantages from delivery and safety perspectives[6].

2.4 ANGIOGENESIS, VASCULOGENESIS, AND ARTERIOGENESIS

The term, vasculogenesis, is usually used in developmental biology, describing new vascular formation in embryo or fetal body by vascular progenitor cells. In this section, vasculogenesis is used to describe new vascular formation in adults by endothelial progenitor cells. When an organ or a tissue becomes ischemia, our body tries to create new vasculature to supply oxygen and nutrients to the ischemic area. There are mainly three ways to create vasculature: angiogenesis, vasculogenesis, and arteriogenesis.

In angiogenesis, the key player to build blood vessels is the endothelial cell. Hypoxic condition at ischemia promotes cells to activate HIF-1 expression and release pro-angiogenic factors including VEGF, EGF, FGF, or TGFβ. Hypoxia also upregulates protease expression such as MMP, leading to the basement membrane degradation and pericyte detachment[43]. Activated endothelial cells by these growth factors migrate towards ischemic areas to build new blood vessels by sprouting from existing blood vessels.

In vasculogenesis, the key player to build blood vessels is endothelial progenitor cells (EPCs). EPCs are usually found in bone marrow, circulating blood, and umbilical cord. After

ischemic events, circulating EPCs are mobilized and recruited to ischemic sites and contribute to vessel growth or repair.

Arteriogenesis describes the growth of functional collateral arteries from preexisting arterio-arteriolar anastomose, usually seen as a maturation and a formation of larger-diameter arteries from preexisting capillaries or collateral arteries. While angiogenesis is induced by hypoxia and results in new capillaries, arteriogenesis is induced by physical forces, most importantly fluid shear stress. Altered fluid stress induces a vascular wall cell proliferation and migration and leads to wall remodeling processes[44].

Our therapeutic angiogenesis using tmSCF protein aims to trigger both angiogenesis and vasculogenesis.

2.5 STEM CELL FACTOR AND TRANSMEMBRANE STEM CELL FACTOR

Stem cell factor (SCF) is known as Kit ligand, mast cell growth factor, or steel factor. SCF is a hematopoietic cytokine that triggers its biological effects by binding to its receptor, c-Kit, and maintains hematopoiesis[14]. Endogenous SCF isoform (SCF248) is initially a transmembrane protein that contains an enzyme cleavable domain allowing the release of soluble SCF (SCF163)[15]. While the main role of SCF is to maintain hematopoiesis, further studies demonstrated that SCF has a potential to induce angiogenesis and help repair ischemic areas *in vitro* and *in vivo*[16-18]. For example, Matsui et al. demonstrated an improved migration and tube formation of endothelial cells after SCF treatment *in vitro*[16], and Yaniz-Galende et al. demonstrated that SCF gene transfer promoted a cardiac repair after myocardial infarction *in vivo*[18]. In addition to these studies, SCF is most known for its synergetic effect with granulocyte colony stimulating factor (G-CSF) in terms of rescuing ischemia. Co-stimulation of SCF and G-CSF enhanced angiogenesis and neurogenesis on stroke models both in animal and clinical studies[17,19,20]. These clinical trials demonstrated a higher number of peripheral blood progenitor cell mobilization after co-stimulation of SCF and G-CSF in comparison to control[45]. Though SCF was a potential protein for ischemia treatment, various clinical studies demonstrated that virtually all patients who have been given SCF have a pruritic wheal and flare response at the injection[23]. Examination of these injection site reactions by transmission electron microscopy revealed evidence of extensive anaphylactic-type degranulation of dermal mast cells[23].

SCF also exists in a membrane bound form, the shorter isoform (SCF220) lacking exon 6, which encodes the cleavable domain and remains as transmembrane protein, transmembrane stem cell factor (tmSCF). Because membrane-bound SCF is produced by and present on bone marrow stromal cells, it functions within the marrow microenvironment to support the proliferation and survival of progenitor cells[25]. Soluble and transmembrane SCF differ in terms of their abilities to activate the c-Kit receptor, induce cellular responses and promote adhesion between hematopoietic stem cells and extracellular matrix[14,26]. Several reports have further demonstrated that tmSCF caused more prolonged activation of the c-Kit receptor[27] and induced longer term proliferation of $CD34^+$ hematopoietic cells in comparison to soluble SCF[28].

2.6 C-KIT RECEPTOR[29]

The c-Kit is a cell surface receptor that binds to SCF, and belongs to receptor tyrosine kinase (RTK). When SCF binds to the extracellular domain of c-Kit, its dimerization is triggered with other adjacent c-Kit. Dimerization leads to a rapid activation of the protein's cytoplasmic kinase domains. The first substrate for being phosphorylated by this kinase domain is the receptor itself. The activated receptor as a result then becomes autophosphorylated on multiple specific intracellular tyrosine residues, driving downstream signal transduction pathway.

The c-Kit is usually detected in various stem cells, cells with self-renewal potency, or progenitor cells. The c-Kit expressing cell type includes hematopoietic cells, germ cells, mast cells, and melanoma cells etc. As stem cells differentiate, they lose c-Kit expression. Approximately 1% to 4% of bone marrow stem cells are c-Kit positive and 1% in peripheral blood. Other than these locations, c-Kit are also found in epithelial cells, neurons, or endothelial cells.

2.7 PROTEOLIPOSOME

Liposome is one kind of lipid based nanocarriers often used as a drug delivery carrier. Liposome is made of phospholipid bilayers mimicking the cellular membrane. Polar head group facing outside, allowing interaction with aqueous solution while having non-polar chains, promoting interaction with one another to create a lipid bilayer vesicle. Liposomes are the most successful drug carrier because of their unique advantages. They can contain hydrophilic agents inside of aqueous core as well as insert lipophilic agents on the membrane. Hydrophilic surface

of the liposomes makes them less likely to be bound with serum, leading to less opsonization. Lamellarity also contributes to drug delivery efficiency. Unilamellar vesicles enclose a large aqueous core, thus they are ideally suited for the encapsulation of hydrophilic drugs. On the other hand, multilamellar vesicles preferentially entrap lipid-soluble drugs[46].

In this study, we used four types of lipid to make liposome. 1,2-Dioleoyl-sn-glycero-3-phosphocholine (DOPC), 1,2-dioleoyl-sn-glycero-3-phosphoethanolamine (18:1 (Δ9-Cis) PE (DOPE)), Sphingomyelin and Cholesterol. Phosphatidylcholine (PC) is generally the most abundant lipid in animal cell membranes, providing structural framework. PC is more common in the outer leaflet where it functions as part of the permeability barrier[47]. DOPE forms a stable lipid layer and fuses with endosomal lipid bilayer. DOPE or DOPC are neutral lipids and usually studied with 1,2-dioleoyl-3-trimethylammonium-propane (DOTAP) for its *in vitro* transfection efficiency[48]. Sphingomyelin is highly abundant in a membrane of nerve cells (i.e. myelin sheaths). Sphingomyelin has a high affinity for cholesterol, they are packed tightly into liquid-ordered domains to form lipid rafts. These raft domains are thought to function as signaling platforms that regulate the localization and interactions of proteins[49]. Cholesterol consists of four linked hydrocarbon rings, forming a bulky steroid structure. Cholesterol is particularly useful in proteoliposome creation since it fills the gaps created by imperfect packing of other lipid species when proteins are embedded in a membrane. Although cholesterol is often used as liposome content, it presents some problems when used in human pharmaceuticals. Since commercially available source is from animals (sheep derived), it may cause a potential viral contamination. Moreover, cholesterol is readily oxidized and these oxidized products tend to be toxic in the biological system (i.e. cholesterol causes aortic smooth muscle cells to die)[50]. Therefore, care must be taken to handle cholesterol not to oxidize it (i.e. store in argon gas). We used DOPE:DOPC:Cholesterol:Shingomyelin = 2:1:1:1 ratio, providing liposome flexibility to incorporate tmSCF protein.

2.8 NANODISC

In 2007, Sligar and coworkers at the University of Illinois at Urbana-Champaign developed a new technology termed as nanodiscs[51]. Nanodiscs are essentially small nanoscale lipid bilayers that allow for the solubilization of membrane protein in a uniform, membrane-mimicking environment. Nanodiscs have several advantages over other types of lipid bilayer-

mimicking technologies, including their homogeneity, control of membrane protein oligomeric state and long-term stability[52]. Because of these advantages, nanodiscs are usually used for studying membrane protein's properties. In our study, we used nanodisc as a protein carrier to improve therapeutic efficiency of membrane protein. Nanodisc is composed of Membrane Scaffold Protein (MSP), lipid, and target protein. It is made through self-assembly using detergent solubilizing methods. MSP is wrapping the lipid and protein, and forming a nanodisc when detergent is removed. The stoichiometric ratio of lipid, MSP, and target protein is important to make nanodisc. If this ratio is off, aggregates of lipid, protein and MSP will be formed. In our protocol, we removed these free proteins/lipids by dialysis with a membrane (the pore size is 300kDa). We use 1-palmitoyl-2-oleoyl-sn-glycero-3-phosphocholine (POPC) as a lipid source, which is typically considered as one of the model lipids for biophysical experiments. Unsaturated lipids in POPC provide nanodisc fluidity, allowing membrane proteins to be incorporated. The structures of all the lipids used in this study are shown in **Figure 2.2**.

2.9 ENDOTHELIAL PROGENITOR CELLS

EPCs were first discovered by Asahara et al. in 1997, reporting the bone marrow derived circulating progenitor cells for endothelial lineage[53]. Stem cells have been traditionally characterized based on three properties: self-renewability, clonogenicity, and plasticity (differentiation capacity). In contrast, progenitor cells lack self-renewability. EPC has self-renewability and clonogenicity but does not have plasticity (**Figure 2.3**) thus it is between stem cell and progenitor cell [54]. In this section, I will describe the origin of EPC, markers for EPC, culture method, subtypes of EPCs, and their niche.

EPCs share a common origin with hematopoietic cells. They originated from hemangioblast, which is a transient cell that forms in embryo during gastrulation and has an ability to rapidly differentiate into an endothelial or a hematopoietic stem cell[54] (**Figure 2.3**). Since EPCs are of hematopoietic origin, EPCs share some common markers with hematopoietic cells. Examples include CD34 (transmembrane phosphoglycoprotein protein), CD133 (prominin-1) and CD45 (Protein tyrosine phosphatase, receptor type, C). CD34 mediates the attachment of hematopoietic stem cells to bone marrow extracellular matrix or directly to stromal cells. The precise function of CD133 remains unknown, but it has been proposed that it acts as an organizer of cell membrane topology. EPCs also share some common markers with endothelial cells such

as CD31 (PECAM-1), FLK-1(Fetal Liver Kinese-1), and CD144(VE-cadherin). CD31 is known as platelet/endothelial cell adhesion molecule-1 (PECAM-1), which regulates cell adhesion thus controlling migration and inflammation of endothelial cell[55]. FLK-1 is known as VEGFR2 and regulates vascular development and angiogenesis. CD144 is VE-cadherin, regulating various cellular processes such as cell adhesion, proliferation, apoptosis and vascular endothelial growth factor receptor function. Though CD34 is a potential marker for EPC, it is a widely expressed molecule on some mesenchymal, epithelial, and even cancer stem cell populations. FLK-1 is also widely expressed on blood, endothelial, and cardiac cells and thus fails to be a helpful discriminator among those cells expressing CD34. Thus, we need multiple markers to detect EPCs. So far, general consensus purports that it would be sufficient to use CD34, CD133, and FLK-1 as EPC marker. In our study, we used CD34, CD133, FLK-1 and CD144 to determine EPCs.

Though there is a general consensus for markers for EPC, it is a very controversial topic since some studies found these markers on EPCs but some claimed not. These discrepancies happen because EPCs have several subtypes and their culture method is modified by various researchers.

The first subtype is early EPC, which can be found after one week of culturing bone marrow mononuclear cells (BMMNCs) from blood or bone marrow in endothelial cell media. Their morphology is spindle shape. To obtain early EPC, we generally have two methods: depletion method or re-plating method. The depletion technique involves plating BMMNCs on fibronectin-coated dishes for approximately four days. The nonadherent cells are then removed by washing with PBS, leaving BMMNCs on a dish. The four-day period is selected because the unwanted platelets, red blood cells, or monocytes are gradually depleted over this period. The number of days is, however, not fixed and has been modified by various researchers. In the re-plating method, we first pre-plate the BMMNCs from bone marrow or blood then re-plate the non-adherent cell. The rationale for pre-plating the BMMNCs is to remove any monocytes, macrophages, or circulating mature ECs that might be present in the BMMNCs sample[54]. In these culture methods, each researcher uses different kinds of endothelial cell media, different days to select EPCs. These inconsistencies may contribute to the variety of marker expressions for EPC.

The second subtype of EPC is called late EPC, which appears after one to three weeks of culturing early EPCs. Their appearance will shift from spindle shape to cobblestone like shape. This phenotype is functionally closer to endothelial cells, having enhanced LDL uptake, nitric oxide production, and lectin binding in comparison to early EPC. Markers for late EPCs are more consistent among articles. Late EPC loses CD133 expression and maintains CD34, FLK-1, CD144. Marker expression, morphology, functional activities are summarized in **Table 1**[54].

EPCs are found in peripheral blood, umbilical cord blood and bone marrow. EPCs are most abundant in umbilical cord blood but their population is still 0.2-1% of total cord blood[56]. Population of EPC in bone marrow and peripheral blood are even less and reported to be around 0.002-0.01%[57]. These resident EPCs will increase in response to physiological and pathological stimuli, including myocardial and peripheral ischemia[58].

2.10 CLATHRIN MEDIATED ENDOCYTOSIS[59]

Clathrin is composed of a clathrin heavy chain (~190 kDa) and a smaller clathrin light chain (~25 kDa). Three clathrin heavy and light chains form a trimeric clathrin 'triskelion', structuring polygonal lattices (**Figure 2.4 A, B**). When a cargo molecule is endocytosed, clathrin is assembled on the membrane. However, clathrin does not have an affinity to the plasma membrane, thus requiring aids of adaptor proteins. Cargo molecules are usually transmembrane proteins and their extracellular ligand. In this research, cargo molecules are c-Kit. After a ligand binds to c-Kit, c-Kit will recruit cascades of adaptor proteins. These adaptor proteins then recruit clathrins, starting to form a clathrin pit and generating vesicles. These processes are relatively fast and only take 120 seconds to generate a vesicle (**Figure 2.4 C**). These vesicles are then fused with an early endosome to initiate an intracellular trafficking event.

2.11 CAVEOLIN MEDIATED ENDOCYTOSIS[60-62]

Caveolin-1 is a small integral membrane protein, whose 34 hydrophobic amino acids are inserted into the inner leaflet of the membrane bilayer in a special hairpin-like form and never reaches the outside of the cell. The rest of the protein is cytosolic and the N-terminal region has been suggested to be important for anchoring caveolin to cholesterol and sphingolipid-rich membrane domains. Biochemical studies revealed that caveolae are detergent resistant and highly hydrophobic, usually surrounded by cholesterol or sphingomyelin, thus believed to be in

lipid raft domain. Caveolin serves an important role in lipid metabolism. Caveolin 1 in adipocyte binds to fatty-acid and supports the formation of lipid droplets (intracellular organelles specialized for lipid storage). Another evidence of linking caveolin and lipid metabolism is that Cav1-knockout mice are resistant to diet-induced obesity and show decreased adiposity as well as decreased levels of free cholesterol in adipocytes. These studies indicate that caveolae may have an affinity to lipids and may interact with our lipid based nanocarriers.

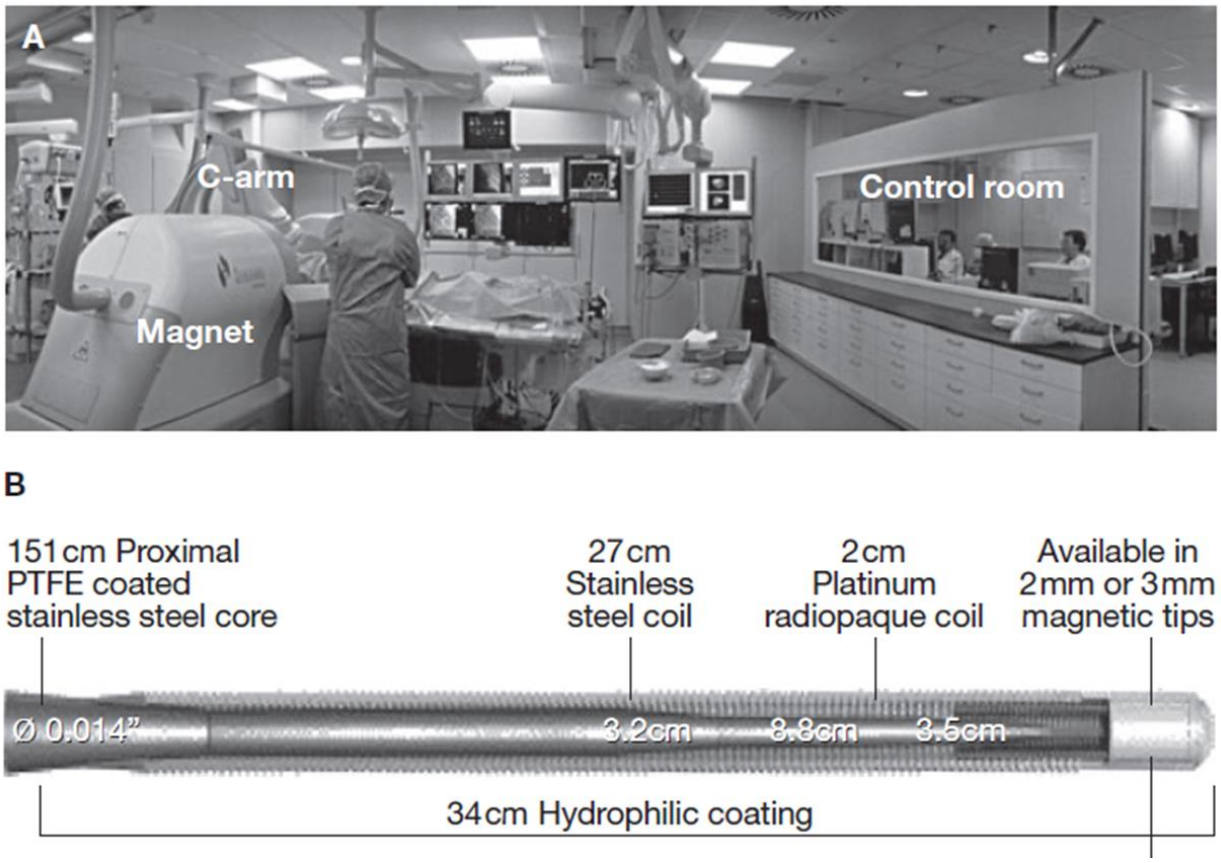

Figure 2.1. Image of magnetic navigation system and catheter head. Physicians control a catheter using a robot in the control room. Images taken from Ramcharitar et al. *Nature Clinical Practice Cardiovascular Medicine* **5**, 148-156

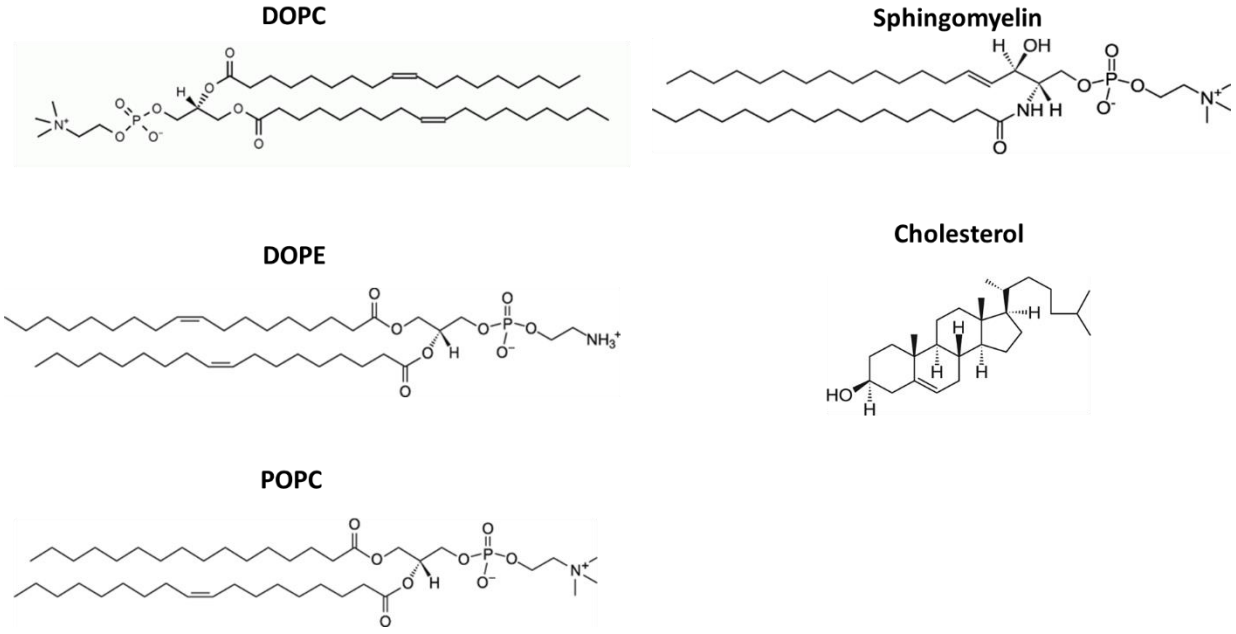

Figure 2.2. Structures of lipids used in this study. 1,2-Dioleoyl-sn-glycero-3-phosphocholine (DOPC), 1,2-dioleoyl-sn-glycero-3-phosphoethanolamine (18:1 (Δ9-Cis) PE (DOPE)), 1-palmitoyl-2-oleoyl-sn-glycero-3-phosphocholine (POPC), Sphingomyelin, and Cholesterol.

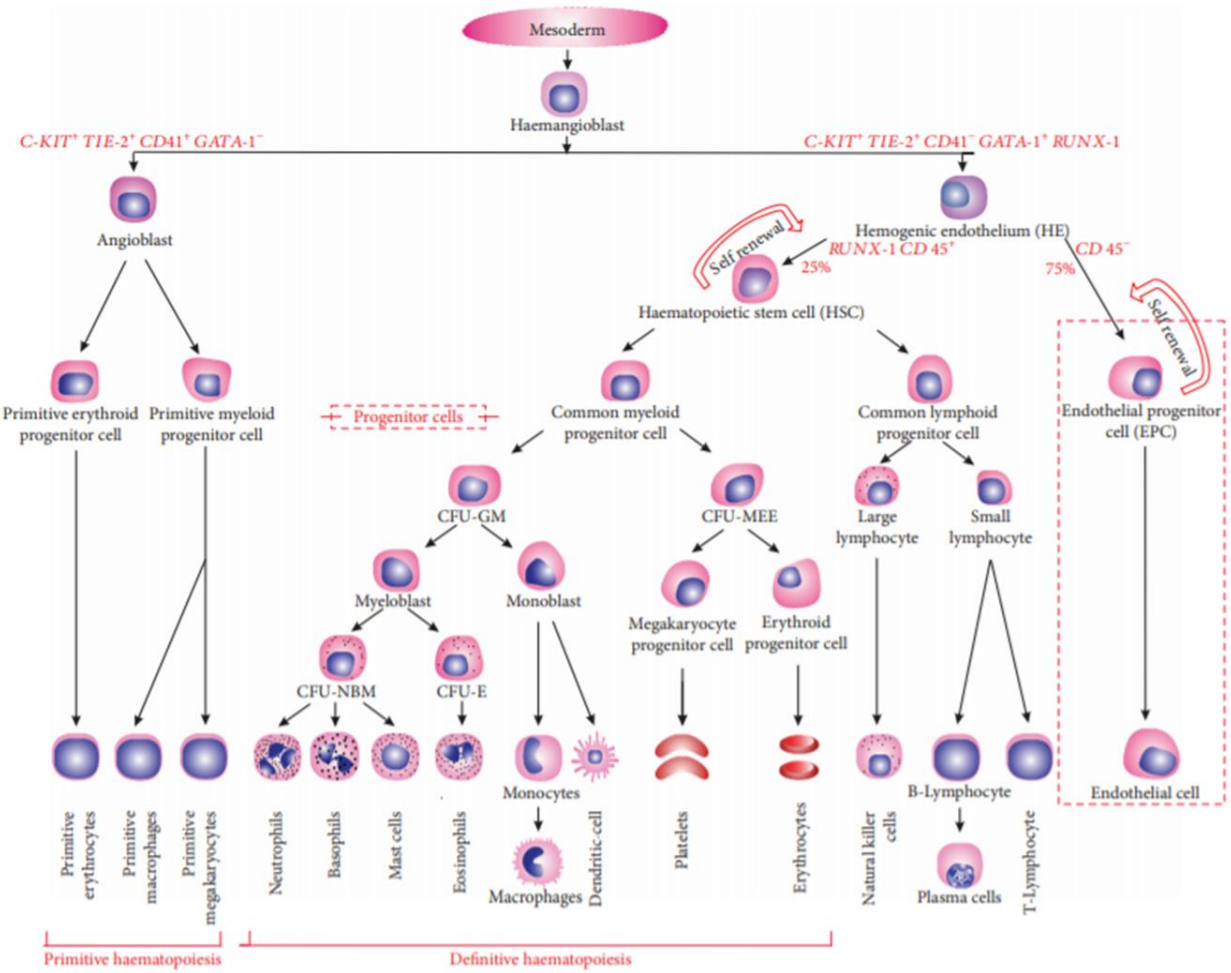

Figure 2.3. Origin of EPCs. EPCs share the same origin with hematopoietic stem cells, and they are differentiated from hemangioblast. Image is taken from Chopra et al. *Stem Cells Int* **2018**, 9847015-9847015

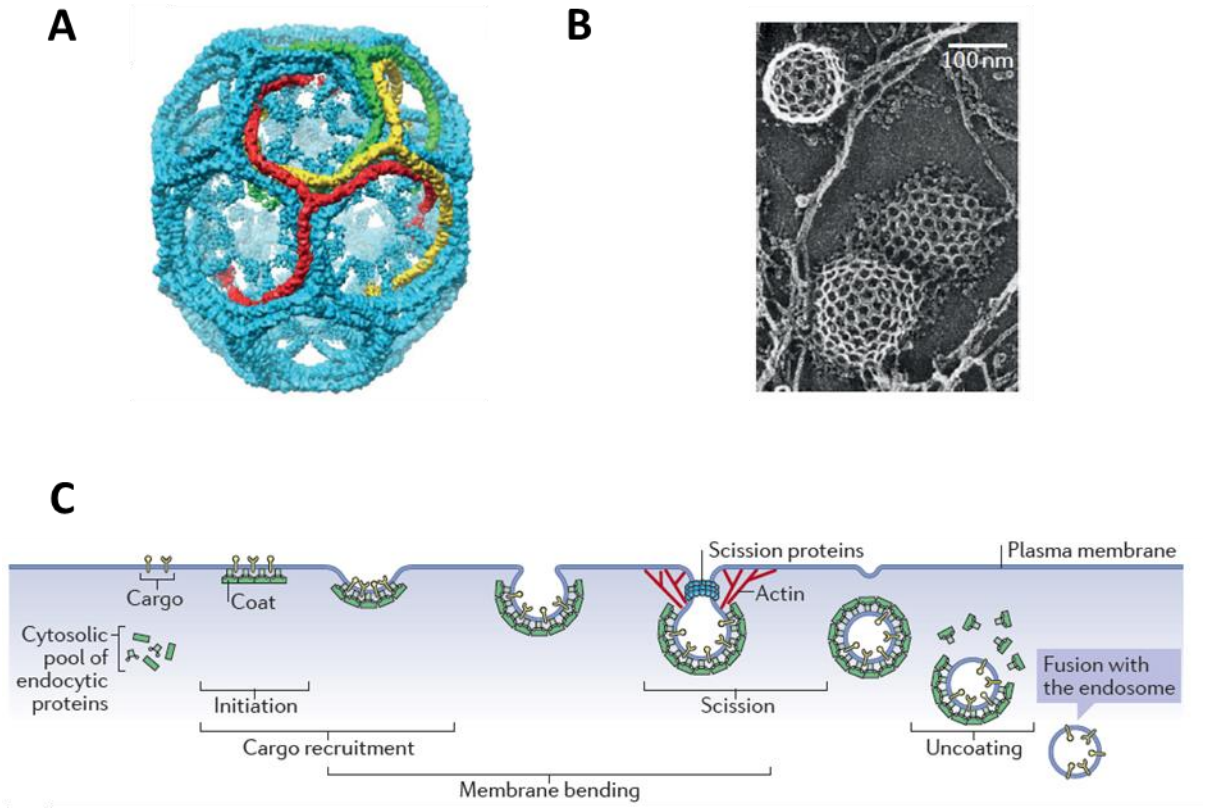

Figure 2.4. Structure of clathrin and schematic illustration of clathrin-mediated endocytosis. (A) 3D model structure of clathrin vesicle. (B) Electron microscopy image of clathrin pit. (C) Schematic illustration of clathrin pit formation. Images taken from Kaksonen, M. & Roux, A. *Nature Reviews Molecular Cell Biology* **19**, 313-326.

Table 2.1 Summary of activity and surface expression of early EPCs and late EPCs. Table taken from Chopra et al. *Stem Cells Int* **2018**, 9847015-9847015.

	Early EPCs	Late EPCs
Synonyms	CACs [82]	OECs [83, 91] or ECFCs [84]
Cell population [81, 91]	Heterogeneous	Homogenous
Cell morphology [81]	Spindle-shaped cells	Cobblestone-like cells
Appearance in culture	<1 week [5, 81]	2–4 weeks [81]
Lifespan [81]	3-4 weeks	≈12 weeks
Morphogenic potential [81]	Low	High
Angiogenic potential [81]	Good	Good
Tube formation *in vitro* [5, 92, 134]		
Tube formation by EPCs alone	*Absent*	*Present*
Tube formation by EPCs with HUVECs	*Absent*	*Present*
Tube formation *in vivo* [92]	Absent	Present
Neovascularization *in vivo* [82, 92, 93, 134]	Indirect paracrine fashion	Directly providing ECs; hence can be referred to as "true EPCs"
Surface expression		
CD34 [88, 134]	+	+
CD45 [81, 88, 134]	+	−
CD14	+ and − [91, 93]/+ [92]	−
CD133	− [88] and + [89, 136]	− [88, 89, 136]
CD31 (PECAM 1) [81, 134, 137]	−/+	++
VEGFR-2 [81, 92, 93, 134, 137]	−/+	++
VE cadherin [81, 93, 134]	−/+	++
vWf [81]	−/+	+
Phenotype [90]	Monocytic	Endothelial
AcLDL uptake [5]	+	++
Lectin binding [5]	+	++
NO production [5]	+	++

+: present; ++: strongly present; −: absent; and −/+: limited/weak/focal.

Chapter 3: Altered Gene Expression in the Skin of Type 2 Diabetes

3.1 INTRODUCTION

Type 2 diabetes affects 29 million people in the U.S., and 170 million people in the world[63]. This condition can often lead to the disturbance of the blood vessel wall through promotion of vascular inflammation and endothelial cell dysfunction[31,32]. These abnormalities increase the severity of vascular disease in diabetic patients[33]. A major complication of diabetes is the formation of non-healing ulcers. Patients with type 2 diabetes are prone to the development of non-healing ulcers, particularly on the lower limbs[34]. These non-healing ulcers are a major factor in the cost of treating diabetes. One estimate suggested that non-healing ulcers add 9-13 billion dollars to the overall annual cost of treating diabetes in the United States alone[35]. A wide variety of treatments have been explored to heal or prevent these ulcers from forming[36]. However, the majority of these treatments have been found to either be ineffective in clinical trials or have limited benefits in a subset of patients[37].

Our group has recently identified that patients with diabetes have a reduction in cell surface proteoglycans in their skin, including syndecan-4 and glypican-1[36,64,65]. These proteoglycans serve as co-receptors for growth factor signaling and their absence would suggest that diabetic tissues would be resistant to growth factor therapies for enhancing angiogenesis and wound healing. Delivery of syndecan-4 and glypican-1 in a proteoliposomal formulation enhanced the effectiveness of growth factor therapies in diabetic animals in models of limb ischemia and wound healing[36,65]. These studies demonstrated that an increased understanding into the biology of non-healing ulcers and the changes that occur in skin with type 2 diabetes could identify potentially treatable deficits in healing and angiogenesis that may improve their treatment.

In this chapter, we used RNA sequencing (RNAseq) to examine the changes in gene expression in the skin between patients with type 2 diabetes and non-diabetic patients. These findings provide a window into the changes that occur in diabetic patients that may predispose them to the formation of non-healing ulcers and could provide pathways for further investigation into the mechanisms of poor healing in diabetic wounds.[1]

[1] Portions of this chapter have been previously published as 66Takematsu, E. *et al.* Genome wide analysis of gene expression changes in skin from patients with type 2 diabetes. *PLoS One* **15**, e0225267, doi:10.1371/journal.pone.0225267 (2020).

3.2 Materials and Method

3.2.1 Human Samples

Human skin samples were obtained from the Glasgow Caledonian University Skin Research Tissue Bank, Glasgow UK. The tissue bank has NHS research ethics approval to supply human skin for research (REC REF: 16/ES/0069). All methods were carried out in accordance with relevant guidelines and regulations. All experimental protocols were approved by the NHS East of Scotland Research Ethics Service. Informed consent was obtained from all subjects (no patients were under 18 years of age). All the patients were Caucasian and from western Scotland. Patients with diabetes were on treatment with metformin. Samples were formalin fixed and embedded in paraffin following standard procedures prior to sectioning. Control skin samples were taken from either clinical cases of breast reduction surgery or lower limb interventions for peripheral arterial disease. Skin samples for diabetic patients were taken from limb amputation surgeries. Metadata for the patients are listed in **Table 1**.

3.2.2 RNA Sequencing and Analysis

RNA was isolated from formalin-fixed, paraffin-embedded tissue sections using the RNeasy FFPE kit (Qiagen). The mRNA was sequenced using an Illumina HiSeq 4000 at the Genomic Sequencing and Analysis Facility at UT Austin. Single reads of 50 base pairs were performed after poly-A mRNA capture used Ambion Poly(A) Tailing Kit and NEBNext Ultra II Directional RNA Library Prep Kit to isolate mRNA and dUTP directional preparation of the mRNA library. Gene expression analysis was performed using DESeq2 and R software. Plots were created using Prism GraphPad and Microsoft Excel.

3.2.3 Statistical Analysis

Gene abundances were then normalized using DESeq2 normalization and log2 transformed using variance-stabilizing transformation (VST). Differential expression testing was performed based on the DESeq2 negative binomial distribution by comparing type II diabetic samples to normal samples, while controlling for sex differences. This was done by including sex as a covariate to control for in the DESeq2 design matrix along with the factor of interest, diabetic state. Genes that met the adjusted p-value cutoffs of 0.05 or lower and an absolute fold change of 2 or higher.

3.3 Results and Discussion

3.3.1 Overall changes in gene expression in the skin in type 2 diabetes

Skin tissues were obtained from 13 non-diabetic and 14 type 2 diabetes donors. We examined expression changes of 58,037 transcribed genes. Differential expression testing was performed based on the DESeq2 negative binomial distribution by comparing type 2 diabetic samples to normal samples. We found 64 significantly upregulated genes and 120 downregulated genes (**Figure 3.1 A, B**). There was significant patient-to-patient variability in the samples (**Figure 3.1 C**). Overall the five most upregulated genes when comparing skin samples from diabetic patients to non-diabetic patients included three non-coding RNA (lncRNA) genes (LINC01118, RP11-545I5.3 and an unknown lncRNA), an enzyme involved in lipid metabolism (ABHD16A) and a potassium channel that is important in smooth muscle tone and nerve function (KCNMA1). Conversely, the most downregulated genes included multiple pseudogenes and lncRNA (LINC01060, HPRT1P2, and CCNYL3) as well as the transcription factor NKX2_1 and a member of the TPD52 protein family associated with proliferation and vesicle trafficking (TPD52L3). Pathway analysis of the significantly altered genes revealed significant alterations in genes relating to epigenetic regulation of gene expression, lipid membrane rafts, growth factor signaling/PDGFRβ signaling, and proteolysis (**Figure 3.2 A**). Gene ontology analysis of the biological processes most regulated in the genes and the functional pathways being regulated supported significant regulation of genes relating to integrin-based adhesion, focal adhesion formation and ECM proteoglycans (**Figure 3.2 B, C**).

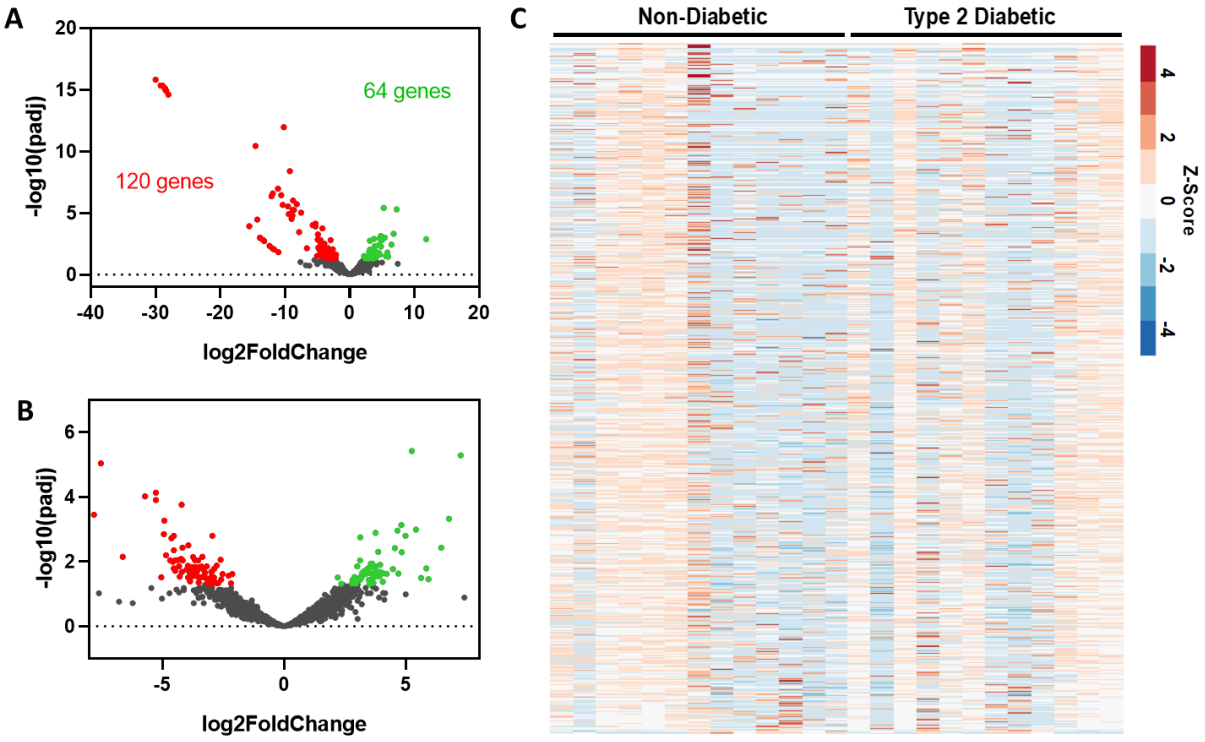

Figure 3.1 Volcano plots and heat map of z-score. (A) Volcano plot of statistical significance against fold change between diabetic and non-diabetic skin. (B) Zoomed volcano plot of statistical significance against fold change between diabetic and non-diabetic skin. (C) Heat map of the z-score for the top 30% varying genes for diabetic and non-diabetic patients.

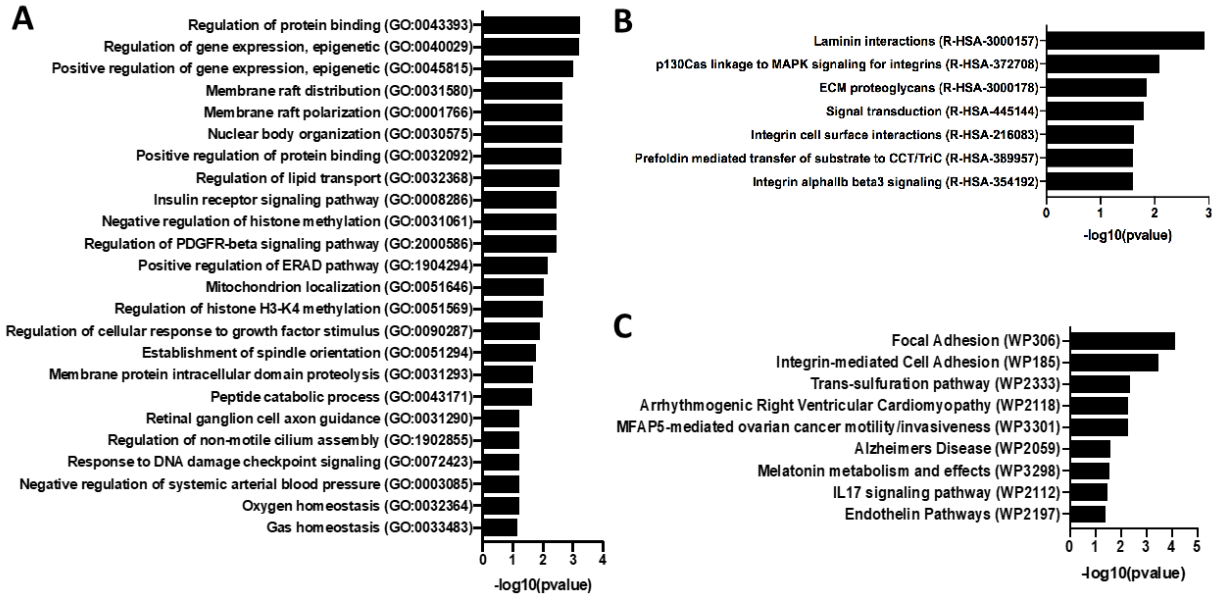

Figure 3.2 Gene and pathway ontology analysis of significantly regulated genes between diabetic and non-diabetic patient skin samples. (A) Most altered pathways between diabetic and non-diabetic skin using the reactome database analysis. (B) Significantly alter pathways for the gene ontology analysis for biological processes when comparing diabetic and non-diabetic patients. (C) Pathways significantly altered using the wikipathways analysis tool comparing diabetic and non-diabetic patients.

Table 3.1. Patient Metadata

Sex	Age	Diabetic State
M	59	Normal
F	49	Normal
F	49	Normal
M	69	Normal
M	69	Normal
F	80	Normal
F	39	Normal
M	62	Normal
F	19	Normal
F	34	Normal
F	60	Normal
F	27	Normal
F	69	Normal
M	73	Type II Diabetic
F	47	Type II Diabetic
M	80	Type II Diabetic
M	81	Type II Diabetic
M	53	Type II Diabetic
M	77	Type II Diabetic
M	61	Type II Diabetic
M	79	Type II Diabetic
M	61	Type II Diabetic
M	49	Type II Diabetic
M	58	Type II Diabetic
F	72	Type II Diabetic
F	59	Type II Diabetic
F	59	Type II Diabetic

3.3.2 *Regulation of Genes Related to Transcription and Gene Regulation*

The largest category of genes with significant regulation was that involved in gene regulation (**Figure 3.3**). Among the 11 upregulated genes, five genes (CAMK4, ZNF106, RC3H2, DMNT1, ZNF148) showed some relationship with type 2 diabetes in the previous studies[67-71]. One of the significantly upregulated genes was for calcium/calmodulin-dependent protein kinase (CAMK4). This protein phosphorylates transcription factors and can thereby regulate gene expression. Its target transcription factors include high-mobility group protein 1 (HMGB1), a proinflammatory mediator of chronic pain development[72]. Increased phosphorylation of CAMK4 is seen in a rat dorsal root ganglion after STZ-induced diabetes. [73].

Another notable gene that was upregulated in patients with diabetes was the transcriptional repressor ZNF224. Overexpression of ZNF224 is linked to the reduction of mitochondrial citrate carrier (CIC)[74,75], a key enzyme in fatty acid and cholesterol synthesis[75]. Rats with STZ-induced diabetes had a reduced CIC activity[76], consistent with our findings.

Among the downregulated genes in our study, seven of these genes were found to also be associated with diabetes in previous studies[77-84]. The most downregulated gene in the gene regulation category was NKX2-1, also known as thyroid transcription factor 1 (TTF1). This transcription factor is involved in differentiation of the thyroid, lung and brain[85] and is linked to neuronal disorders[86,87]. Mutation of NKX2-1 is also related to the reduction in mitochondrial respiratory chain complex activity[88]. Notably, reduced mitochondrial activity is one of the characteristics of diabetes[89]. Another highly downregulated transcription factor was SIX4, a key transcription factor in the development of sensory neurons and myogenesis[90-92]. Peripheral neuropathy is a common finding in diabetic patients and underlies alterations in biomechanics that leads to increased risk of ulcer formation[93]. In addition, diabetes can cause muscle weakness by altering muscle progenitor cells and other mechanisms[94,95]. Thus, further investigation of these genes in the context of reduced mitochondrial activity and deficits in neural and muscular healing in diabetes would be merited.

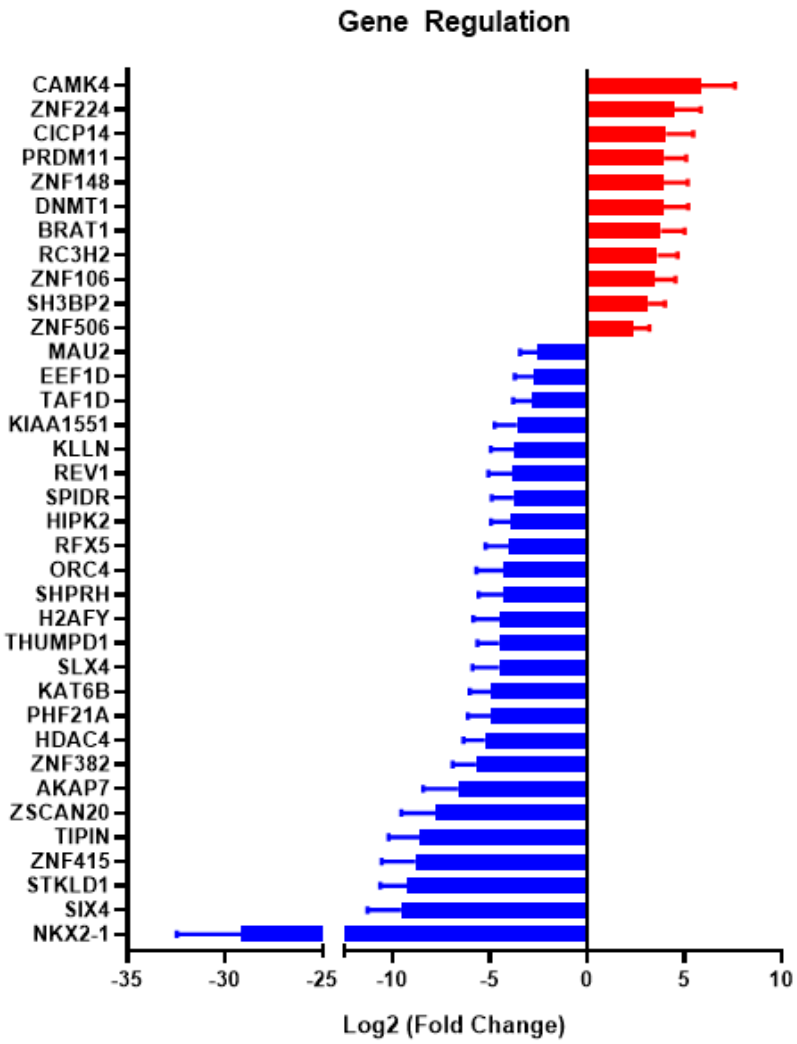

Figure 3.3 Transcription- and regulation-related genes that were significantly regulated in type 2 diabetic patient skin samples.

3.3.3 *Regulation of Metabolism and Mitochondrial Related Genes.*

We observed significant regulation in a number of genes relating to metabolism (**Figure 3.4 A**). The most upregulated gene in this category was α/β hydrolase domain containing 16A (ABHD16A), which is a member of the α/β hydrolase domain-containing (ABHD) protein family and is expressed in dendritic cells, macrophages, lymphocytes, and lymphoid organs. Interplay between ABHD16A and ABHD12 dynamically regulates immunomodulatory lysophosphatidylserines and can alter the release of proinflammatory cytokines from macrophages[96]. Other studies found several associations between ABHD16A and the genetic predisposition to coronary artery aneurysm and Kawasaki disease[97].

We also found an 11.8 fold increase in gene expression for LDL Receptor Related Protein 1 (LRP1) in skin from diabetic patients in comparison to control patients. LRP1 interacts with many ligands including lipoproteins, extracellular matrix proteins, protease, cytokines and growth factors. Biological roles of LRP1 covers broad ranges of activities such as lipid metabolism, cell growth, migration and tissue invasion, but the most notable role of LRP1 in terms of wound healing should be extracellular matrix (ECM) remodeling. A recent study found that LRP1 markedly inhibited fibronectin remodeling by regulating cell-surface urokinase receptors and plasminogen activation[98]. This process may be relevant to reduced healing of wounds and altered ECM remodeling observed in diabetic patients. Another study found upregulation of LRP1 in the epicardial fat tissue from patients with type 2 diabetes[99]. Interestingly, GULP1, a ligand that binds to LRP1, was significantly decreased in patients with type 2 diabetes in our study. GULP1 is an adapter protein necessary for the engulfment of apoptotic cells by phagocytes[100] and also functions as a modulator of glycosphingolipid and cholesterol transport[101].

We also found an 8.7 fold increase in NOTCH3 expression in skin from patients with type 2 diabetes. The Notch3 protein plays a key role in the function and survival of vascular smooth muscle cells, and is essential for the maintenance of blood vessels[102]. Recently, several studies found that NOTCH3 polymorphism seems to be a risk factor for both ischemic disease and diabetes. For example, NOTCH3 381C>T and 1735T>C polymorphisms found in the peripheral blood were associated with ischemic stroke and to be the risk factors for ischemic stroke[103]. The C381T (rs3815188) variants in exon 3 and A684G (rs1043994) variants in exon 4

of the NOTCH3 gene in the peripheral blood were also strongly associated with type 2 diabetes[104].

Superoxide dismutase 2 (SOD2) was increased 4.6-fold in patients with type 2 diabetes in our study. This gene encodes a mitochondrial protein, also known as manganese superoxide dismutase (MnSOD), that is a manganese-dependent enzyme that acts on superoxide produced as a byproduct of oxidative phosphorylation. SOD2 converts superoxide into hydrogen peroxide, which can be further detoxified by other enzymes. This enzyme is induced by oxidative stress and is increased in chronic ischemic wound models[105,106]. In addition to its role in protecting oxidative damage, SOD2 also regulates signaling through reactive oxygen species (ROS)[107]. Low levels of SOD2 impair wound healing and enhancing SOD2 expression/activity enhanced wound repair[108,109]. Polymorphisms in the SOD2 gene are associated with type 2 diabetes in the Japanese American population. The A16V polymorphism of SOD2 was seen frequently in the peripheral blood of type 2 diabetes patients, and study confirmed that this polymorphism decreases SOD2 activity, which successively will increase oxidative stress[110]. The C47T polymorphism in SOD2 gene has also been associated with a protective effect against diabetic microvascular complications[111].

The most downregulated gene in the metabolism category was tumor protein D52-like family of proteins (TPD52L3; **Figure 3.4 A**). This gene has not been linked to type 2 diabetes or wound healing yet, but a study found that exogenous expression of human TPD52 in cultured cells resulted in significantly increased numbers of lipid droplet.[112] Lipid droplets store excess fatty acids within adipocytes. Thus, TPD52L3 seems to be associated with excess lipid storage in adipose cells. We hypothesize that lowering of TPD52L3 in type 2 diabetes, may lead to alterations in lipid storage and altered function of adipocytes.

Previous studies have linked diabetes to the development of mitochondrial dysfunction[113]. For example, point mutations resulting in amino acid substitutions in MT-CYB (D214N) showed defective mitochondrial ATP production[114-116]. Therefore, it is imperative to examine how diabetes affects the expression of mitochondrial related genes. The only significantly upregulated mitochondrial gene was HEBP2, which codes for the Heme Binding Protein 2 (**Figure 3.4 B**). The protein encoded by this gene plays a role in the loss of mitochondrial membrane potential prior to cell death in necrosis. Methylation on this gene has been found in diabetic patients[117,118]. The most strongly downregulated mitochondrial gene was

MFN1, which codes for the mitofusin-1 protein. This protein is expressed on the mitochondrial membrane and is involved in the regulation of mitochondrial fusion. A study showed that type 2 diabetes was related to mitochondrial network fragmentation in myocardium and a large decrease in MFN1 expression[119]. Interestingly, mice with MFN1 knockout displayed a higher preference for lipid use as energy substrate[120]. Among five downregulated genes, three genes were downregulated in previous studies, including PDP2, NGRN, and MFN1[119,121].

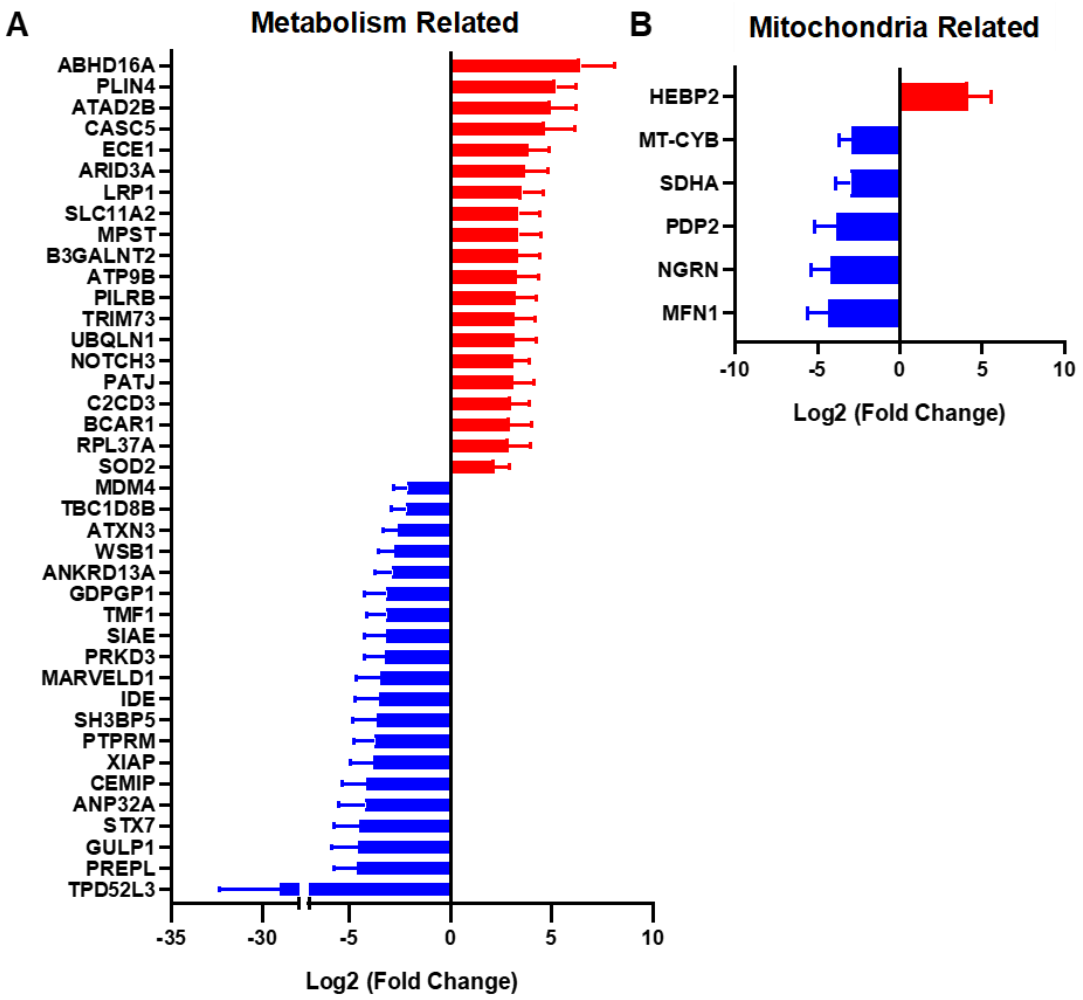

Figure 3.4 Metabolism genes and mitochondrial genes are significantly upregulated or downregulated in patients with diabetes. (A) Alterations in metabolism-related genes when comparing patients with T2D and non-diabetic patients. (B) Mitochondrial genes that were significantly altered between the patient groups.

3.3.4 Alterations in Pseudogene, lncRNA, RNA Gene, RNA Processing Genes

Pseudogene is a DNA sequence that is an imperfect copy of a functional gene. Pseudogenes were once thought to be junk DNA, but it has since been recognized that some pseudogenes play essential roles in gene regulation of their parent genes[122]. We found two genes upregulated and nine genes downregulated in the pseudogene category (**Figure 3.5 A**). Putative Cyclin-Y-Like Protein 3 is a pseudogene for cyclin-dependent protein serine/threonine kinase. The function of CCNYL3 is not yet fully understood, but overall it is expected to relate to the regulation of cell proliferation. Double Homeobox 4 Like 9 (DUX4L9), also known as DUX4c, is a pseudogene that has similarity to DUX4 transcription factor that was suggested to be a risk gene to cause facioscapulohumeral muscular dystrophy[123]. This gene rapidly downregulates the transcription factor Myogenic Differentiation 1 (MyoD), resulting in impaired myogenic differentiation and muscle regeneration[124]. Low expression of DUX4 impairs myogenesis through a reduction in myogenic gene expression[125]. DUX4L9 expression impairs myofibrillogenesis and potentially has a role in controlling muscle cell differentiation through association with type III intermediate filament protein desmin[126,127].

Recent studies showed that deregulation of lncRNAs is associated with various diseases such as cancer, Alzheimer's disease, and heart disease[128-132]. We found five upregulated genes and six downregulated genes under the long non-coding RNA (lncRNA) category (**Figure 3.5 B**). Within the lncRNA category, CPS1-IT1 seems to be involved in type 2 diabetes. In the previous study, an impairment in neovascularization results from a high glucose induced defect in transactivation of hypoxia-inducible factor-1α (HIF-1α), and HIF-1α is controlled by CPS-IT1[133,134]. The lncRNA LINC01118 was the most upregulated lncRNA in patients with type 2 diabetes in our study. LINC01118 has been associated with chemoresistance and increased cell migration in cancer[135]. The lncRNA LINC01060 was strongly decreased in our study in patients with type 2 diabetes. This lncRNA has been associated with poor prognosis in pancreatic cancer and inhibited pancreatic cancer proliferation and invasion[136]. Thus could also potentially contribute to poor wound healing prognosis.

In the RNA gene category, we found eight downregulated genes (**Figure 3.5 C**). One of the downregulated RNA genes was Calcium-Activated Neutral Proteinase 10 Antisense 1 (CAPN10-AS1). In a previous study, CAPN10 expression was elevated in a pancreatic islet from type 2 diabetes[137]. It is generally known that antisense interferes the transcription of paired RNA

(sense RNA)[138]. We also found the RNA gene ERICH3-AS1 to be highly downregulated in patients with type 2 diabetes. Consistent with our findings, this gene is downregulated in a sciatic nerve in diabetic mice[139]. Little is known about the function of ERICH3, however it is highly expressed in airway cilia and has been associated with major depressive disorder[140,141].

In the RNA processing category **(Figure 3.5 D)**, we found a downregulation of Zinc Finger Protein 1 (ZPR1). The ZPR1 binds to the promoter of peroxisome proliferator-activated receptor gamma (PPARG) proteins 1 and 2, which play a key role in insulin sensitivity and obesity[142,143]. A previous study reported the evidence linking the genetic susceptibility of common variants in *ZPR1* to type 2 diabetes with the levels of fasting plasma glucose and blood hemoglobin A1c, suggesting *ZPR1* might be involved in abnormal glucose metabolism[144]. However, the expression tendency seems to be different in skin tissue and others. ZPR1 mRNA in the brain is upregulated in mice fed a high-fat diet[145], whereas our result showed downregulation in the skin.

Several other notable genes were regulated in the RNA processing category including cysteinyl-tRNA synthetase 2 (CARS2), Heterogeneous Nuclear Ribonucleoprotein R (HNRNPR), and DEAH-box helicase 37 (DHX37). CARS2 plays a critical role in protein biosynthesis by charging tRNAs with their cognate amino acids. In a previous study, CARS2 was upregulated in a muscle tissue of patients with type 2 diabetes[146]. Heterogeneous Nuclear Ribonucleoproteins are RNA binding proteins and associated with pre-mRNAs in the nucleus. HNRNPR appears to influence pre-mRNA processing and other aspects of mRNA metabolism and transport. HNRNPR was downregulated in the islet-specific CD4 + T cells in type 1 diabetes -susceptible NOD mice[147]. DHX37 encodes a DEAD box protein. DEAD box proteins are characterized by the conserved motif Asp-Glu-Ala-Asp (DEAD), and implicated in alteration of RNA secondary structure such as translation initiation, nuclear and mitochondrial splicing, and ribosome and spliceosome assembly. In the previous study, DHX37 was downregulated in rat corneal epithelia in type 1 diabetes[83,148]. Our result also showed a significant downregulation of DHX37, implying the malfunction in constructing RNA secondary structures may occur in the diabetic skin or corneal epithelia.

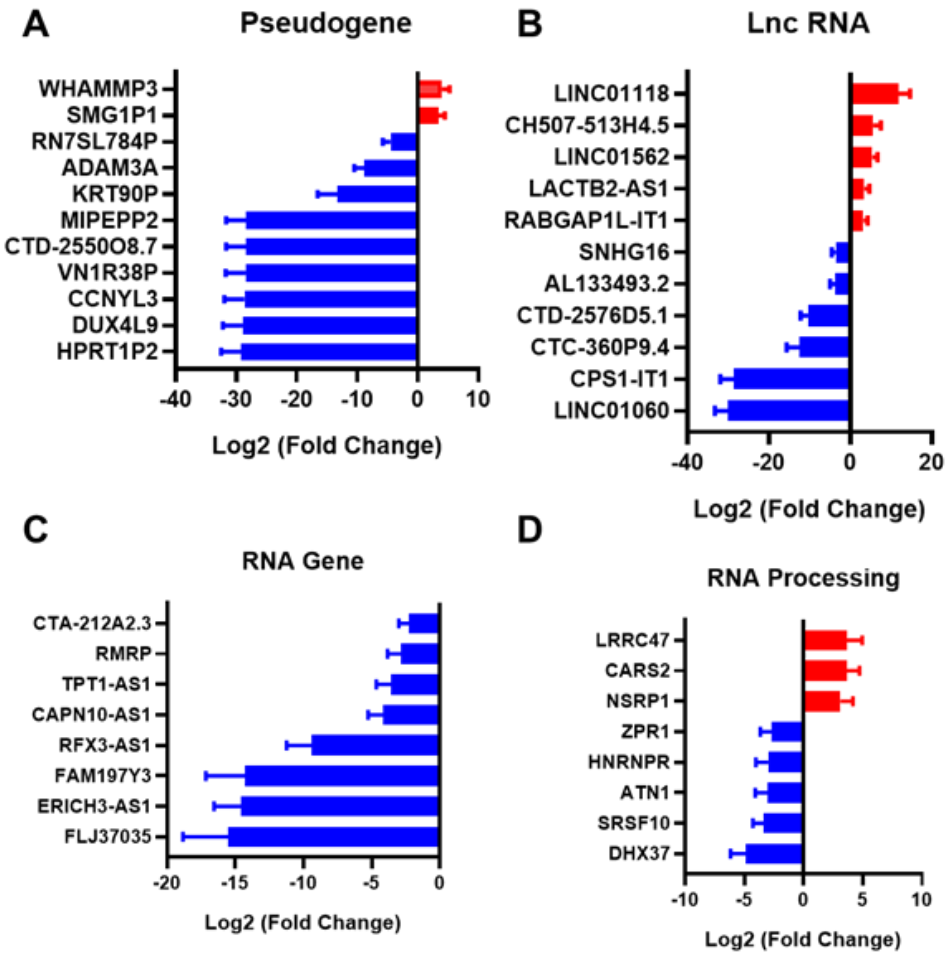

Figure 3.5 Pseudogene, lncRNA, RNA gene, and RNA processing genes are significantly upregulated or downregulated in patients with diabetes. (A) Pseudogenes that were altered inin skin from patients with type 2 diabetes. (B) Long non-coding RNAs (lncRNAs) that were altered in the skin of patients with type 2 diabetes (C) RNA genes with significant regulation in comparing the two patient groups. (D) Genes involved in RNA processing that were significantly changed between diabetic and non-diabetic patient groups.

3.3.5 *CYTOSKELETON, MEMBRANE, AND ADHESION RELATED GENES*

Elevated glucose levels can alter the mRNA and protein expression of contractile smooth muscle markers[149]. **Figure 3.6 A** shows significantly up and downregulated cytoskeleton related genes in type 2 diabetic skin. We found β-actin (ACTB) to be significantly upregulated in the skin of type 2 diabetic patients. We also found increases in the Myosin-IF (MYO1F) gene. MYO1F exacerbates atherogenesis and is reported to be a biomarker candidate for patients with obstructive coronary artery disease or advanced atherosclerosis[150]. Among downregulated genes, Tropomyosin (TPM3) was downregulated ten-fold in the type 2 diabetic test group. This gene is translated into α-tropomyosin, which controls contraction in type I skeletal muscle fibers. Consistent with our findings, a previous study showed the downregulation of TPM3 in rats with alloxan-induced diabetes[151].

We found 12 genes in this category that were significantly altered in the skin of diabetic patients in comparison to control patients **(Figure 3.6 B)**. Cell membrane lipid composition can alter the effectiveness of glucose transporters and has been implicated in the microvascular pathophysiology in diabetes[152]. The most upregulated gene in our study was the huntingtin interacting protein 1 related protein (HIP1R). This protein serves an important role in clathrin mediated endocytosis[153]. A recent study revealed its function in β-cell survival and glucose-stimulated insulin secretion, and HIP1R is downregulated in type 1 diabetes[154]. On the other hand, HIP1R expression is increased in the pancreas in type 2 diabetes[155].

We found a significant decrease in plasmolipin (PLLP) in the skin of patients with type 2 diabetes. A recent study showed that Notch signaling is mediated by PLLP and STX7 in epithelial cells: silencing STX7 impairs activation of Notch through PLLP[156,157]. In our study, both of STX7 and PLLP were significantly downregulated in diabetic patient skin. The Notch1 pathway is a key regulator of wound healing[158]. Thus, defects in this pathway may be potential targets for improving healing in diabetes.

Tissue repair or wound healing process requires the regulation of cell adhesion molecules to control proliferation or migration of cells. The most upregulated gene in this category was RPSA, which codes for the Laminin Receptor 1 (**Figure 3.6 C**). This gene is differentially expressed in wound margins at different sites on the body and has a role in adhesion and migration in the intestinal epithelia[159,160]. We also observed increases in the genes for integrin α3 and α9, as well as a decrease in gene expression for integrin αv. Integrin α3β1 is suppressed by

α9β1 during the resolution wound angiogenesis[161]. In one study, integrin α3β1 also inhibited re-epithelialization in wound healing[162]. Another study demonstrated that ITGA3 knockout mice had inhibited wound healing and that integrin α3β1 served as an inhibitor of Smad7 during the wound healing process[163]. Integrin αv is overexpressed in endothelial cells during the formation of new blood vessels and is a key adhesion receptor in many steps of angiogenesis[164]. In addition, αv integrins have a role in wound healing through the regulation of TGF-β and regulation of cell migration[165]. We also found an increase in von Willebrand factor (vWF) gene expression in patients with type 2 diabetes. The protein is involved in platelet adhesion and has a role in vascular inflammation and thrombosis[166]. There have been previous studies showing that high levels of VWF are associated with type 2 diabetes[167-169]. Our study adds to these findings in showing a significant upregulation in skin from diabetic patients.

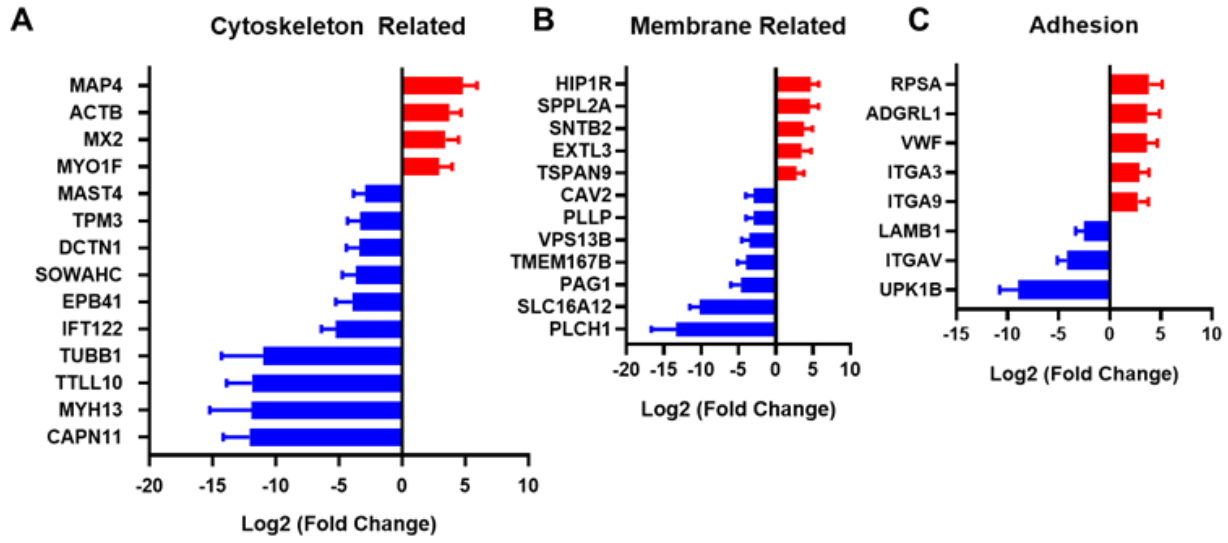

Figure 3.6 Cytoskeleton, membrane and adhesion genes are significantly upregulated or downregulated in patients with diabetes. (A) Cytoskeletal genes altered in the skin in patients with type 2 diabetes. (B) Membrane related genes that were significantly different between diabetic and non-diabetic patients. (C) Cell adhesion related genes that were altered in type 2 diabetes.

3.3.6 *CALCIUM SIGNALING AND INFLAMMATION RELATED GENES*

In the calcium-signaling gene category, we found a large increase in expression of KCNMA1 in patients with type 2 diabetes (**Figure 3.7 A**). This gene encodes the calcium- and voltage-dependent potassium channel KCa1.1. This channel has been implicated in rheumatoid arthritis, the regulation of integrins, and myoblast function[170-172]. We also found decreases in expression for the genes for striatin (STRN) and calmodulin 2 (CALM2). Calmodulin 2 is involved in regulating a large number of proteins through calcium-mediated mechanisms and striatin is a calmodulin binding protein.

Among the significantly regulated genes to inflammation, we found a significant increase in the gene expression NF-κB inhibitor zeta (NFKBIZ) in patients with type 2 diabetes (**Figure 3.7 B**). The protein encoded by this gene inhibits NF-κB, a key transcription factor in inflammation. We also found three significantly downregulated inflammatory genes including a receptor for IL-17 family members (IL17RA), TRAF3 Interacting Protein 2 (TRAF3IP2) and Interleukin 1 Receptor Like 2 (IL1RL2; IL-36 receptor). Interleukin-17A is a proinflammatory cytokine that promotes the recruitment of neutrophils during wound healing. In wound healing, it likely delays wound healing while enhancing an inflammatory response that would promote the removal of microbes[173]. TRAF3IP2 alters keratinocyte differentiation in the skin and inhibits response to IL-17[174]. Both IL-17A and tumor necrosis factor-α (TNF-α) are induced by IL-36 cytokines in keratinocytes[175]. The cytokine IL-36γ promotes wound closure through a mechanism involving toll-like receptor 3 (TLR3), TIR-domain-containing adapter-inducing IFN-β (TRIF) and the transcription factor SLUG[176]. Thus, our findings suggest that IL17/IL36 mediated inflammatory pathways may be altered in diabetic skin. Indeed, the IL17/IL36 signaling axis is associated with psoriasis and targeted therapies are showing success. Psoriatic skin has hallmarks to some aspects of the hyperproliferative status of chronic non-healing wounds and comparisons between these established pathways are worthy of further investigation. We have summarized a comparison of our results to others in previous studies in **Table 2**[177-179].

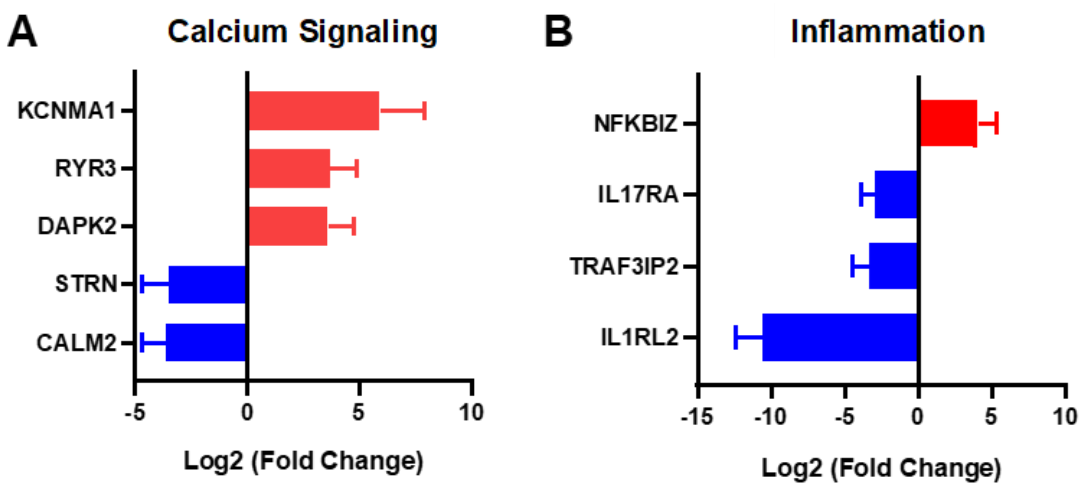

Figure 3.7 Inflammation and calcium signaling related genes that are significantly upregulated or downregulated in patients with diabetes. (A) Calcium signaling related genes that were significantly altered between the patient groups. (B) Inflammation-related genes that were significantly different between the non-diabetic and type 2 diabetic groups.

Table 3.2. Comparison of Study Results with Previous Studies

Gene	This Study	Previous Studies	Model animal
CAMK4	Increase in T2D	Increased phospho-CAMK4	STZ-Induced Diabetes in Rat
ZNF224	Increase in T2D	Reduced CIC activity	STZ-Induced Diabetes in Rat
ABHD16A	Increase in T2D	Genetic predisposition to coronary artery aneurysm and Kawasaki disease	Human
LRP1	Increase in T2D	Upregulation in the epicardial fat tissue	T2D in Human
NOTCH3	Increase in T2D	NOTCH3 polymorphism is a risk factor for ischemic disease and diabetes	Ischemic Stroke in Human
SOD2	Increase in T2D	SOD2 polymorphism is assocated with T2D	T2D in Human
HEBP2	Increase in T2D	Methylation on this gene is found in T2D	T2D in Human
CARS2	Increase in T2D	Upregulated in muscle tissue	T2D in Human
MYO1F	Increase in T2D	MYO1F exaerbates atherogenesis	Coronary Artery Disease in Humar
HIP1R	Increase in T2D	Downregulated in β-cell in T1D, but upregulated in the pancreas in T2D	T1D/T2D in Human
vWF	Decrease in T2D	High levels of vWF	T2D in Human
NKX2-1	Decrease in T2D	Mutation in NKX2-1 links to reduced mitochondrial activity	Human
MFN1	Decrease in T2D	Downregulated	T2D in Human
PDP2	Decrease in T2D	Decreased protein expression	T2D in Human
NGRN	Decrease in T2D	Downregulated	T2D in Human
CAPN10	Decrease in T2D	Upregulated in pancreatic islet	T2D in Human
ERICH3-AS1	Decrease in T2D	Downregulated in a sciatic nerve	Diabetic Mice
ZPR1	Decrease in T2D	Upregulated in brain	High-Fat Diet Fed Mice
HNRNPR	Decrease in T2D	Downregulated in the islet-specific CD4 + T cells	T1D-Susceptible NOD Mice
DHX37	Decrease in T2D	Downregulated in corneal epithelia	T1D Rat
TPM3	Decrease in T2D	Downregulated	Alloxan-Induced Diabetes in Rat

3.4 CONCLUSIONS.

We examined the gene expression in the skin from patients with type 2 diabetes and non-diabetic patients. Among the genes regulated, there were many that had been identified as being modulated in diabetic animals and this study serves to provide confirmation that these changes also occur in the skin of human patients. This information could be useful in identifying the causal factors and potential therapeutic targets for the prevention and treatment of diabetic related diseases.

Chapter 4: Transmembrane Stem Cell Factor Protein Therapy for Therapeutic Angiogenesis

4.1 INTRODUCTION

Diabetes mellitus affects approximately 350 million people worldwide, leading to the death of about 4.6 million people per year[2,29]. As a complication of diabetes, 30 to 40 percent of patients age 50 and older develop peripheral artery disease (PAD)[3]. Severe PAD increases the risk of non-healing ulcers, pain from intermittent claudication and limb amputation. The current standard of care for PAD include surgical revascularization with bypass grafting or percutaneous interventions such as angioplasty, stenting and atherectomy. However, these interventions cannot be performed in a significant portion of patients, and many do not respond to these therapies[4]. An alternative approach for treating ischemic disease is to stimulate the body to create new vasculature to restore blood flow through its own regenerative processes. Several approaches have been attempted: the delivery of progenitor cells[5,6], viral vectors to express growth factor/angiogenic transcription factor genes[7-10] or through the delivery of growth factors[11-13]. While cell therapy is labor-intensive and gene therapy has safety issues, protein therapeutics such as growth factor treatments have potential advantages from delivery and safety perspectives[6].

One potential therapeutic protein for treating ischemic disease is stem cell factor (SCF), which signals through the receptor (c-Kit/CD117)[14]. The endogenous SCF isoform (SCF248) is initially a transmembrane protein that contains an enzyme cleavable domain allowing its release as soluble SCF (SCF163)[15]. While a major role of SCF is to maintain hematopoiesis, studies demonstrated that SCF induces angiogenesis, enhances recovery from stroke and improves recovery after myocardial infarction[16-18]. In many studies, SCF has a synergetic effect with G-CSF to enhance angiogenesis and neurogenesis after stroke in animal studies[17,19,20]. There are also several clinical trials demonstrating a higher amount of peripheral blood progenitor cell mobilization after co-stimulation of SCF and G-CSF (Filgrastim)[21,22]. Though SCF seems to be a potential protein for ischemia treatment, various clinical studies demonstrated that patients who have been given SCF have a pruritic wheal and flare response at the injection[23]. Examination of these injection site reactions by transmission electron microscopy has revealed evidence of extensive, anaphylactic-type degranulation of dermal mast cells[23]. Moreover, Johnsen et al. reported in phase II clinical study that 13% of the patients who received the combination therapy

of SCF and G-CSF suffered from allergic, febrile and rigor episodes, and 3% of the patients experienced hepatic failure[24]. Based on these and other findings, researchers concluded that phase III trials of treatments using soluble SCF were very unlikely[24].

The shorter isoform of SCF (SCF220) lacking exon 6, which encodes the cleavable domain and remains as a transmembrane protein, is known as transmembrane stem cell factor (tmSCF). Transmembrane SCF is found in the stromal cells of the bone marrow where it functions to support the proliferation and survival of progenitor cells[25]. The soluble and transmembrane forms of SCF differ in their properties in terms of degree of c-Kit activation, cellular response and adhesion between hematopoietic stem cells and the ECM[14,26]. Several reports demonstrated the advanced properties of tmSCF in comparison to SCF[26]. For example, previous reports showed that tmSCF causes prolonged activation of the c-Kit receptor than the soluble isoform[27] and induces long term proliferation of $CD34^+$ hematopoietic cells[28].

While soluble SCF has been studied extensively for its therapeutic properties, tmSCF has not been examined as a potential protein therapy. In this chapter, we explored the potential of tmSCF protein therapeutics. To further enhance the therapeutic efficiency, we embedded tmSCF in lipid nanocarriers: liposomes and nanodiscs. Liposomes are frequently used in drug or protein delivery due to its amphiphilic character. Lipid bilayer is hydrophobic thus enabling it to incorporate hydrophobic molecules such as membrane proteins between lipid bilayers. Inside of the lipid bilayer is filled with aqueous solution, allowing hydrophilic chemicals to be incorporated. In this study, we inserted tmSCF protein between lipid bilayers of liposomes, aiming to improve the therapeutic efficiency. Nanodiscs are also made by lipid bilayer, shaping in disc-like structure, allowing an access of receptor protein from both directions (front and back). Both formulations of lipid nanocarriers will enhance the therapeutic efficiency of tmSCF protein thanks to the lipid bilayers that resembles cell membrane, allowing membrane protein to work in its native-like environment.

4.2 Materials and Methods

4.2.1 Preparation of tmSCF proteoliposomes

For the production of recombinant tmSCF, HEK-293Ta cells were transduced with lentiviral vector with constitutive expression of 6X His tagged tmSCF. Viruses were produced in

HEK-293Ta cells using human lentiviral packaging system according to the manufacturer's instructions (Genecopoeia). Puromycin was used to select only for transduced cells. The cells were lysed in a buffer containing 20mM Tris (pH 8.0), 150mM NaCl, 1% Triton X-100, 2mM sodium orthovanadate, 2mM PMSF, 50mM NaF, and protease inhibitors (Roche) at room temperature. Transmembrane stem cell factor (tmSCF) was then isolated using cobalt chelating column (Chelating column; GE Healthcare), and the buffer was exchanged in 1X PBS. After concentrating the protein solution with Centriprep concentrators (Millipore), the final working concentration of protein was found to be 100 μg/ml using a BCA Protein Assay kit (Thermo Scientific). Purity of the protein was confirmed by SDS-PAGE followed silver staining of the gel. To prepare liposomes, stock solutions (10 mg mL^{-1}) of 1,2-dioleoyl-sn-glycero-3-phosphocholine, 1,2-dioleoyl-sn-glycero-3-phosphoethanolamine, cholesterol, and sphingomyelin were prepared in chloroform. The lipids were mixed in the volumetric ratio 2:1:1:1 in a round bottom flask and the chloroform was removed on rotary evaporator attached to a vacuum pump. Liposomes were resuspended in 4-(2-hydroxyethyl)-1-piperazineethanesulfonic acid buffer by vortexing, sonication, and freeze thawing. Extruding device (Avanti Polar Lipids) with polycarbonate membranes (400 nm) was used to homogenize the liposome population. A mild detergent, n-octyl-β-D-glucopyranoside (1% w/v) was added to both the liposome and the recombinant tmSCF. The protein and liposomes were then combined and the detergent was removed by timed serial dilution (every 30 min, 10% dilution up to 2h), dialysis, and treatment with Biobeads (Biorad). The final tmSCF concentration in tmSCFPLs was 55 μg/ml.

4.2.2. PREPARATION OF TMSCF NANODISCS

As a lipid source, 1-palmitoyl-2-oleoyl-sn-glycero-3-phosphocholine (POPC) was used in this study. POPC was stored in chloroform, so we first removed chloroform by rotary evaporator. After that, POPC was resuspended in sodium cholate (100 mM). MSP protein was then added to phospholipid solution, and the detergent concentration was adjusted between 14-40 mM. This construct was incubated for 15 minutes at 4°C. To solubilize the membrane protein, tmSCF was incubated in the n-octyl-β-D-glucopyranoside (1% w/v) for 15 minutes at 4°C. After 15 minutes incubation of lipid construct and tmSCF protein, these were combined and incubated for 1 hour at 4°C. Detergent concentration during this incubation was adjusted to 20 mM with sodium

cholate. Finally, detergent was removed by dialysis and biobeads. The final tmSCF concentration in tmSCFNDs was 77 μg/ml.

4.2.3. LIPOSOME CHARACTERIZATION

The size and dispersion of the proteoliposomes were characterized by dynamic light scattering (Malvern Zetasizer Nano ZS). Calibration was performed using 54 nm polystyrene particles. For TEM imaging of proteoliposomes, carbon support grids (300 mesh Cu; EM Sciences) were treated with glow discharge at 50 mA for two minutes (Emitech K100X; Quorum Technologies). The samples were then applied to the grids and the excess liquid removed with a filter paper. 2% uranyl acetate solution was used to stain glids, and images were taken using an FEI Tecnai Transmission Electron Microscope (TEM). For cryo-electron microscopy imaging, the liposomes were plunge-frozen in liquid ethane on carbon holey film grids (R2X2 Quantifoil; Micro Tools GmbH, Jena, Germany). The grids were transferred to a cryo-specimen holder (Gatan 626) under liquid nitrogen and put in a microscope (JEOL 2100 LaB6, 200 keV), Grids were maintained at close to liquid nitrogen temperature during EM session (-172 to -180^{o}C).

4.2.4. TMSCF PROTEIN RELEASE KINETICS FROM ALGINATE BEADS

Purified tmSCF protein was first labeled with Alexa Fluor™ 488 Microscale Protein Labeling Kit (Thermo Scientific), then tmSCFPLs and tmSCFNDs were fabricated using this labeled protein. Equal volume of treatments and 4% sodium alginate solution were mixed, then the solution was extruded from a 30G needle into a 1.1% calcium chloride solution to crosslink for 1 hour. Protein amount was calibrated based on the protein fluorescent signal. Fabricated alginate beads were incubated in the 5 ml of 1% BSAPBS in plastic scintillation vial and incubated at 37^{o}C. 100 μl of released protein was collected each time point and fluorescent intensity was measured by plate reader. The same amount of 1% BSAPBS was replaced each time point to compensate.

4.2.5. TUBE FORMATION ASSAY

Cells were stained with cell tracker green, cultured and starved 24h prior to the experiment. Growth factor reduced Matrigel (Corning) were coated on the 96 well plate, and endothelial cells were seeded on top of it with seeding density of 4×10^{4}/well. Treatments were

then added and cells incubated for 6 or 10 hours. Images were taken using a high throughput imaging system (Cytation 5 Cell Imaging Multi-Mode Reader; Biotek) at each time point and the number of loops was quantified using Photoshop (Adobe).

4.2.6. CELL PROLIFERATION ASSAY

Endothelial cells were passaged into a 96-well plate and cultured in low serum media with 2% FBS for 24h. Treatments were then added to cells. After 24h, BrdU was added to the cells and proliferation was assessed 12h later using a colorimetric BrdU assay (Cell Signaling, Inc.).

4.2.7. CELL MIGRATION ASSAY

Endothelial cells were stained with cell tracker green, and passaged to confluence in 96-well migration assay kit (Platypus). Treatments were added for 24h before assay starts. A cell stopper was then removed to allow cells to migrate. Migration area and green fluorescent intensity were measured after 16 and 24 hours.

4.2.8. HIND LIMB ISCHEMIA MODEL

Prior to surgery, alginate beads containing the treatments were fabricated by mixing equal volume of 4% sodium alginate solution and treatments. Beads were created through extruding the alginate solution through a 30G needle into a 1.1% calcium chloride solution to crosslink for 1 hour. Wild-type mice and ob/ob mice (n = 12-13 for WT, n = 11-12 for ob/ob; Jackson Labs) were used in the studies. To perform the hind limb ischemia studies, mice were anesthetized with 2-3% isoflurane gas and a longitudinal incision was made in the inguinal region of the right thigh. The femoral artery was separated from the femoral vein and nerve, and then double ligated with 6-0 silk sutures at two locations and the artery severed at each ligation. Treatments were then implanted in the pocket created by the surgery and the wound was closed with resorbable sutures (4-0 Vicryl; Ethicon, Inc.).

4.2.9. IMMUNOHISTOCHEMISTRY ON HUMAN SKIN

Human skin samples were obtained from the Glasgow Caledonian University Skin Research Tissue Bank, Glasgow UK. The tissue bank has NHS research ethics approval to

supply human skin for research (REC REF: 16/ES/0069). All methods were carried out in accordance with relevant guidelines and regulations. All experimental protocols were approved by the NHS East of Scotland Research Ethics Service. Informed consent was obtained from all subjects (no patients were under 18 years of age). Samples were formalin fixed and embedded in paraffin following standard procedures prior to sectioning. The sections were then deparaffinized in xylene and treated for 3 hours with antigen retrieval solution (Dako) at 80°C. The sections were cooled to room temperature and blocked with 20% fetal bovine serum for 45 minutes and then immunostained overnight with 1:100 dilution of primary antibody to PECAM-1 (Cell Signaling), SCF (Abcam), FSP1 (Abcam), c-Kit (Abcam), and mast cell tryptase (Abcam). Secondary staining was performed with secondary antibodies conjugates with Alexa Fluor 488 or 594 dye (Thermo Scientific). Following staining, the samples were imaged using confocal microscopy. For quantification, double-positive areas were quantified using Photoshop and ImageJ.

4.2.10 IMMUNOHISTOCHEMISTRY ON MICE

The thigh and calf muscles were formalin fixed and embedded in paraffin following standard procedures prior to sectioning. The sections were deparaffinized in xylene and treated for 3 hours with antigen retrieval solution (Dako) at 80°C. The sections were cooled to room temperature and blocked with 20% fetal bovine serum for 45 minutes and then immunostained overnight with 1:100 dilution of primary antibody to PECAM-1 (Cell Signaling), αSMA (Abcam), CD34 (Santa Cruz), and VE-cadherin (Abcam). Secondary staining was performed with secondary antibodies conjugates with Alexa Fluor 488 or 594 dye (Thermo Scientific). Following staining, the samples were imaged using confocal microscopy. The number of small blood vessels was counted from the PECAM-1 positive area, and the number of matured blood vessels was counted from the αSMA positive area. For the quantification of the double-positive areas of CD34 and VE-cadherin were quantified using Photoshop and ImageJ.

4.2.11 EPC COLONY FORMATION ASSAY

Bone marrow cells (BMCs) were harvested, and Bone marrow mononuclear cells (BMMNCs) were then separated by using Ficoll density centrifugation. Semisolid culture medium was prepared by mixing methylcellulose (MethoCult™ SF M3236; Stem Cell

Technologies), 15% fetal bovine serum, 50 ng/ml murine vascular endothelial growth factor, 50 ng/ml murine basic fibroblast growth factor, 50 ng/ml murine insulin like growth factor-1, 20 ng/ml murine interleukin- 3, 50 ng/ml murine epidermal growth factor, and 100 ng/ml stem cell factor in IMDM. SCF is replaced with the same concentration of tmSCF, tmSCFPL, and tmSCFND respectively for each treatment group. Both of the BMCs and BMMCs are adjusted to 7×10^5 cells / ml, then resuspended in the semisolid culture medium. Cell medium is added to 6 well cell culture plates and incubated for 7 days. The number of small and large colonies was counted by two investigators who were blinded to the experimental conditions.

4.2.12 BONE MARROW CELL INDUCTION TO $CD34^-CD133^+CD146^+$EPCS

BMCs were harvested freshly for the experiment and cultured in DMEM high glucose media with 10% FBS. 100 ng/ml of SCF, tmSCF, tmSCFPLs, tmSCFNDs were added to the BMCs media, and cells were incubated for 30 minutes. Treatment was stopped by placing the cell plate on ice. Then cells are stained for CD34-Alexa647 (BD Biosciences), CD133-PE (BioLegend) and CD146-Alexa488 (BD Biosciences). $CD34^-CD133^+CD146^+$ cells are quantified by FlowJo software.

4.2.13 EPCS INDUCTION TO PERIPHERAL BLOOD

To measure the ability of treatments to induce EPCs to peripheral blood, 240μg/kg of SCF, tmSCF, tmSCFPLs, and tmSCFNDs were injected subcutaneously for consecutive 4 days. At the end of day 4, peripheral blood was collected for EPC marker analysis. As EPCs markers, flk1, CD146, CD34, and CD133 were used for flow cytometry analysis.

4.2.14 EVANS BLUE EXTRAVASATION ASSAY

Male C57BL/6J wild-type mice were anesthetized with 2 % isoflurane and initial ear thickness was measured using Mitsutoyo Micrometer (Uline). 250 mL sterile-filtered 1% Evans blue (Sigma) in PBS was injected into the retro-orbital vein and allowed to recover. After 15 minutes later, mice were anesthetized again and intradermally injected into the ear pinnae with 25 mL of PBS alone (into the left ear pinna) or containing 50 mg/mL SCF, tmSCF, tmSCFPLs, or tmSCFNDs (into the right ear pinna) using a 1 mL syringe equipped with a 30 G x 1/2 needle. Two and three hours after injections, mice were anesthetized again, and ear pinnae thickness was

measured and photographs were taken. Three hours after injections, mice were euthanized, ear pinnae were harvested. Ear pinnae was incubated in 300 mL dimethyl sulfoxide (DMSO) in a 48-well tissue culture plate for 20 hours on a shaker at room temperature. Evans blue containing supernatant was collected, transferred into 96-well flat-bottom plate and absorbance at 620 nm wavelength was measured using a plate reader.

4.2.15 STATISTICAL ANALYSIS

All results are shown as mean ± standard error of the mean. Comparisons between only two groups were performed using a two-tailed Student's t-test. Differences were considered significant at $p<0.05$. Multiple comparisons between groups were analyzed by two-way ANOVA followed by a Tukey post-hoc test. A two-tailed probability value <0.05 was considered statistically significant.

4.3 RESULTS

4.3.1 DIABETIC PATIENTS HAVE REDUCED ENDOTHELIAL STEM CELL FACTOR EXPRESSION

Our group and others have identified mechanisms of therapeutic resistance to growth factors[65,180-183], including the loss of cell surface proteoglycans[65,180,181,184-186] and expression of angiogenesis inhibiting growth factors[182]. Diabetic patients have reduced recruitment of stem cells to ischemic regions, circulating endothelial progenitor cells and endothelial cell function[187,188]. We examined the expression of SCF/tmSCF in skin samples from diabetic and non-diabetic patients to assess differences in these proteins with diabetes. We found a marked reduction of SCF expression in endothelial cells in the skin of type 2 diabetic (T2D) patients (**Figure 4.1 A, B**). Conversely, SCF levels were similar between the groups in skin fibroblasts (**Figure 4.1 C, D**). The expression of c-Kit in endothelial cells was higher in patients with T2D in comparison to non-diabetic patients (**Figure 4.1 E, F**). In addition, we found an increase in c-Kit in mast cells in the skin from diabetic patients (**Figure 4.1 G, H**). These results support that there is a significant alteration in SCF and c-Kit in the skin of diabetic patients that may contribute to altered ischemia recovery.

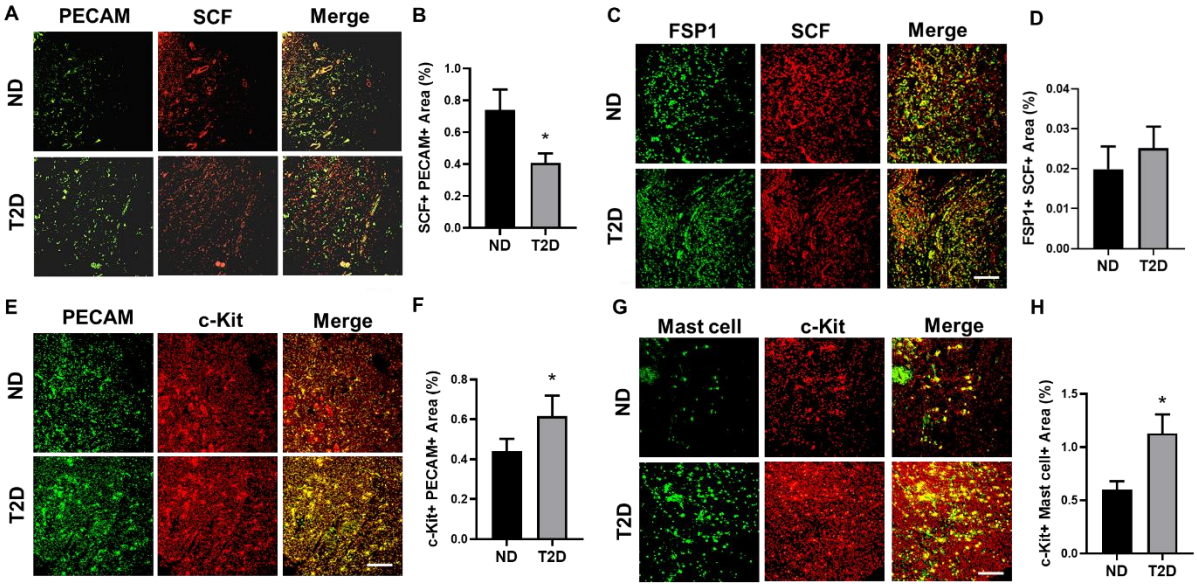

Figure 4.1. SCF is deficient in the skin of patients with diabetes. Immunostaining was conducted on the skin of non-diabetic (ND) and type 2 diabetic patients (T2D). (A) Representative immunostaining images for PECAM and SCF. Scale bar is 300 μm. (B) Quantification of area of double positive area for PECAM and SCF. *p<0.05 versus nondiabetic group (n = 6). (C) Representative immunostaining images of FSP1 and SCF. Scale bar is 300 μm. (D) Quantification result of double positive area of FSP1 and SCF. *p<0.05 versus nondiabetic group (n = 6) (E) Representative immunostaining images for PECAM-1 and c-Kit. Scale bar is 300 μm. (F) Quantification result of double positive area of PECAM and c-Kit. *p<0.05 versus nondiabetic group (n = 6). (G) Representative immunostaining images of mast cell tryptase and c-Kit. Scale bar is 300 μm. (H) Quantification result of double positive area of Mast cell and c-Kit. *p<0.05 versus nondiabetic group (n = 6).

4.3.2 SYNTHESIS OF TRANSMEMBRANE STEM CELL FACTOR PROTEOLIPOSOMES AND NANODISCS

We first created several formulations of recombinant tmSCF to test the effectiveness and differential response in comparison to soluble SCF. Our previous studies had identified that embedding transmembrane proteins in proteoliposomes can alter their therapeutic and signaling properties[65,189]. In addition, recent work has identified methods for creating lipid nanodiscs that are stabilized by membrane scaffolding proteins (MSPs). Thus, we aim to create two types of nanocarriers, tmSCF proteoliposomes and nanodiscs to deliver tmSCF effectively to ischemic sites (**Figure 4.2 A**). Transmembrane stem cell factor (tmSCF) protein was first harvested and purified as described in method section. SDS-PAGE, western blotting and silver staining were performed to analyze the purity of the final concentrated samples. The results of silver staining and western blotting indicate the high purity of tmSCF protein (**Figure 4.2 B, C**). We measured the size of the purified tmSCF and found that there is likely self-association/aggregation that gives it has a much larger size than soluble SCF (**Figure 4.3 A**). We fabricated tmSCF proteoliposomes (tmSCFPLs) using detergent depletion methods as previously described[65,189]. We confirmed the size of the liposomes before and after the addition of tmSCF (**Figure 4.3 B**). The liposomes were around 350 nm in diameter as expected from the extrusion membrane used. After embedding tmSCF, the size increased to 450 nm. We further verified the liposomal structure using TEM and cryo-EM (**Figure 4.3 C**). We also created nanodiscs based on MSP1D1. Purified nandiscs had a size of 20-30 nm and following tmSCF embedding and detergent depletion, the size increased to 150 nm (**Figure 4.4 A**). The structure of the nanodiscs was further verified using TEM and cryo-EM, which revealed disc-like structures (**Figure 4.4 B**).

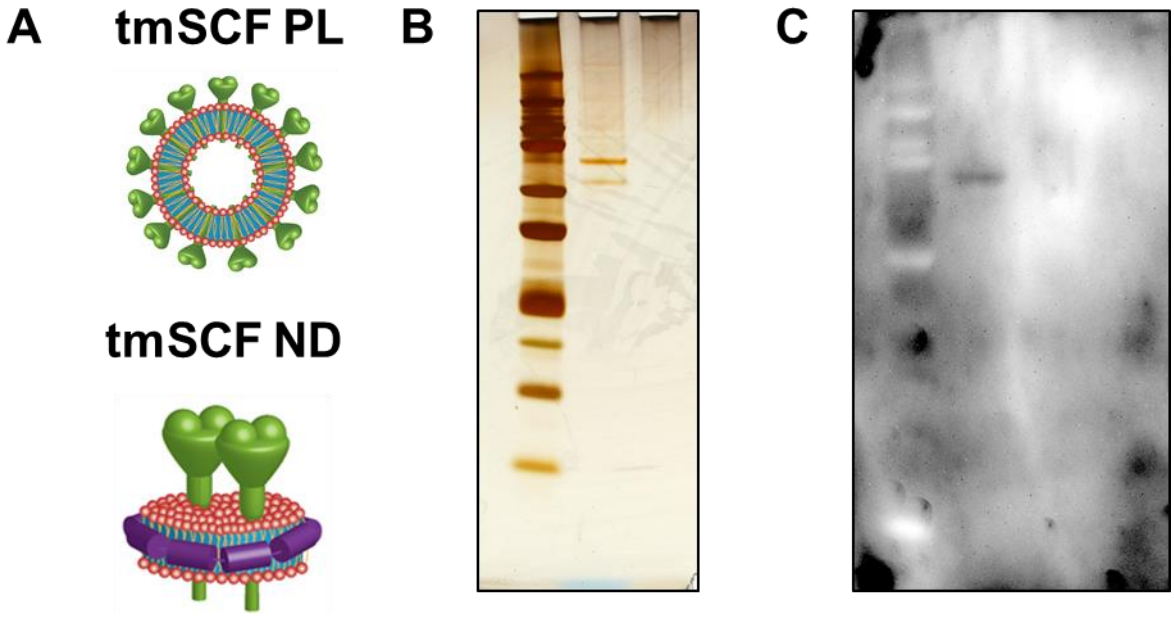

Figure 4.2. Schematic illustration of tmSCFPLs and tmSCFNDs. Purification of tmSCF protein. (A) Schematic illustration of tmSCFPLs and tmSCFNDs. (B) Western Blot result of purified tmSCF protein, showing its corresponding band. (C) Silver staining result of purified tmSCF protein.

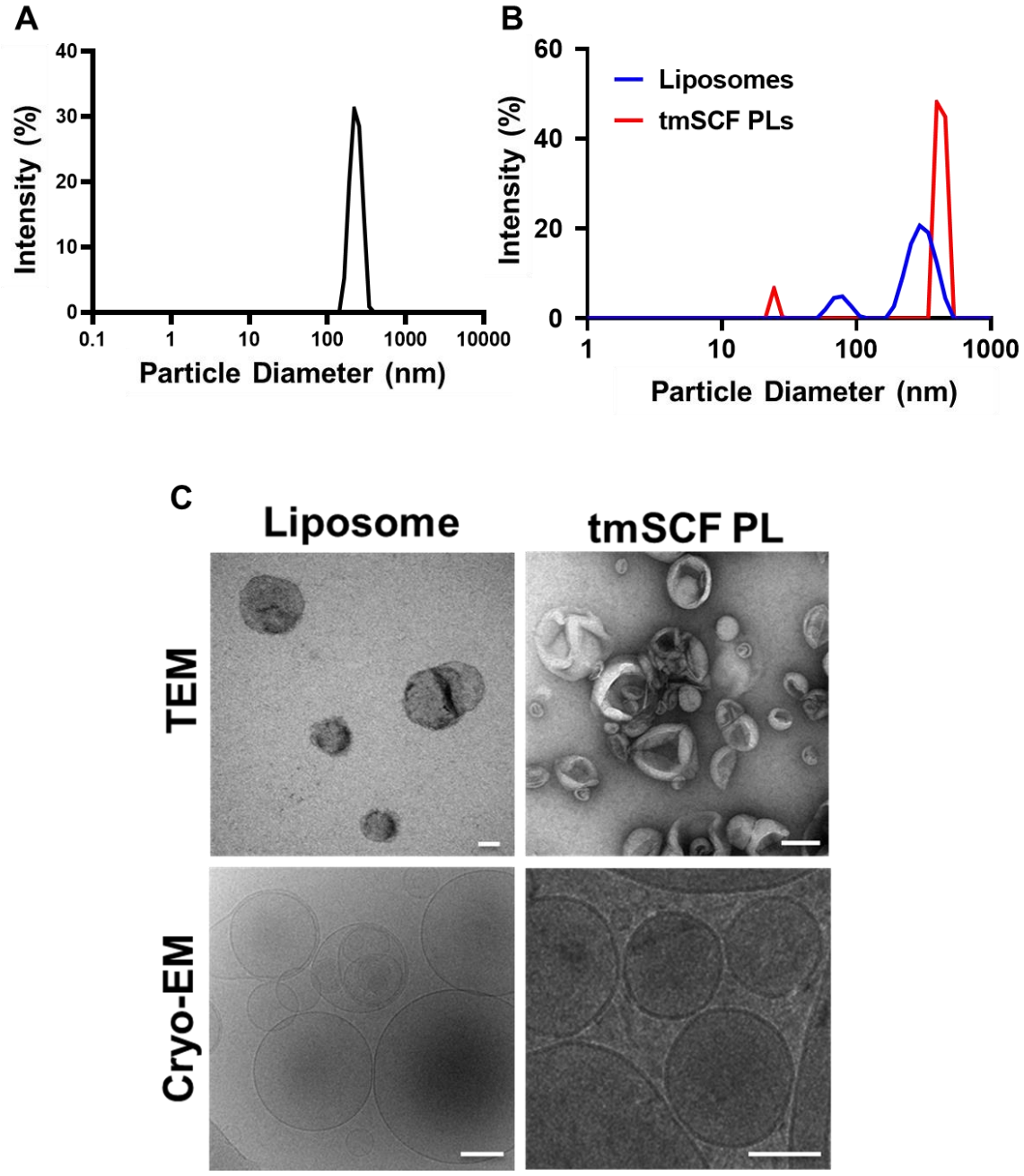

Figure 4.3. Characterization of tmSCFPLs using DLS, TEM, and Cryo-EM. (A) Size distribution for tmSCF measured by dynamic light scattering. The average size of tmSCF was approximately 200 nm. (B) Size distribution for liposomes and proteoliposome with tmSCF measured by dynamic light scattering. The average size of tmSCFPLs were around 450 nm. (C) Representative TEM and cryo-EM images of liposomes and tmSCFPLs. Scale bar is 100 nm.

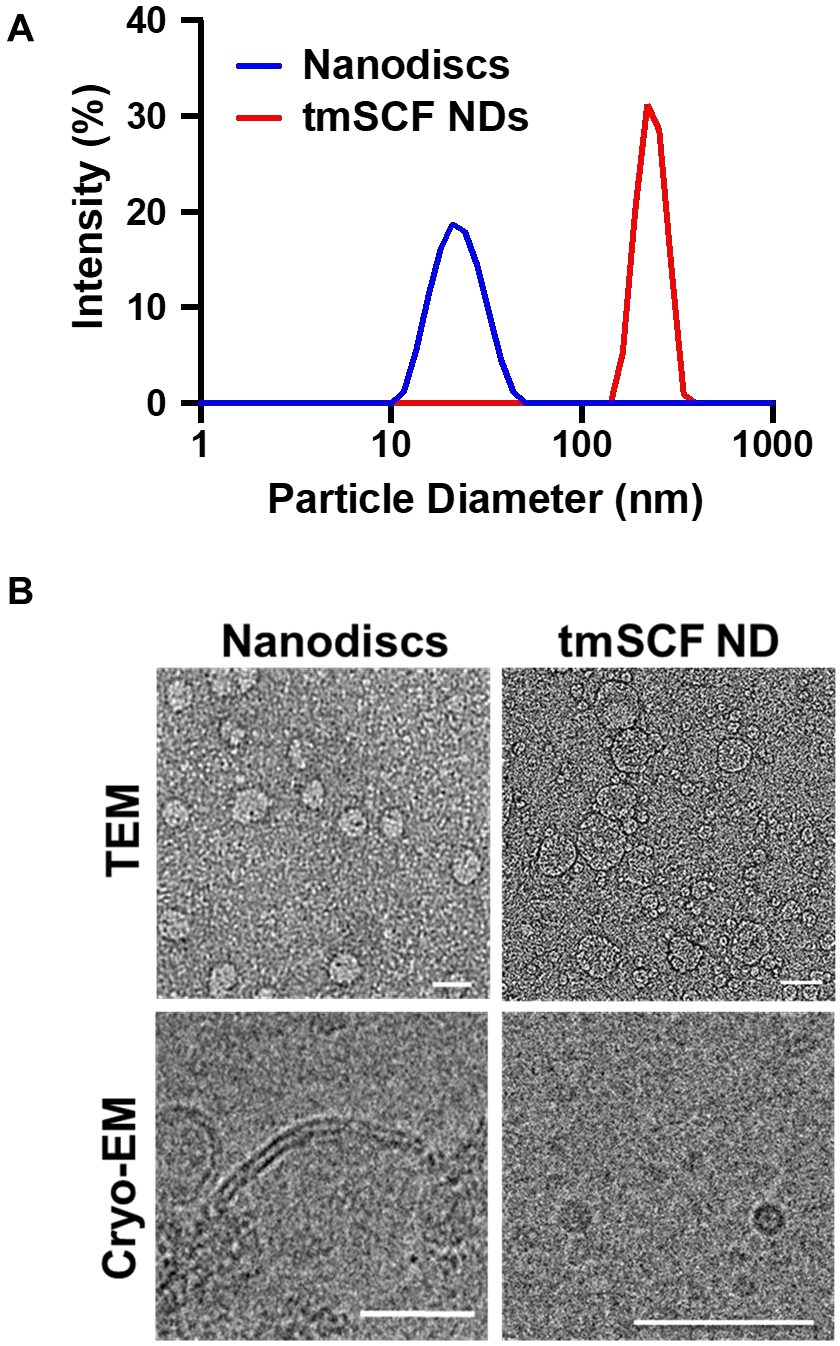

Figure 4.4. Characterization of tmSCFNDs using DLS, TEM, and Cryo-EM. (A) Size distribution for empty nanodics and nanodiscs with tmSCF. The average size of tmSCFNDs was around 150 nm. (B) Representative TEM and cryo-EM images of nanodiscs and tmSCFNDs. Scale bar is 100 nm.

4.3.3 TRANSMEMBRANE STEM CELL FACTOR-BASED TREATMENTS DO NOT INDUCE MAST CELL ACTIVATION

A major limiter in the clinical use of soluble SCF is the activation of mast cells and potential induction of anaphylaxis[190,191]. While SCF is known to induce mast cell activation, it is unclear whether tmSCF shares this property or if nanocarrier encapsulation alters these properties. We injected mice with Evan's blue dye and then locally injected PBS, soluble SCF, tmSCF, tmSCFPL or tmSCFND into the ears of the mice. After three hours, we imaged the ears and extracted the dye with DMSO to quantify the vascular leakage induced by the treatments. We found that SCF induced vascular leakage but tmSCF-based therapies did not induce this response (**Figure 4.5**). It is widely known that mast cell activation triggers histamine release, causing vascular leakage. Thus, our Evan's blue extravasation assay implies that tmSCF-based treatments do not induce mast cell activation.

4.3.4 TRANSMEMBRANE SCF PROTEOLIPOSOMES INDUCED GREATER ANGIOGENIC TUBE FORMATION IN ENDOTHELIAL CELLS THAN TRANSMEMBRANE SCF OR TRANSMEMBRANE SCF NANODISC

To measure the angiogenic activity of tmSCF based therapies, we performed a tube formation assay on endothelial cells. While tmSCF protein itself induced limited tube formation, tmSCFPLs had 16 to 18 fold greater activity (**Figure 4.6 A, B**). In contrast, we did not see a significant induction of tube formation tmSCFND treatment (**Figure 4.6 C, D**). We also tested endothelial cell migration and proliferation but did not see any significant difference for any of our treatments compared to the control (**Figure 4.7**).

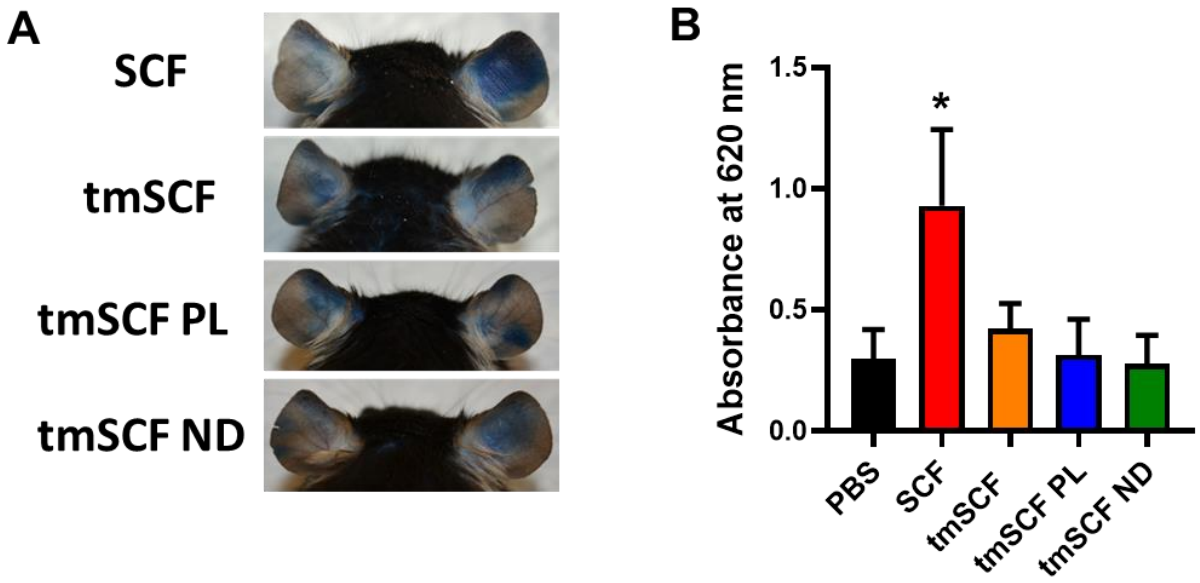

Figure 4.5. Evan's blue dye extravasation assay, showing tmSCF-based therapy had a minimal activation of mast cell. (A) Representative pictures of mice ears after Evan's blue extravasation assay. PBS was injected to the left ear as a control and treatments were injected to the right ear. (B) Quantification result of the absorbance at 620 nm (n = 7-8).

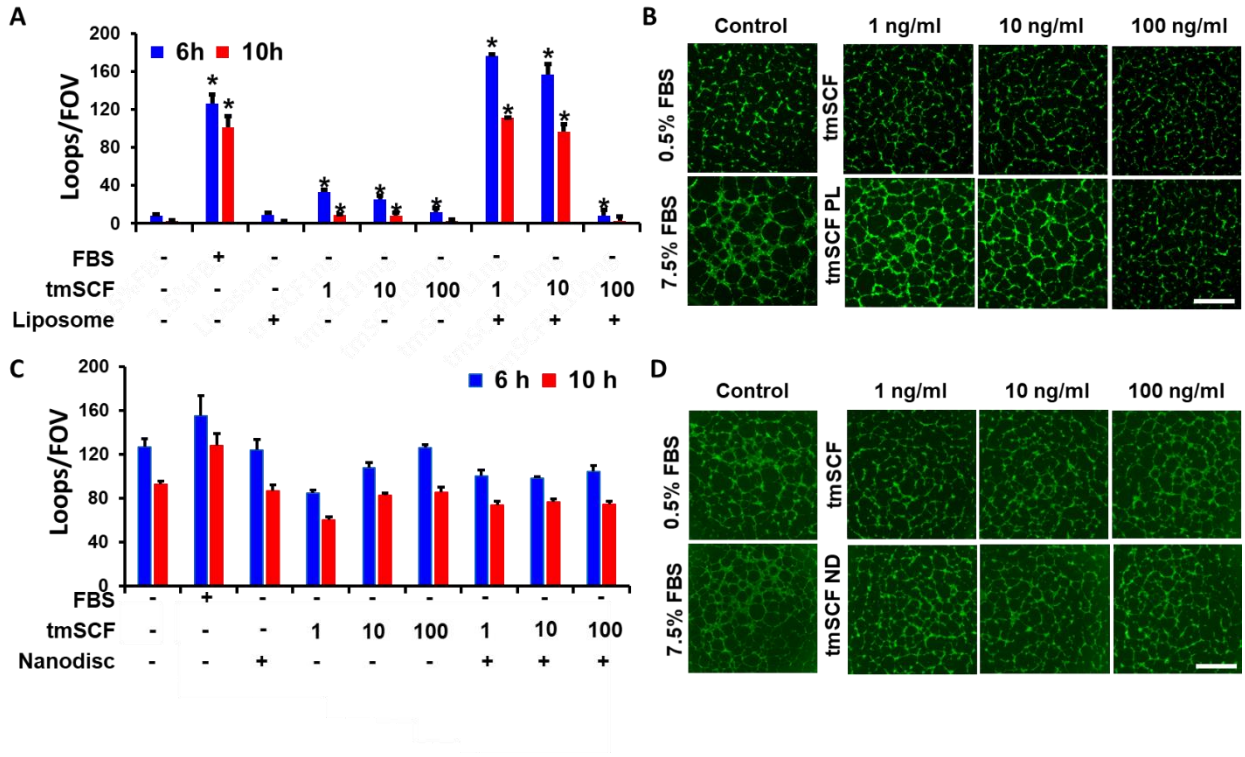

Figure 4.6 Endothelial cell tube formation assay. (A) HUVECs were starved in MCDB131 (Thermo Scientific) supplemented with 0.5% FBS, L-glutamine and Penicillin-Streptomycin 24 hours prior to the experiment and treated with tmSCF or tmSCFPLs. Loop number was counted after 6 and 10 hours of incubation. Significantly higher numbers of loops were formed in 1 ng/ml and 10 ng/ml concentrations of tmSCFPLs groups compared to negative control. (B) Representative images of HUVECs after 6 hours of tmSCF or tmSCFPLs treatment. Scale bar is 300 µm. (C) HUVECs were treated with tmSCF or tmSCFNDs. No significant difference was confirmed in any of the treatment groups. (D) Representative images of HUVECs after 6 hours of tmSCF and tmSCFNDs treatment. Scale bar is 300 µm.

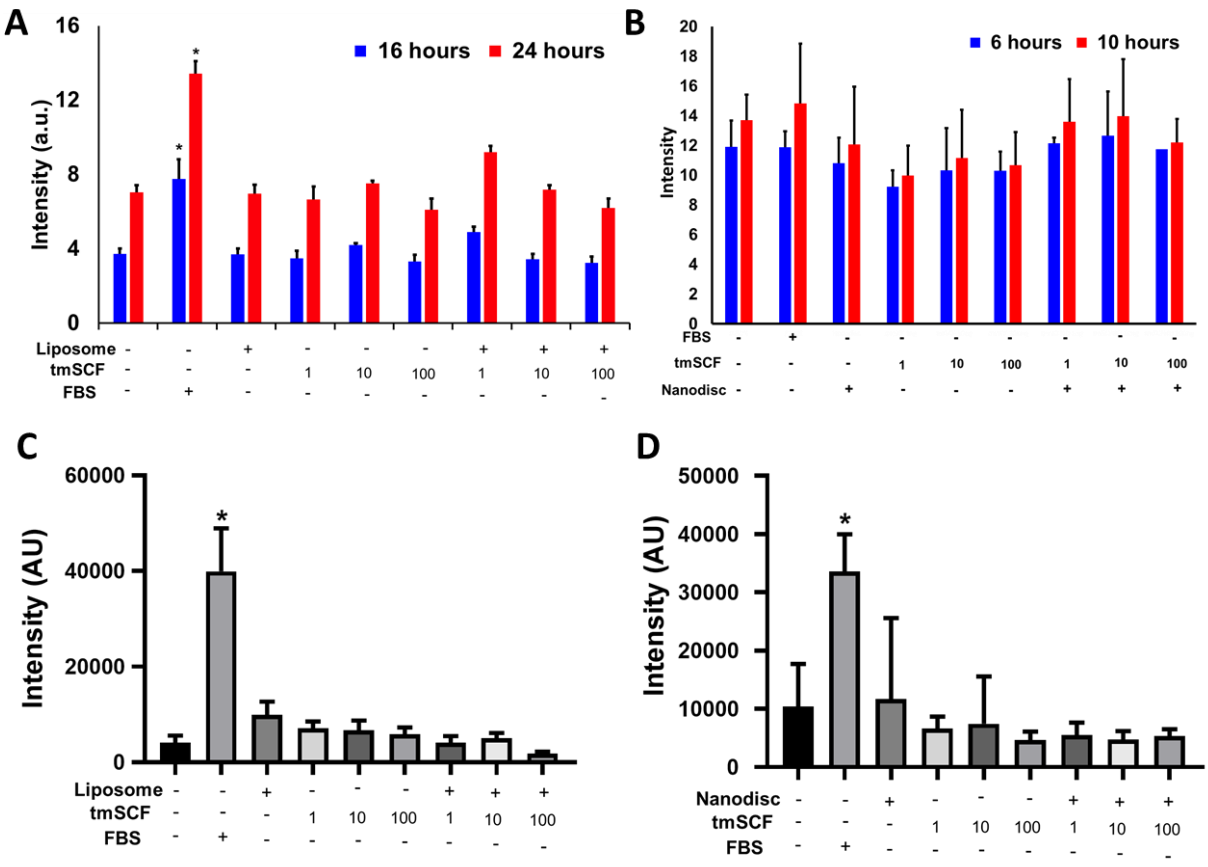

Figure 4.7. Endothelial cell migration and proliferation assay. (A) Quantification results of migration assay, HUVECs were treated by tmSCFPLs. The number of the cells migrated towards the center were counted by green fluorescent signals. (B) Quantification results of migration assay, HUVECs were treated by tmSCFNDs. The number of the cells migrated towards the center were counted by green fluorescent signals. (C) BrdU intensity was measured after HUVECs were treated by tmSCFPLs. (D) BrdU intensity was measured after HUVECs were treated by tmSCFNDs.

4.3.5 TRANSMEMBRANE STEM CELL FACTOR PROTEOLIPOSOMES AND NANODISCS ENHANCE REVASCULARIZATION IN WILD TYPE MICE

To examine whether tmSCF-based treatments could enhance revascularization, we ligated the femoral artery of the mice and implanted alginate beads that encapsulated treatments at the ischemic site. We found significantly higher relative blood flow recovery in tmSCFPLs/NDs groups in comparison to alginate group (**Figure 4.8 A, B**). Immunohistochemical staining for PECAM-1 and α-smooth muscle actin (α-SMA) revealed that there was a significant increase in small blood vessels formed at Day 14 in the tmSCFNDs treatment group while there was increased mature blood vessels in mice treated with tmSCFPLs (**Figure 4.9 A-D**).

4.3.6 TRANSMEMBRANE STEM CELL FACTOR PROTEOLIPOSOMES AND NANODISCS ENHANCE REVASCULARIZATION IN OB/OB TYPE MICE

To examine the effect of the treatments under diabetic conditions, we repeated the hind limb ischemia model on ob/ob mice. After 14 days, significantly higher blood flow recoveries were seen in tmSCFPLs and tmSCFNDs treated groups in comparison to an alginate only control (**Figure 4.10 A, B**). Immunohistochemical staining on ob/ob mice to detect endothelial cells (PECAM-1) and smooth muscle cells (αSMA) showed a higher number of small blood vessels under tmSCFNDs treatment while there was a higher number of matured blood vessels under tmSCFPLs treated group (**Figure 4.11 A-D**). Treatment with tmSCF alone did not enhance the mature blood vessel formations in ob/ob mice in comparison to WT mice, indicating the better treatment potential with nanocarriers. Overall, tmSCF treatment with nanocarriers improved blood flow recoveries in both WT and ob/ob mice on hind limb ischemia model.

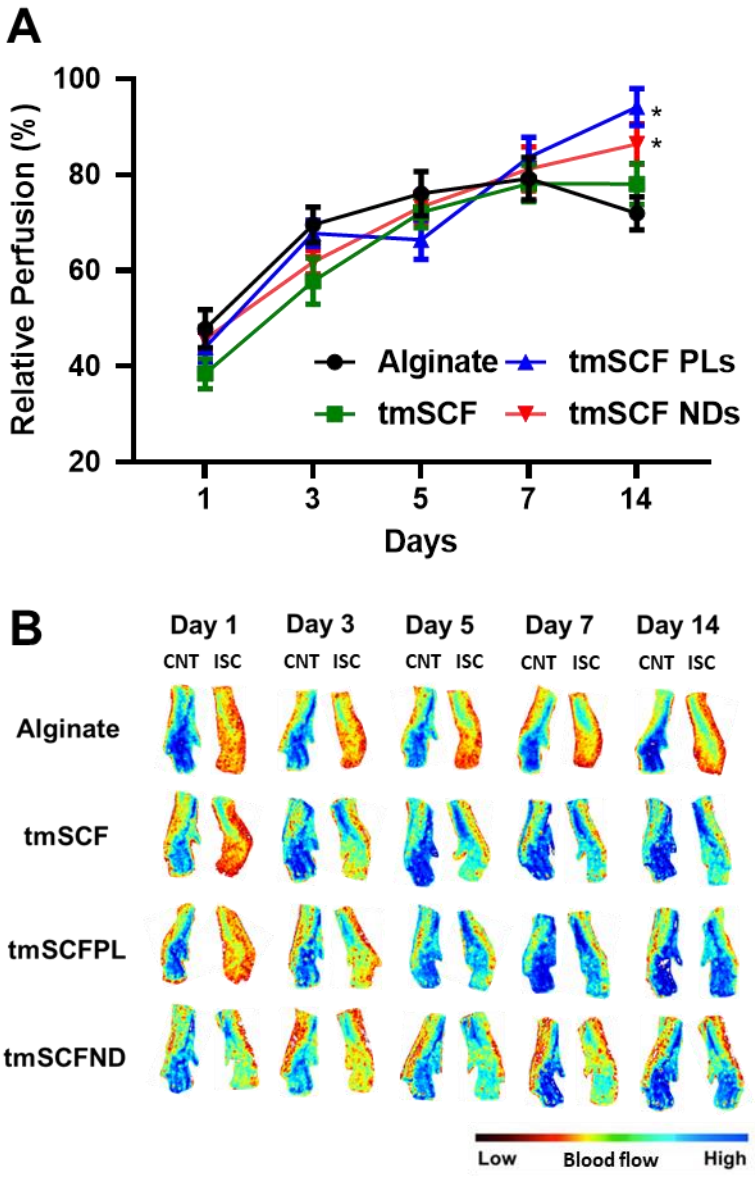

Figure 4.8. The result of hindlimb ischemia model on wild type mice. (A) Relative blood flow recovery after hindlimb ischemia surgery on WT mice (n =12-13). (B) Representative mice foot images taken by laser speckle imaging. Left foot is control (no surgery) and right foot is ischemic foot (surgery + treatments).

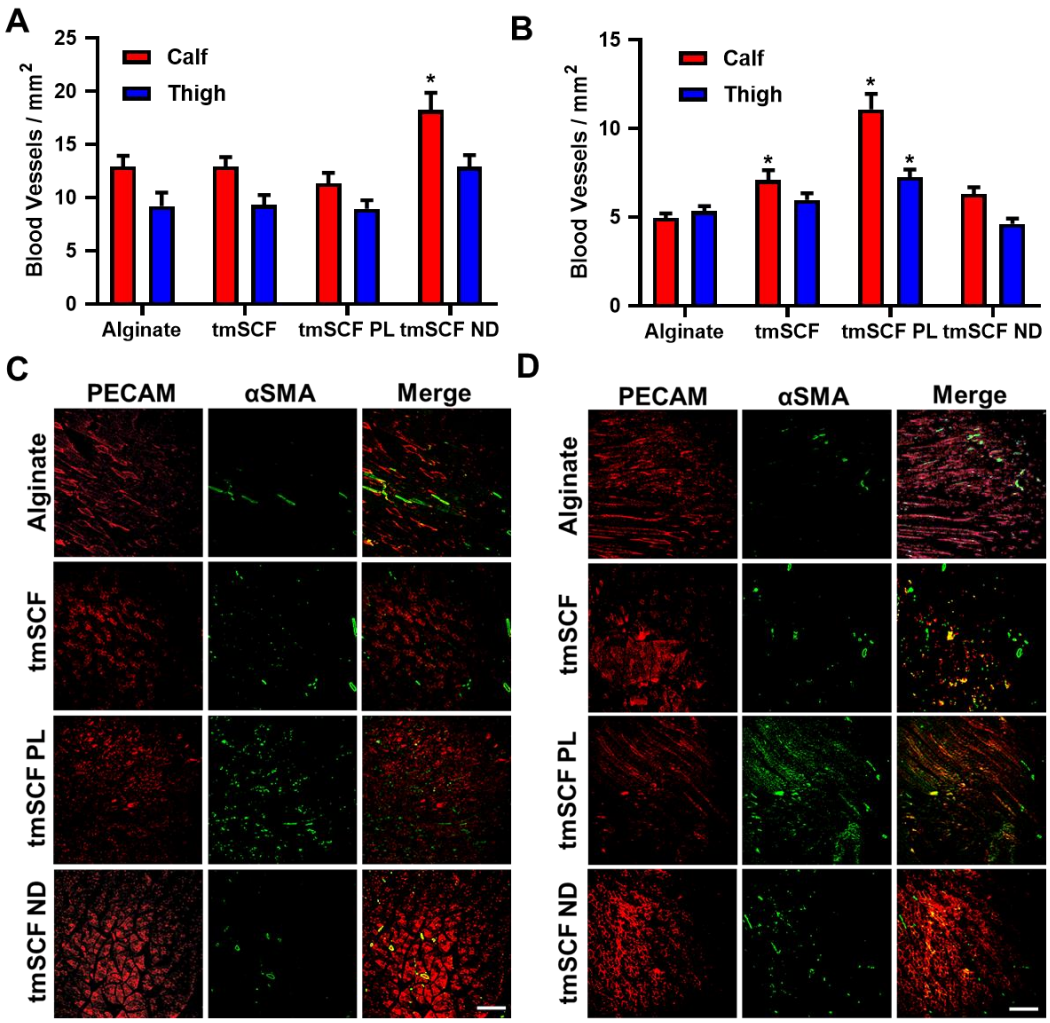

Figure 4.9. PECAM and αSMA immunostaining on ischemic foot of WT mice.

(A) The number of small blood vessels in the calf and thigh muscle counted from PECAM immunostaining images (n = 4-7). (B) The number of large blood vessels counted from αSMA immunostaining images (n = 4-7). (C) Representative immunostaining images of PECAM (red) and αSMA (green) on WT mice calf muscle. Scale bar is 300 μm. (D) Representative immunostaining images of PECAM (red) and αSMA (green) on WT mice thigh muscle. Scale bar is 300 μm. *p<0.05 versus alginate.

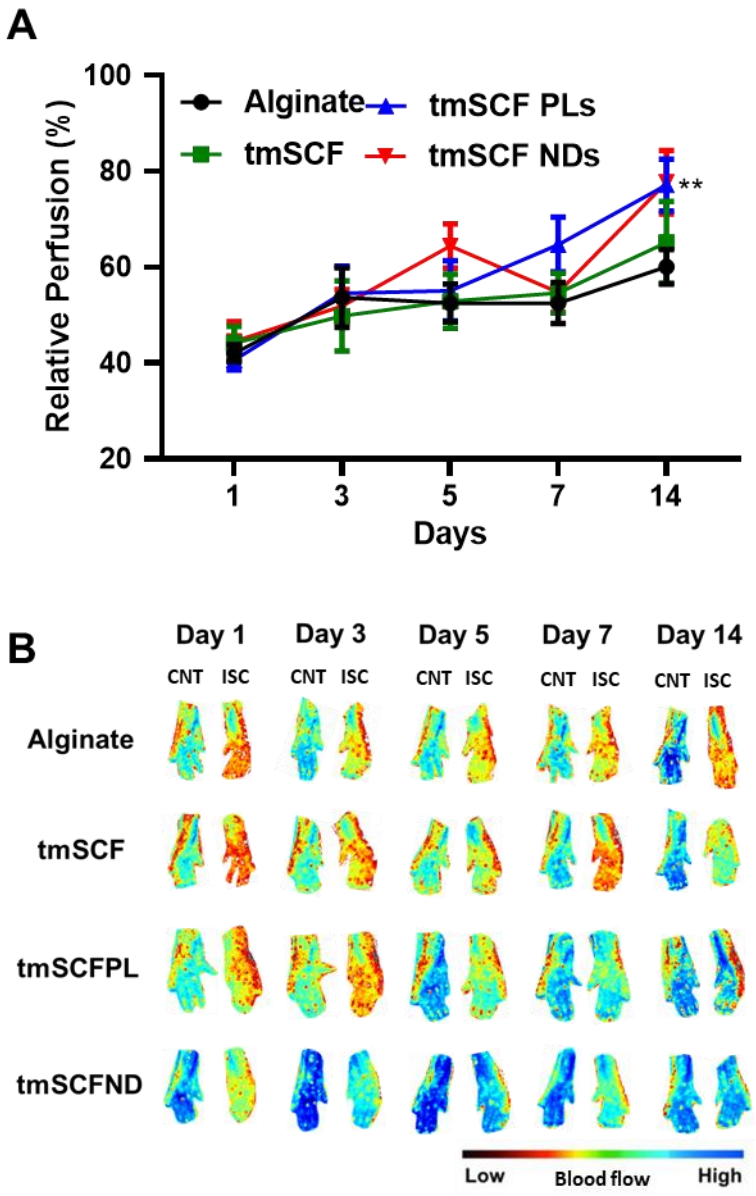

Figure 4.10. The result of hindlimb ischemia model on ob/ob mice. (A) Relative blood flow recovery after hindlimb ischemia surgery on ob/ob mice (n =11-12). (B) Representative mice foot images taken by laser speckle imaging. Left foot is control (no surgery) and right foot is ischemic foot (surgery + treatments).

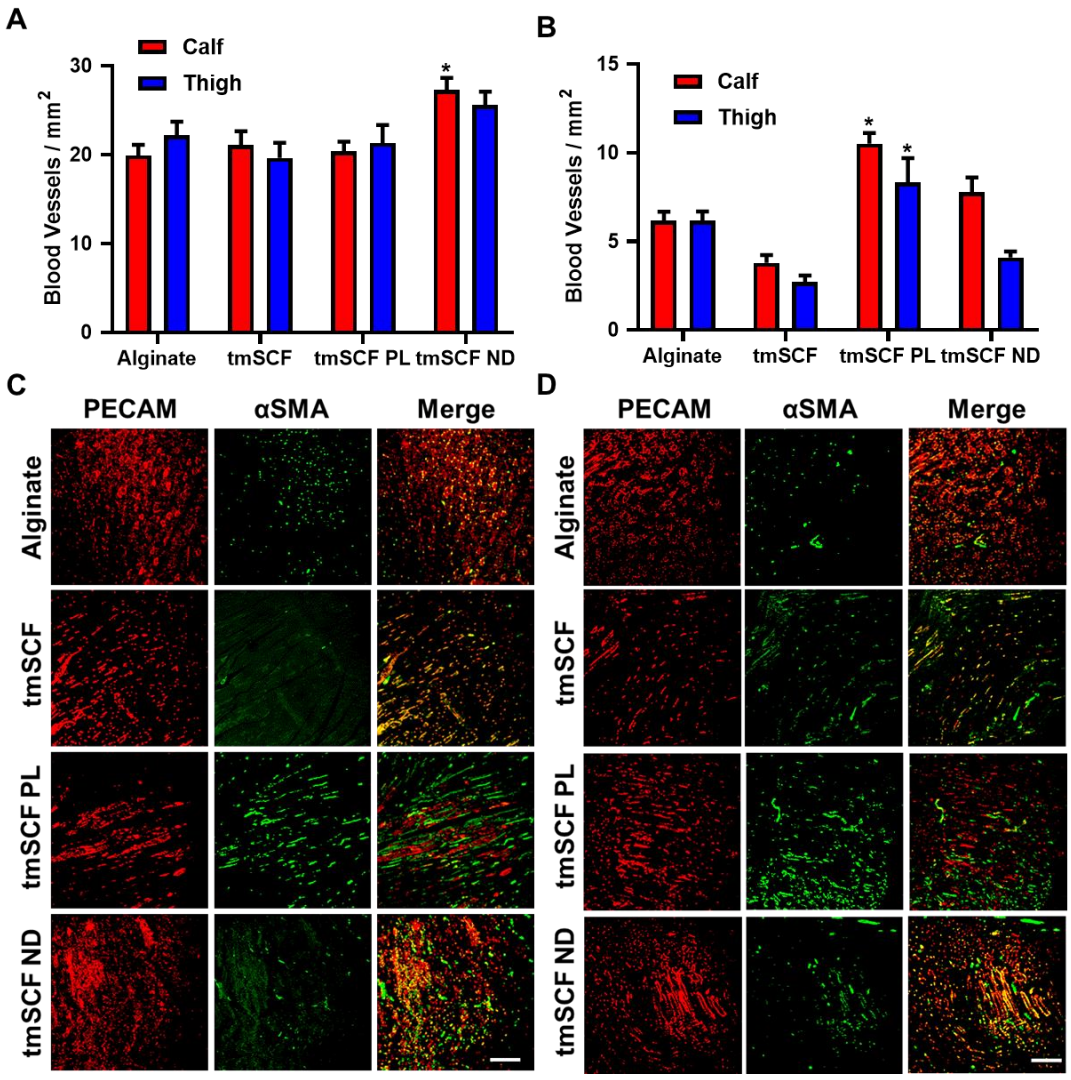

Figure 4.11. PECAM and αSMA immunostaining on ischemic foot of ob/ob mice. (A) The number of small blood vessels in the calf and thigh muscle counted from PECAM immunostaining images (n = 4-10). (B) The number of large blood vessels counted from αSMA immunostaining images (n = 4-10). (C) Representative immunostaining images of PECAM (red) and αSMA (green) on ob/ob mice calf muscle. Scale bar is 300 μm. (D) Representative immunostaining images of PECAM (red) and αSMA (green) on ob/ob mice thigh muscle. Scale bar is 300 μm. *p<0.05 versus alginate.

4.3.7 TRANSMEMBRANE STEM CELL FACTOR NANODISCS INDUCED POTENT SUBTYPES OF ENDOTHELIAL PROGENITOR CELLS

In section 4.3.4, we found enhanced tube formation of HUVECs with tmSCFPL treatments, indicating a potential angiogenesis of endothelial cells. In this section, we examined potential vasculogenesis of endothelial progenitor cells with our treatments. We first conducted an EPC colony formation assay. We quantified the number of small EPCs and large EPCs after 7 days of bone marrow mononuclear cells (**Figure 4.12 A**). Small EPCs indicate primitive EPCs with highly proliferative activity, and large EPCs indicate definitive EPCs with vasculogenic properties. There is no significant difference in the number of small colony formation between groups (Data not shown). However, we confirmed a significantly higher number of large EPC colonies formed in SCF, tmSCFPLs and tmSCNFDs treated groups in comparison to control, indicating their high vasculogenic potential (**Figure 4.12 B**).

We then investigated the effect of our treatment on bone marrow cells by incubating them with treatments for 30 minutes. We examined markers for EPCs including CD34, CD133, CD146, and found that tmSCFPLs and tmSCNDs increased the population of $CD34^{-}CD133^{+}CD146^{+}$ cells in comparison to the control or tmSCF treated cells (**Figure 4.12 C**). Notably, a population of $CD34^{-}CD133^{+}$ EPCs was identified to be the most potent EPC phenotype for rescuing ischemia in a recent study[192], suggesting that tmSCFPLs and tmSCFNDs induced this potent EPC phenotype. We next immunostained for $CD34^{+}/CD144^{+}$ in the muscles of WT mice after the hind limb ischemia study and found increased EPCs in the ischemic muscles of tmSCFNDs treated mice, indicating the recruitment of EPCs to the ischemic region (**Figure 4.13**). We also immunostained for EPCs in the muscles of ob/ob mice from the hind limb ischemia study and found increased $CD34^{+}/CD144^{+}$ in the ischemic muscles of tmSCF treated mice (**Figure 4.14**). It is noted that the percentage of the double positive area is much lower in ob/ob mice, indicating the reduced effect of our treatment in ob/ob mice. Together, these results suggest that nanocarrier formulations of tmSCF are more active in inducing potent subtype of EPCs and contributing to vasculogenesis.

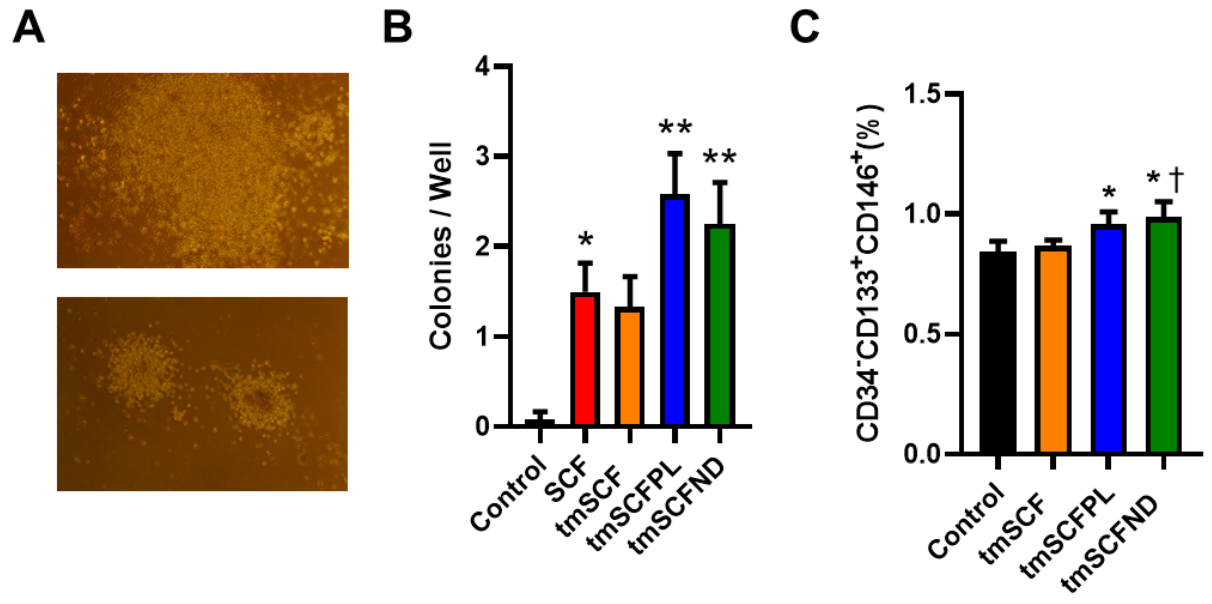

Figure 4.12. EPC colony formation assay demonstrated significantly more large EPC colonies by tmSCFPLs and tmSCFNDs. (A) Representative picture of large EPC colony (Top) and small EPC colony (Bottom). (B) Quantification result of number of large EPC colonies per well. (C) Bone marrow cells are incubated with treatments for 30 minutes. tmSCFPLs and tmSCFNDs induced more $CD34^{-}CD133^{+}CD146^{+}$EPCs than control. *p<0.05 versus control, **<0.01 versus control. † <0.05 versus tmSCF.

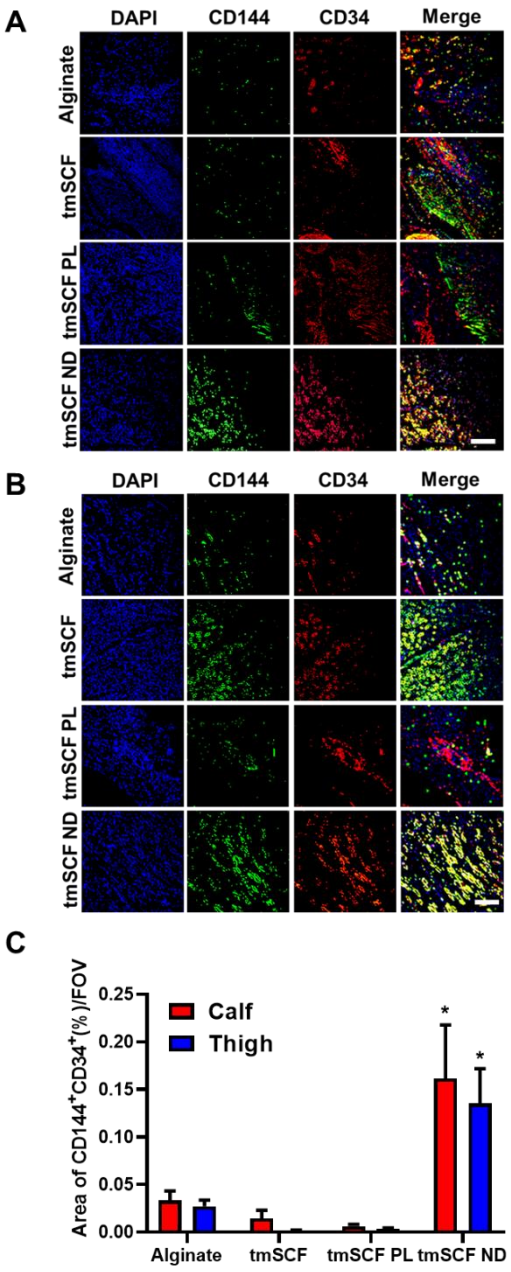

Figure 4.13. Immunostaining of calf and thigh muscle of WT mice after hind limb ischemia. (A) Representative images of calf muscle of WT mice after hind limb ischemia (Day 14). CD144 (Green), CD34 (Red), and DAPI (Blue). Scale bar is 300 μm. (A) Representative images of thigh muscle of WT mice after hind limb ischemia (Day 14). CD144 (Green), CD34 (Red), and DAPI (Blue). Scale bar is 300 μm. (C) Quantification results of double positive area (%) of CD144 and CD34, indicating that tmSCFND mobilized EPCs to ischemic site after injury.

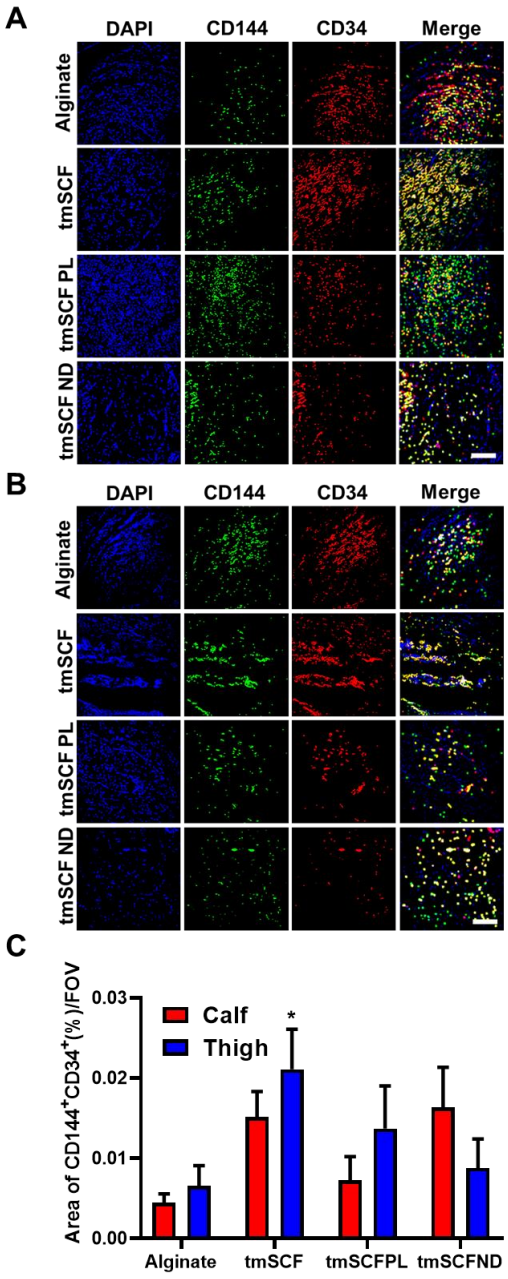

Figure 4.14. Immunostaining of calf and thigh muscle of ob/ob mice after hind limb ischemia. (A) Representative images of calf muscle of ob/ob mice after hind limb ischemia (Day 14). CD144 (Green), CD34 (Red), and DAPI (Blue). Scale bar is 300 μm. (A) Representative images of thigh muscle of ob/ob mice after hind limb ischemia (Day 14). CD144 (Green), CD34 (Red), and DAPI (Blue). Scale bar is 300 μm. (C) Quantification results of double positive area (%) of CD144 and CD34, indicating that the effect of our treatments are reduced in ob/ob mice.

4.3.8 TRANSMEMBRANE STEM CELL FACTOR NANODISCS INDUCED MOBILIZATION OF $CD34^-CD133^+$EPCS TO PERIPHERAL BLOOD

Following injury or development of ischemia, EPCs mobilize and home to the region of injury[193]. Soluble SCF is known to participate in both the mobilization and homing of EPCs in concert with other cytokines[194]. To test if the tmSCF-based treatments induced EPC mobilization, we performed subcutaneous injections of the treatments in mice for four days consecutively and then performed flow cytometry on the peripheral blood to identify EPCs. While we did not observe significant changes in the conventional EPC population of $CD34^+CD133^+CD146^+FLK1^+$ cells (**Figure 4.15 A**), we found that there were increases in $CD34^-CD133^+CD146^+FLK1^+$ and $CD34^-CD133^+CD146^+FLK1^-$ cells in the tmSCFNDs treated group (**Figure 4.15 B, C**). This result indicates that tmSCFNDs induce mobilization of the potent subtypes of EPCs to peripheral blood described in previous work[192]. We also examined the EPC population in bone marrow after four consecutive days of subcutaneous injection of our treatments, but neither the $CD34^-CD133^+CD146^+FLK1^+$ nor $CD34^+CD133^+CD146^+FLK1^+$ population were enriched in bone marrow following the treatments (**Figure 4.15 D, E**).

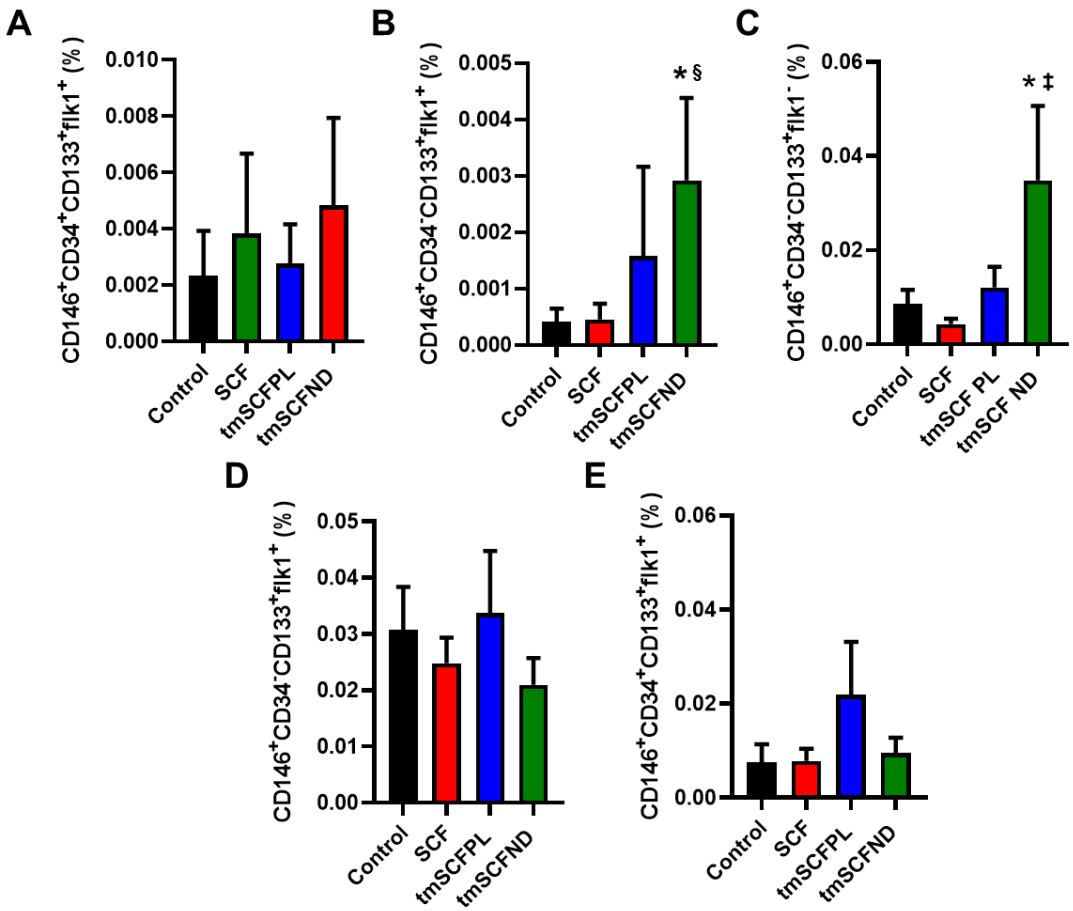

Figure 4.15. EPC mobilization to peripheral blood after tmSCFND treatment. (A) Frequency of $CD34^+CD133^+CD146^+FLK1^+$ cells in peripheral blood after subcutaneous injection (n = 11-12). (B) Frequency of $CD34^-CD133^+CD146^+FLK1^+$ cells in peripheral blood after subcutaneous injection (n = 10-13). (C) Frequency of $CD34^-CD133^+CD146^+FLK1^-$ cells in peripheral blood after subcutaneous injection (n = 10-13). (D) $CD34^-CD133^+CD146^+FLK1^+$ subpopulation in bone marrow was analyzed after four days of subcutaneous injection of our treatment. (E) $CD34^+CD133^+CD146^+FLK1^+$ subpopulation in bone marrow was analyzed after four days of subcutaneous injection of our treatment.*, †, ‡ and § indicate significant difference over alginate control, tmSCF, tmSCFPL, and SCF, respectively ($p < 0.05$; Kruskal–Wallis one-way analysis of variance).

4.4 DISCUSSION

The treatment of ischemia in diabetes has been a recurrent clinical problem, especially among diabetic patients receiving bypass surgery or percutaneous interventions for limb ischemia who have significantly worse outcomes than non-diabetic patients.[195,196] To examine abnormal protein expression in type 2 diabetic patients, we first conducted immunostaining on the skin of type 2 diabetes. Our data revealed significantly reduced SCF expression while upregulated c-Kit expression in endothelial cells of type 2 diabetes (**Figure 4.1**). There may be a feedback mechanism behind these phenomena. According to the previous study, Ets homologous factor (Ehf), a member of the Ets family transcription factors, is upregulated by TGF-b/Smad signaling in mouse bone marrow–derived mast cells, which reduces the expression of c-Kit on mast cell.[197] It may be possible that regulation of Ehf transcription factor may be disrupted in type 2 diabetes, thus causing abnormal c-Kit expression in mast cell.

Surgeries or percutaneous interventions for limb ischemia on diabetic patients may lead to the recurring occurrence of limb ischemia, thus our lab aims to develop a protein therapy using tmSCF protein. While soluble form of SCF has been explored as a therapy for multiple indications, its pleiotropic effects including mast cell activation and induction of anaphylaxis have prevented SCF from being adopted for clinical use. Our study supports that local delivery of tmSCF protein may be a viable alternative to soluble SCF for limb ischemia and does not activate mast cells. Evan's blue extravasation assay demonstrated that all of tmSCF, tmSCFPLs, and tmSCFNDs did not induce vascular leakage, indicating little or no mast cell activation. (**Figure 4.5**).

Our hind limb ischemia model on WT demonstrated that tmSCFPLs and tmSCFNDs increased relative blood flow recovery significantly more than control group (**Figure 4.8**). Our immunostaining results on the calf and thigh muscle after hindlimb ischemia surgery showed a significantly more of small blood vessels formation after tmSCFNDs treatment and matured blood vessels formation after tmSCFPLs treatment. These results suggest that tmSCFPLs may enhance remodeling of pre-existent arterioles and maturing blood vessels, and tmSCFNDs enhanced *de novo* blood vessels formation possibly by EPCs. Hind limb ischemia study on ob/ob mice also showed a similar trend. We confirmed increased blood flows on tmSCFPLs and tmSCFNDs groups at day 14 (**Figure 4.10**), and significantly more of small blood vessel formations by tmSCFND and mature blood vessel formations by tmSCFPLs (**Figure 4.11**).

Our endothelial tube formation assay demonstrated an enhanced tube formation only by tmSCFPLs (**Figure 4.6**). It is generally known that low density lipoprotein (LDL) is preferentially taken up by endothelial cells. The structure of proteoliposome may resemble that of LDL, which may lead to the preferential enhancement of endothelial tube formation by tmSCFPLs. Our EPC mobilization assay also demonstrated increased EPC mobilization exclusively by tmSCFND. The reason why EPCs respond to tmSCFNDs remains unknown. However, High Density Lipoprotein (HDL) which is structurally similar to nanodisc is known to enhance mobilization of EPCs. These observations may support a claim that the type of nanocarrier used to deliver tmSCF elicited a differential response based on cell type.

Our EPC mobilization assay showed a significantly higher number of $CD34^{-}CD133^{+}$EPCs in peripheral blood after subcutaneous injection of tmSCFNDs in comparison to control (**Figure 4.15**). $CD34^{-}CD133^{+}$EPCs are unconventional type of EPCs, but it is suggested to be a potent subtype of EPCs[192]. Friedrich et al. demonstrated that homing ability of $CD34^{-}CD133^{+}$EPCs are significantly higher than that of $CD34^{+}CD133^{+}$EPCs. Moreover, $CD34^{-}CD133^{+}$EPCs injection significantly reduces the lumen circumference and neointima formation after vascular injury. Interestingly, we confirmed a significantly higher amount of $CD34^{+}$EPCs at ischemic limb in tmSCFNDs treated group (**Figure 4.13, 14**). Previous studies demonstrated that $CD34^{+}$EPCs are more matured and adherent than $CD34^{-}$EPCs, which can be found in stable plaques[192,198]. Considering our findings and others, tmSCFNDs may induce $CD34^{-}$EPCs to peripheral blood, then these EPCs become mature at ischemic site of injury.

4.5 CONCLUSION

In this chapter, we developed a tmSCF protein therapy. Two types of nanocarriers, liposomes and nanodiscs, were used to enhance the functional activities of tmSCF protein. Hind limb ischemia model on WT and ob/ob mice demonstrated that tmSCFPLs and tmSCFNDs significantly increased the blood flow recovery. Endothelial tube formation assay suggested that tmSCFPLs may have an angiogenic potential on endothelial cells. EPC mobilization assay revealed that tmSCFNDs significantly induced the number of $CD34^{-}CD133^{+}$EPCs in peripheral blood, indicating the vasculogenic potential of tmSCFNDs. These results suggest that we may be able to achieve targeted protein delivery to a specific cell type by controlling nanocarriers.

Chapter 5: Endocytosis and Signaling Mechanism in tmSCF Protein Therapy

5.1 INTRODUCTION

Previous section demonstrated the alteration of mast cell activation in SCF and tmSCF-based therapy while maintaining angiogenic ability in endothelial cells and EPCs. In this chapter, we demonstrate cellular mechanistic studies to elucidate the functional difference. In mast cell, SCF and tmSCF interact with their cognate receptor c-Kit, leading to dimerization, signaling and internalization through either a clathrin or caveolin-mediated endocytosis[199,200]. Clathrin-mediated endocytosis is the most well studied endocytosis pathway, where clathrin proteins assemble to form a clathrin-coated pit followed by budding of the pits away from a surface membrane, bringing receptor to endosomes. Reaction rate of clathrin-mediated endocytosis is faster (Rate constant, K_e = 0.2 - 0.4 min^{-1}) in comparison to clahtrin independent endocytosis (K_e = 0.05 - 0.1 min^{-1})[201]. Previous study suggested that clathrin-mediated endocytosis leads to increased proliferation and migration of mast cells[202]. Another major endocytosis pathway is caveolin-mediated endocytosis. This endocytosis has slower uptake kinetics and leads to reduced proliferation and migration of mast cell[202]. Based on these studies, we hypothesized that mast cells use caveolin to uptake tmSCF-based therapies, thus attenuating mast cell degranulation and preventing anaphylaxis. On the other hand, mast cells use clathrin to uptake SCF, causing mast cell degranulation. To examine this hypothesis, we measured the colocalization of clathrin or caveolin with c-Kit to examine which endocytosis mechanism cells use to uptake protein therapies.

Other than endocytosis, signaling downstream of the c-Kit receptor also influences functional activities of cells. The main signaling pathway downstream of c-Kit is Phosphoinositide 3-kinase (PI3K) pathway, mitogen-activated protein kinase (MAPK) pathway, and signal transducers and activators of transcription (STAT) pathway. In general, phosphorylation of c-Kit activates PI3K, leading to the phosphorylation of AKT, activating mTOR, ultimately contributing to cell survival. Phosphorylation of c-Kit also activates RAS GTPase, causing ERK phosphorylation and leading to increased cell proliferation[203]. Dimerization of c-Kit receptor activates Janus Kinase (JAK), which phosphorylates STATs, allowing STATs to translocate into the nucleus where they act on target gene promoters. STAT5 contributes to mast cell homeostasis by mediating proliferation, survival, and mediator release[204].

Such that, signaling downstream of c-Kit leads to critical cellular activities. In this chapter, we will first closely examine the endocytosis mechanism of mast cell, EPCs, and endothelial cells to figure out what may cause the activation differences in SCF and tmSCF-based therapy. Later in this chapter, we will investigate the signaling pathway downstream of c-Kit in mast cell and bone marrow mononuclear cells to decipher the activation difference in each cell type.

5.2 MATERIALS AND METHODS

5.2.1 C-KIT INTERNALIZATION BY FLOW CYTOMETRY

MC9 mast cells, bone marrow cells, and HUVECs were starved overnight with 0.5% serum prior to the experiment. The cells were treated with Brefeldin A (5 µg/ml; Cayman Chemicals, Inc.) for 2 hours to inhibit a repopulation of surface c-Kit. For clathrin and caveolin inhibitor study, we treated cell with 25nM of nystatin (caveolin inhibitor) for 30 minutes, 100 nM of wortmannin (clathrin inhibitor) for 15 minutes, and pitstop (clathrin inhibitor) for 10 minutes before tmSCF treatments. The cells were washed with 37C^{o} HEPEs buffer (10 mM HEPES, 137 mM NaCl, 2.7 mM KCl, 0.4 mM Na2HPO4·7H2O, 5.6 mM glucose, 1.8 mM CaCl2·2H2O, and 1.3 mM MgSO4·7H2O with 0.04% BSA) and resuspended at 5×10^5 cells/ml in HEPES buffer without BFA. The cells were then treated with either of SCF, tmSCF, tmSCFPLs, and tmSCFNDs (100 ng/ml) for 5, 10, 20, and 30 minutes. After the treatment, cells were plunged into ice to stop the c-Kit internalization. For HUVECs, accutase was used to detach cells. The surface c-Kit was stained with PE-Cy™7 anti-Mouse CD117 antibody (BD Biosciences) or PE-Cy7 anti-Human CD117 antibody (Biolegend) then surface c-Kit intensity was read by flow cytometry. Population above the intensity of 10^4 was calculated. The surface c-Kit intensity was normalized to initial time point (0 min).

5.2.2 CLATHRIN, CAVEOLIN AND C-KIT COLOCALIZATION ASSAY

Prior to the experiment, bone marrow cells were harvested from 10 weeks old female C57BL/6J wild-type mice and mononuclear cells are isolated by Ficoll density centrifugation. These bone marrow mononuclear cells are cultured for seven days under endothelial media to induce spindle shaped adherent EPCs. The EPCs, MC9 mast cells, and HUVECs were starved overnight with 0.5% serum prior to the experiment. 100 ng/ml of SCF, tmSCF, tmSCFPLs and tmSCFNDs were then treated for two minutes and immediately plunged into ice to stop the internalization. After washing with PBS, and fixing with 4% PFA, immunostaining with clathrin (Abcam), caveolin (Abcam) and c-Kit (Invitrogen, NOVUS Biological) were conducted. Images of 30 cells are taken by confocal microscopy and we analyzed the colocalization of clathrin and c-Kit and caveolin and c-Kit by coloc 2 in Image J. Pearson's R value was used for analysis.

5.2.3 IMMUNOSTAINING OF PHOSPHOR-C-KIT

Prior to the experiment, the cells were starved overnight with 0.5% serum prior to the experiment. 100 ng/ml of SCF, tmSCF, tmSCFPLs and tmSCFNDs were then treated for five minutes and immediately plunged into ice to stop the phosphorylation. After washing with PBS, and fixing with 4% PFA, immunostaining with p-c-Kit (R&D) and c-Kit (Invitrogen, NOVUS Biological) were conducted. Images of 30 cells are taken by confocal microscopy and we analyzed the mean intensity of p-c-Kit inside of a single cell by photoshop.

5.2.4 FLOW CYTOMETRY OF P-AKT, ERK, STAT1, STAT5 IN MC9 MAST CELL AND BONE MARROW MONONUCLEAR CELLS

Prior to the experiment, the cells were starved overnight with 0.5% serum prior to the experiment. 100 ng/ml of SCF, tmSCF, tmSCFPLs and tmSCFNDs were then treated for five minutes and immediately plunged into ice to stop the phosphorylation. After washing with PBS with sodium orthovanadate, cells are permeabilized with 100% methanol for 10 minutes followed by fixation with 4% paraformaldehyde for 10 minutes. Antibodies to PE anti-mouse p-AKT (BD Biosciences), Alexa fluor 647 anti-mouse p-ERK(BD Biosciences), Pacific Blue anti-mouse p-STAT1 (BD Biosciences), PE-cy7 anti-mouse p-STAT5 (BD Biosciences) are used and cells were stained for 30 minutes on ice. The intensities of phosphor-proteins were read by flow cytometry. Median intensity of the population above 10^3 was quantified using FlowJo.

5.2.5 STATISTICAL ANALYSIS

All results are shown as mean ± standard error of the mean. Comparisons between only two groups were performed using a two-tailed Student's t-test. Differences were considered significant at $p<0.05$. Multiple comparisons between groups were analyzed by two-way ANOVA followed by a Tukey post-hoc test. A two-tailed probability value <0.05 was considered statistically significant.

5.3 RESULTS

5.3.1 TRANSMEMBRANE SCF-BASED TREATMENTS CAUSE SLOWER C-KIT INTERNALIZATION

SCF interacts with its cognate receptor c-Kit leading to dimerization, signaling and internalization through either a calveolin or clathrin-mediated pathway[199]. We next examined how tmSCF and its nanocarrier formulations altered its uptake by the c-Kit receptor. We measured the surface c-Kit internalization by flow cytometry and found that tmSCF-based treatments had slower uptake in mast cells (MC9 cells), bone marrow mononuclear cells (BMMNCs) and endothelial cells in comparison to soluble SCF (**Figure 5.1 A-C**). In endothelial cells, the internalization of c-Kit was the fastest for the proteoliposomal formulation (tmSCFPLs) in comparison to other tmSCF formulation but still significantly slower than soluble SCF (**Figure 5.1 C**).

5.3.2 TRANSMEMBRANE SCF FORMULATIONS ALTER THE UPTAKE MECHANISMS IN MAST CELLS, EPCS, AND ENDOTHELIAL CELLS

Previous studies have shown that there are two pathways of uptake for SCF in mast cells[202]. One uptake pathway is mediated by caveolin. This pathway has slower uptake kinetics and leads to reduced proliferation and migration of mast cell[202]. The alternative pathway is mediated by clathrin, has faster uptake kinetics, and leads to increased proliferation and migration of mast cells[202]. To examine the uptake mechanism of the tmSCF formulation, we treated cells with SCF and the tmSCF-based treatments and then performed immunostaining for c-Kit and clathrin or calveolin followed by an analysis for co-localization between the markers. We found that mast cells preferentially use clathrin to internalize SCF and caveolin to internalize tmSCFNDs (**Figure 5.2**). Mast cells use both clathrin and caveolin to uptake tmSCF or tmSCFPL. These results correspond well with the protein uptake kinetics results, showing the faster uptake by SCF (a hallmark of clathrin-mediated uptake[202]) and slower uptake of tmSCF-based therapy (a hallmark of caveolin mediated uptake; **Figure 5.1**).

Next, we conducted the same experiment on bone marrow derived EPCs and found that early EPCs preferentially use clathrin to uptake SCF while they use caveolin to uptake tmSCF, tmSCFPLs and tmSCFNDs (**Figure 5.3**). We found that endothelial cells use both clathrin and caveolin to uptake SCF, tmSCF, tmSCFPLs and tmSCFNDs (**Figure 5.4**). These results indicate

that the different cell types use different uptake mechanisms. Most notably, mast cells appear to preferentially use clathrin to uptake SCF and caveolin to uptake tmSCF formulations, which may be the key difference why we see mast cell degranulation in SCF treatment but not in tmSCF-based treatments.

5.3.3 TRANSMEMBRANE SCF-BASED THERAPIES ACTIVATE C-KIT PATHWAY ENDOTHELIAL CELLS AND EPCS BUT NOT MAST CELLS

To elucidate the mechanism of c-Kit/SCF signaling pathway upon SCF or tmSCF-based treatments, we examined the phosphorylation of c-Kit by SCF or tmSCF-based treatments by immunostaining of p-c-Kit. In MC9 mast cells, we found that SCF leads to a significantly higher c-Kit phosphorylation than tmSCF-based treatments (**Figure 5.5**). Next, we examined the degree of phosphorylation on early EPCs and found that SCF and tmSCFNDs treatments lead to a significantly higher c-Kit phosphorylation than control, indicating that SCF and tmSCFNDs may have angiogenic activity related to SCF/c-Kit pathway of early EPCs (**Figure 5.6**). Lastly, we conducted a parallel experiment on endothelial cells and found that SCF, tmSCF, tmSCFPLs and tmSCFNDs lead to a significantly higher c-Kit phosphorylation than control in endothelial cells (**Figure 5.7**). These results support that there is lower pleiotropic activity from tmSCF treatments on mast cells because of their minimal phosphorylation induction of c-Kit in mast cell. In addition, the type of formulation used for delivering tmSCF tailors its trophic specificity, with preferential activation and faster internalization of tmSCFPLs by matured endothelial cells and greater activity towards early EPCs using tmSCFNDs.

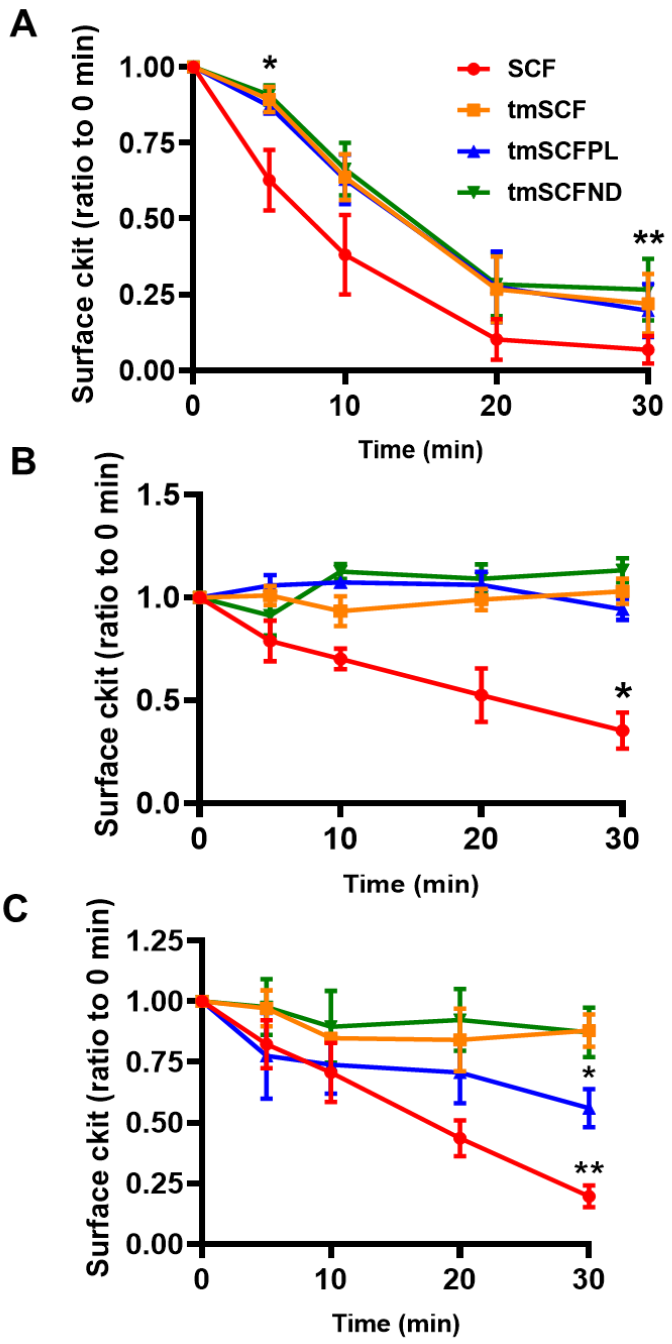

Figure 5.1 c-Kit uptake measurement by flow cytometry on mast cell, endothelial progenitor cells, and endothelial cells. (A) Surface staining for c-Kit on MC9 mast cells was monitored by flow cytometry. The intensity was normalized to 0 min time point to evaluate the treatment uptake kinetics (n = 6). (D) Surface c-Kit on bone marrow mononuclear cells were monitored by flow cytometry (n = 3-6). (E) Surface c-Kits on HUVECs were monitored by flow cytometry (n = 4-8). *p<0.05 versus control, **p<0.01 versus control**.**

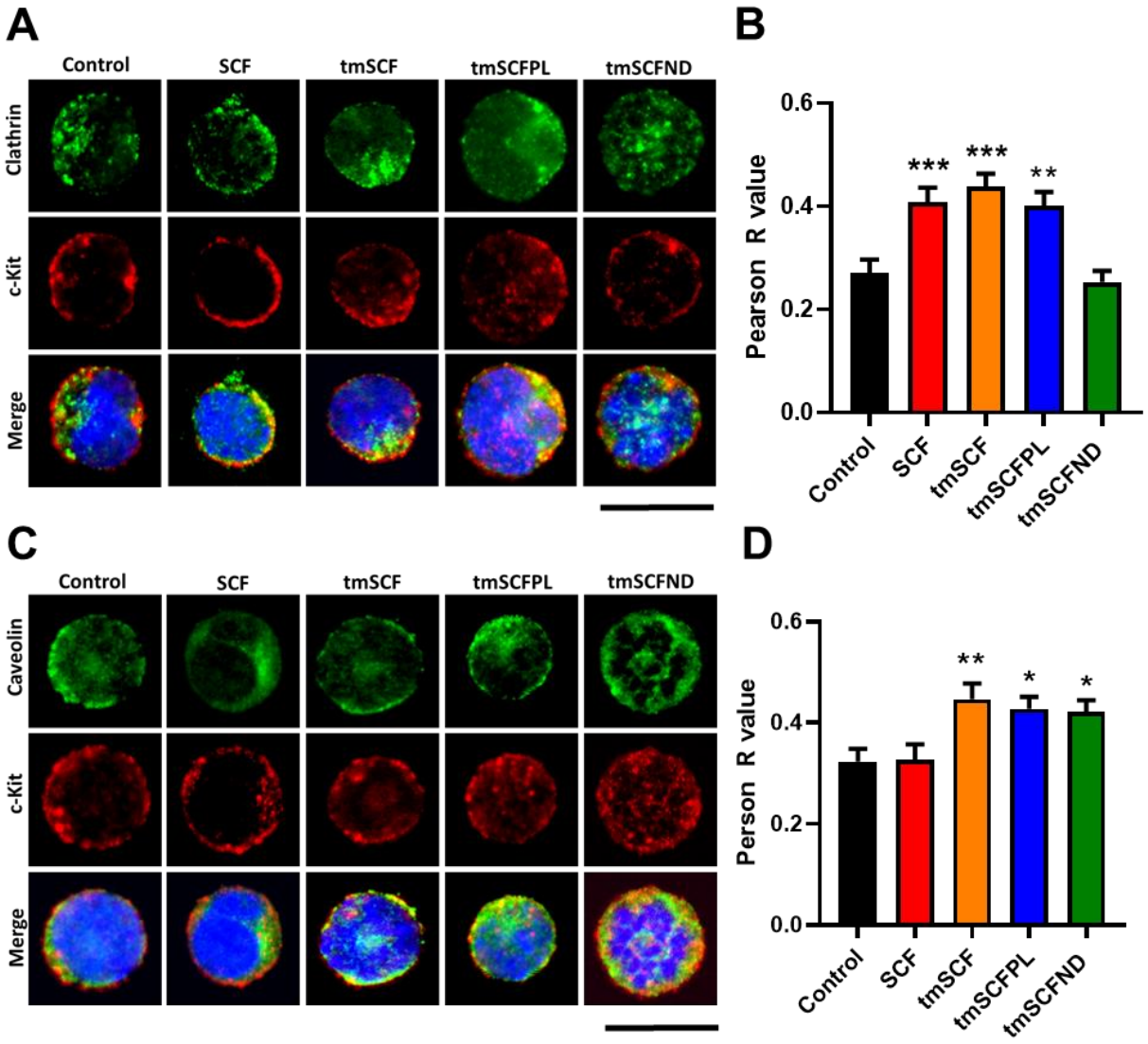

Figure 5.2 c-Kit and clathrin/caveolin colocalization on MC9 mast cell. (A) Representative pictures of single mast cell stained with clathrin and c-Kit. (B) Pearson's R value of the colocalization of clathrin and c-Kit (n = 30). (C) Representative pictures of single mast cell stained with caveolin and c-Kit. (D) Pearson's R value of the colocalization of caveolin and c-Kit (n = 30). Scale bar is 30µm. *p<0.05 versus control, **p<0.01 versus control, ***p<0.001 versus control.

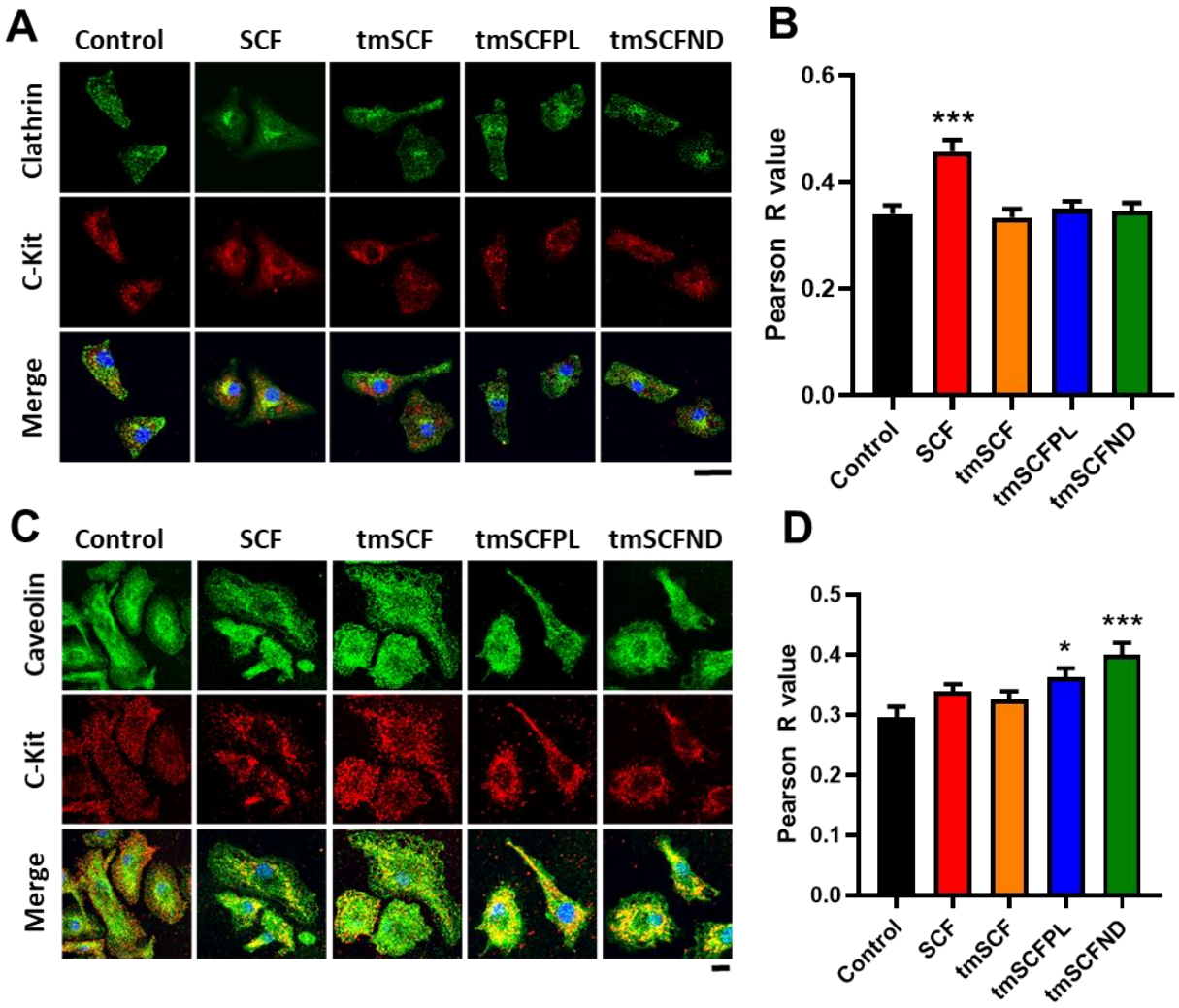

Figure 5.3 c-Kit and clathrin/caveolin colocalization on endothelial progenitor cell. (A) Representative pictures of EPCs stained with clathrin and c-Kit. (B) Pearson's R value of the colocalization of clathrin and c-Kit (n = 30). (C) Representative pictures of EPCs stained with caveolin and c-Kit. (D) Pearson's R value of the colocalization of caveolin and c-Kit (n = 30). Scale bar is 30μm. *p<0.05 versus control, ***p<0.001 versus control.

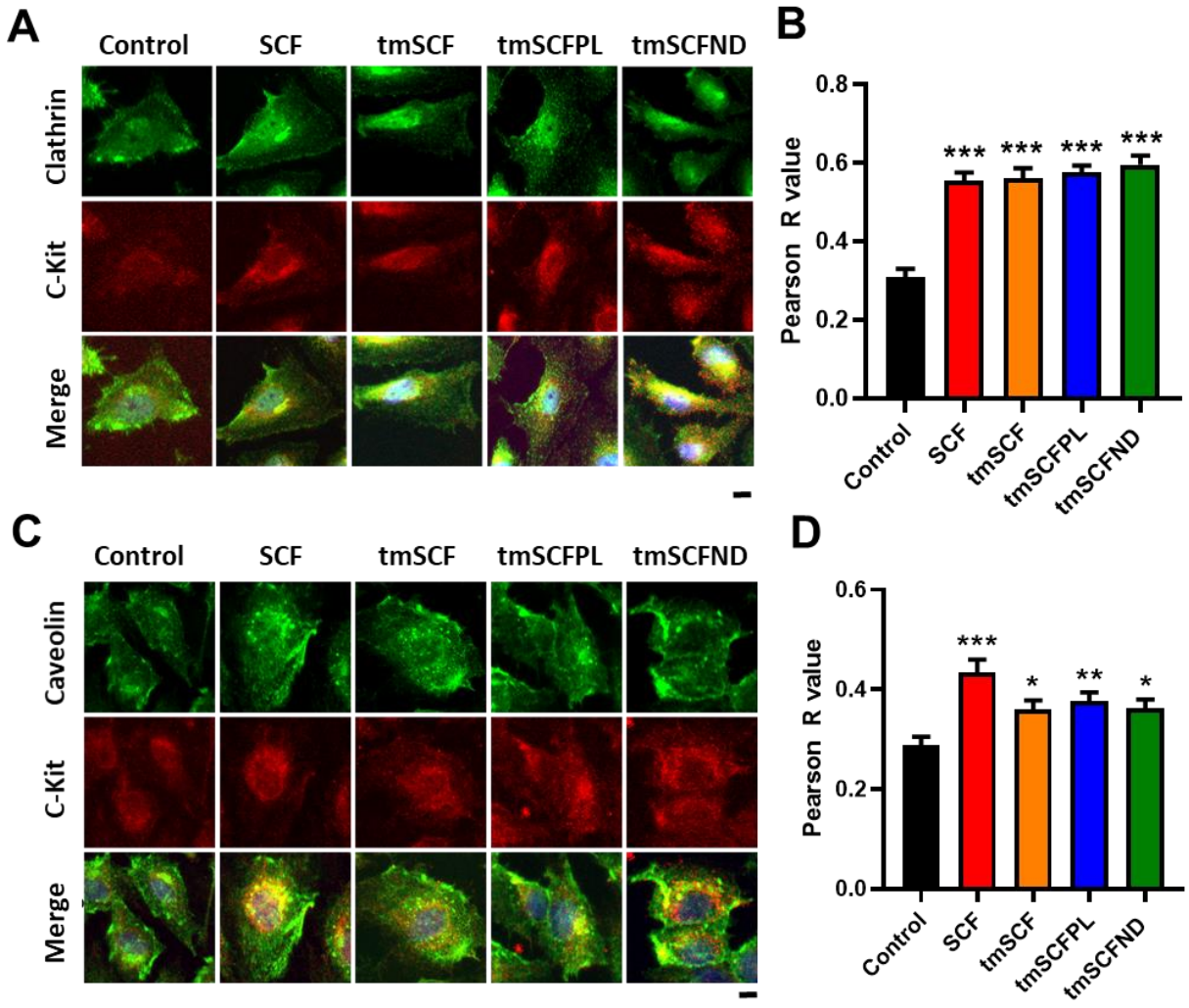

Figure 5.4 c-Kit and clathrin/caveolin colocalization on endothelial cells (HUVECs). (A) Representative pictures of endothelial cells stained with clathrin and c-Kit. (B) Pearson's R value of the colocalization of clathrin and c-Kit (n = 30). (C) Representative pictures of endothelial cells stained with caveolin and c-Kit. (D) Pearson's R value of the colocalization of caveolin and c-Kit (n = 30). Scale bar is 30μm. *p<0.05 versus control, **p<0.01 versus control, ***p<0.001 versus control.

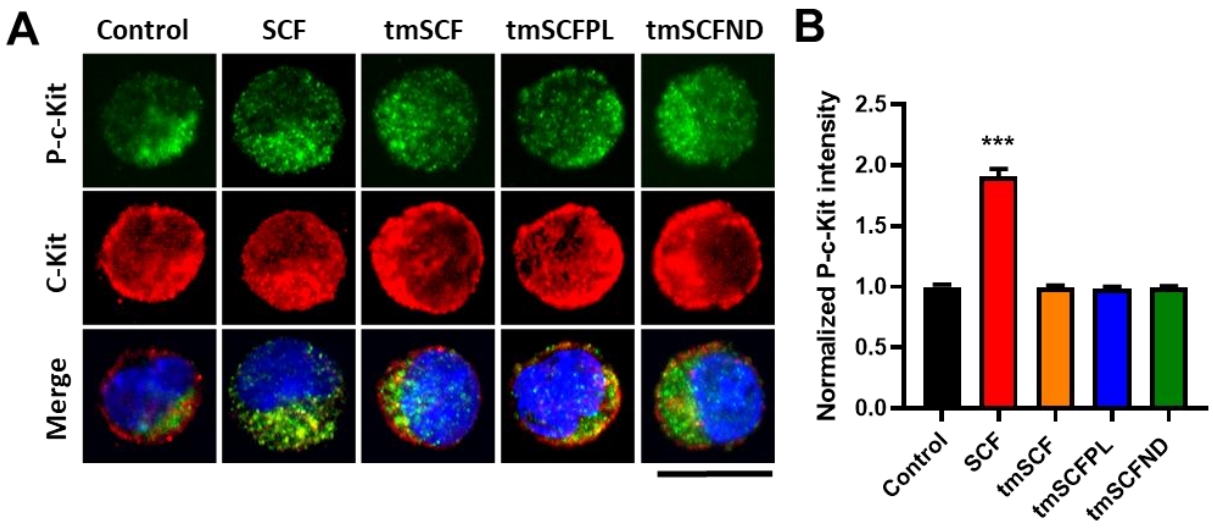

Figure 5.5 Phosphorylation of c-Kit on MC9 mast cell. (A) Representative pictures of single mast cell stained with p-c-Kit and c-Kit. Scale bar is 30μm. (B) The mean p-c-Kit intensity inside of a single cell was quantified (n = 30). ***p<0.001 versus control.

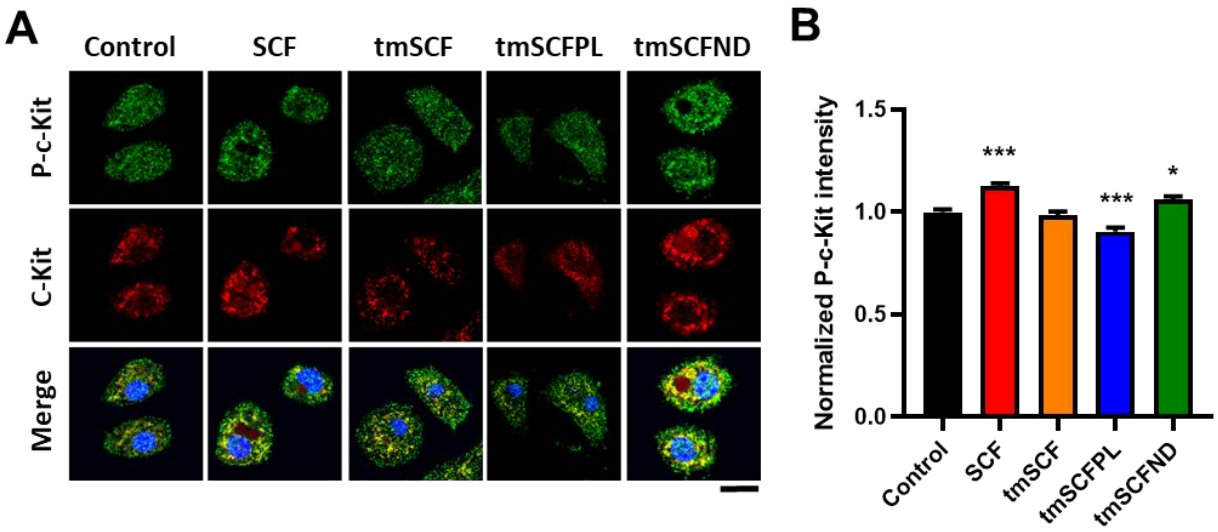

Figure 5.6 Phosphorylation of c-Kit on endothelial progenitor cells. (A) Representative pictures of EPCs stained with p-c-Kit and c-Kit. Scale bar is 30μm. (B) The mean p-c-Kit intensity inside of a single cell was quantified (n = 30). *p<0.05 versus control, ***p <0.001 versus control.

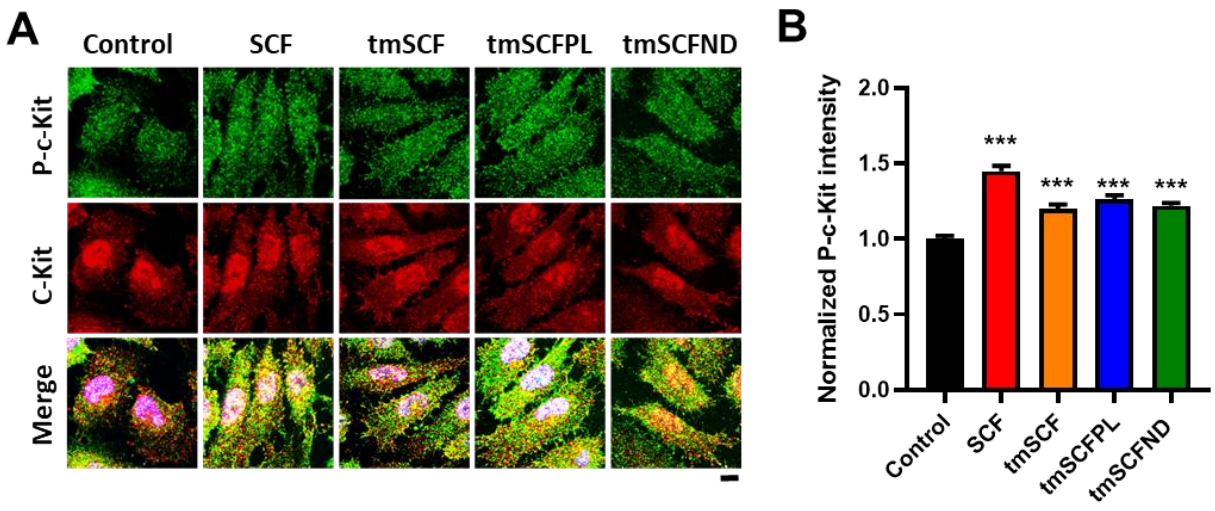

Figure 5.7 Phosphorylation of c-Kit on endothelial cells. (A) Representative pictures of HUVECs stained with p-c-Kit and c-Kit. (B) The mean p-c-Kit intensity inside of a single cell was quantified (n = 30). ***p<0.001 versus control.

5.3.4 INHIBITOR STUDIES FURTHER CONFIRMED ENDOCYTOSIS MECHANISMS IN ENDOTHELIAL CELLS

To further confirm whether endothelial cells use clathrin- or caveolin-mediated endocytosis to uptake protein therapy, we used a caveolin inhibitor (Nystatin) and a clathrin inhibitor (Wortmannin) to inhibit the either endocytosis, and measured the surface c-Kit on HUVECs. We treated cells with Breferdin A to stop c-Kit repopulation, then treated cells with drugs to inhibit the either endocytosis pathway. After 30 minutes of incubation with SCF, tmSCF, tmSCFPLs, or tmSCFNDs, we measured the surface c-Kit intensity by flow cytometry. Surface c-Kit intensity was normalized to time zero c-Kit intensity. With nystatin treatment, tmSCFPLs treated HUVECs showed a significantly increased surface c-Kit in comparison to the group without nystatin treatment (**Figure 5.7 A**). With wortmannin treatment, both SCF and tmSCFPLs treated HUVECs showed a significantly increased surface c-Kit in comparison to the group without wortmannin treatment (**Figure 5.7 B**). These results indicate that endothelial cells use both caveolin- and clathrin-mediated endocytosis to uptake tmSCFPLs, and they use clathrin-mediated endocytosis to uptake SCF.

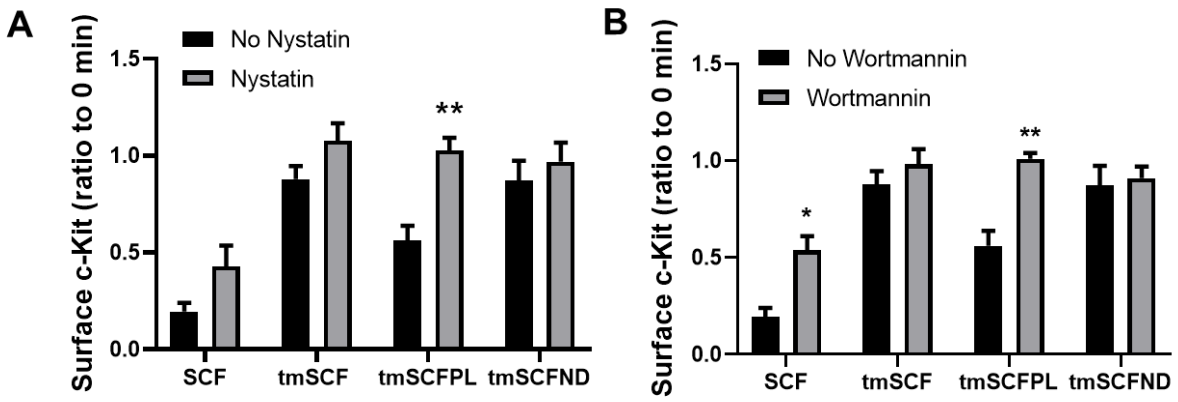

Figure 5.8 c-Kit uptake study with nystatin and wortmannin. (A) The amount of surface c-Kit was measured after 30 minutes treatment of SCF, tmSCF, tmSCFPLs, or tmSCFNDs with and without nystatin treatment. (B) The amount of surface c-Kit was measured after 30 minutes treatment of SCF, tmSCF, tmSCFPLs, or tmSCFNDs with and without wortmannin treatment.

5.3.5 C-KIT DOWNSTREAM SIGNALING

We examined the degree of phosphorylation on c-Kit receptors after treatments in the previous section. In this section, we further investigated the downstream signaling of c-Kit including PI3K pathway, MAPK pathway, and STAT pathway. In general, phosphorylation of c-Kit activates PI3K, leading to the phosphorylation of AKT, activating mTOR, ultimately contributing to cell survival. Phosphorylation of c-Kit also activates RAS GTPase, causing ERK phosphorylation, leading to increased cell proliferation. Dimerization of c-Kit receptor activates JAK, which phosphorylates STATs, allowing STATs to translocate into the nucleus where they act on target gene promoters.

We first investigated the degree of phosphorylation in mast cells over time. MC9 cells were treated with SCF, tmSCF, tmSCFPLs, or tmSCFNDs for one, five, ten, and 15 minutes then plunged into ice to stop phosphorylation. As expected, SCF leads to a significantly higher phosphorylation of ERK, AKT, and STAT1 while tmSCF-based treatments did not induce phosphorylation of these downstream signaling molecules (**Figure 5.9**). Next, we repeated the same experiment on bone marrow mononuclear cells and found that tmSCFNDs induced significantly higher degrees of phosphorylation of ERK, AKT, and STAT1 (**Figure 5.10**). This result corresponds well with our EPC mobilization assay (**Figure 4.15**), suggesting that tmSCFNDs might preferentially work on bone marrow derived EPCs to enhance proliferation and mobilization of EPCs.

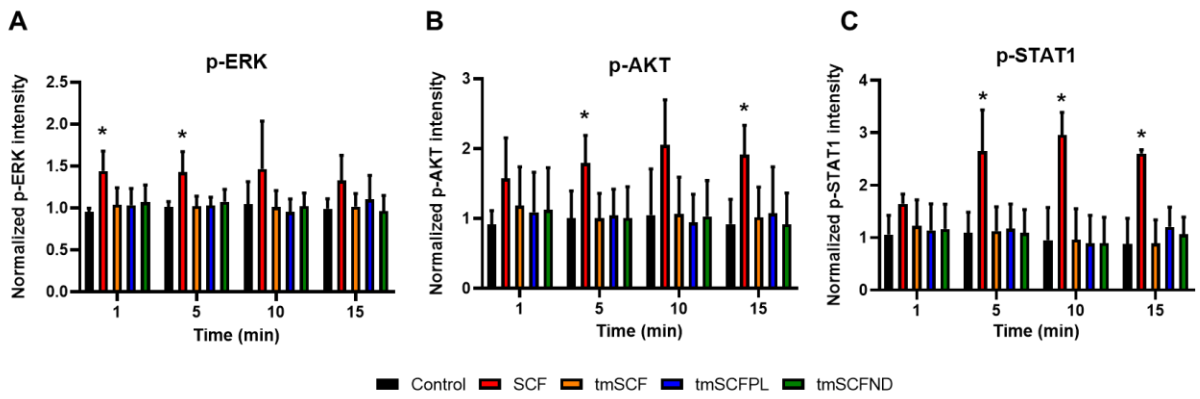

Figure 5.9 Phosphorylation of ERK, AKT, STAT1 in MC9 mast cell after treatments. (A) Normalized p-ERK intensity was quantified from flow cytometry. Significantly higher median intensity of p-ERK was observed by SCF treatment at one and five minutes time point. (B) Normalized p-AKT intensity was quantified from flow cytometry. Significantly higher median intensity of p-AKT was observed by SCF treatment at five and 15 minutes time point. (C) Normalized p-STAT1 intensity was quantified from flow cytometry. Significantly higher median intensity of p-STAT1 was observed by SCF treatment at one, five and ten minutes time point. *$p<0.05$ versus control.

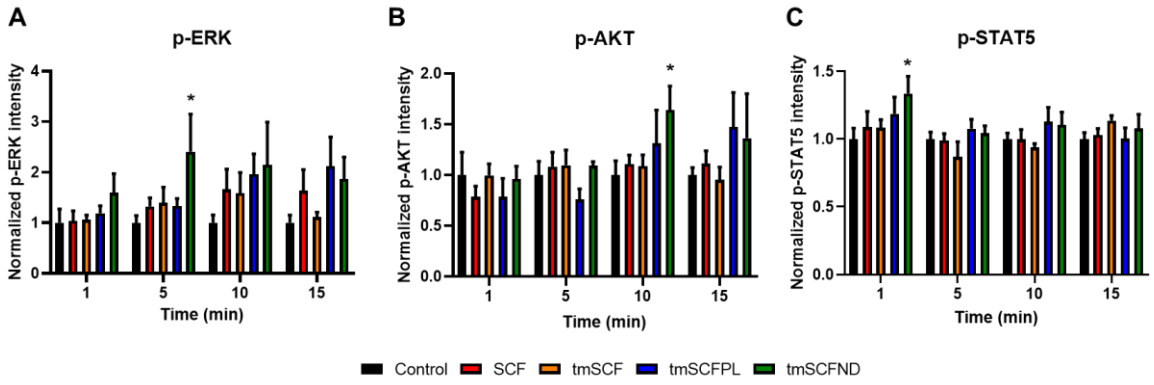

Figure 5.10 Phosphorylation of ERK, AKT, STAT5 in bone marrow mononuclear cells after treatments. (A) Normalized p-ERK intensity was quantified from flow cytometry. Significantly higher median intensity of p-ERK was observed by tmSCFNDs treatment at five minutes time point. (B) Normalized p-AKT intensity was quantified from flow cytometry. Significantly higher median intensity of p-AKT was observed by tmSCFNDs treatment at ten minutes time point. (C) Normalized p-STAT5 intensity was quantified from flow cytometry. Significantly higher median intensity of p-STAT5 was observed by tmSCFNDs treatment at one minute time point. *$p<0.05$ versus control.

5.3.6 PROPOSED DIAGRAM

Overall, this study demonstrated a potential use of tmSCF as a therapeutic protein for PAD treatment. The major negative pleiotropic activity of mast cell activation was not observed on the tmSCF-based treatments. A major difference in the tmSCF-based treatments in comparison to soluble SCF was the slower uptake kinetics and preferential trophism of tmSCF based on the nanocarrier for either endothelial cells or EPCs. Mast cells use clathrin to uptake SCF (small size protein), and caveolin to uptake tmSCF-based treatments (large size protein/lipids), causing different physiological responses such as vascular permeabilization (**Figure 4.5**). In cellular level, this hypothesis is supported by the protein uptake kinetics, showing the fast uptake by SCF and the slow uptake by tmSCF-based treatments (**Figure 5.11 A**). We also revealed that, depending on the nanocarriers to use, different cell types respond differently to tmSCF-based therapeutics. When liposomes are used as the carriers for tmSCF, endothelial cells respond and enhance tube formation and angiogenesis while no tube formation was observed when endothelial cells were treated with tmSCFNDs (**Figure 5.11 B**). When nanodisc is used as a carrier for tmSCF protein, EPCs respond, enhancing colony formation and mobilization of $CD34^{-}CD133^{+}$EPC to peripheral blood, and therapeutic angiogenesis (**Figure 5.11 C**). Our study suggested that caveolin seems to be the key to uptake relatively large size protein-lipid therapeutics. Previous studies reported that caveolin is used to endocytose low density lipoprotein[205-207] which may be resembled with our protein-lipid therapeutics in structure. This may explain why mast cells or EPCs preferentially use caveolin to uptake our protein-lipid therapeutics. Our discovery provides a new approach to targeted protein therapeutics for PAD.

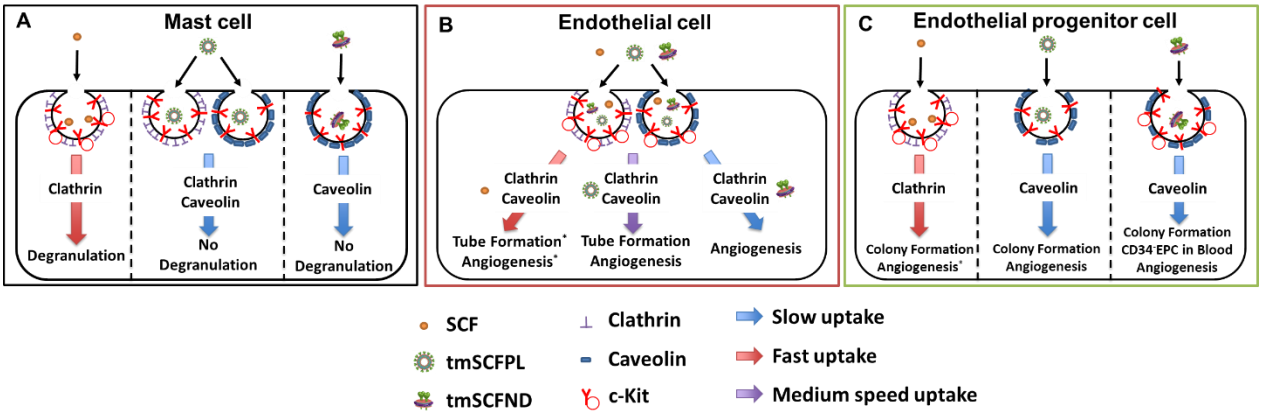

Figure 5.11 Summary diagram. (A) Mast cells use clathrin to uptake SCF (fast uptake), causing degradation and anaphylaxis, while they use caveolin/clathrin to uptake tmSCF-based treatments (slow uptake), reducing the degradation and anaphylaxis. (B) Endothelial cells use both clathrin and caveolin to uptake SCF (fast uptake), triggering tube formation of endothelial cells. Endothelial cells use both of clathrin and caveolin to uptake tmSCFPL (medium speed uptake), triggering tube formation of endothelial cells and therapeutic angiogenesis. (C) EPCs use clathrin to uptake SCF (fast uptake), triggering colony formation of EPC. EPCs use caveolin to uptake tmSCF-based treatments (slow uptake), leading to colony formation and angiogenesis. Treatment with tmSCFND further induced $CD34^{-}CD133^{+}$EPC peripheral blood mobilization in addition to colony formation and therapeutic angiogenesis.

5.4 DISCUSSION

While SCF has been explored as a therapy for multiple indications, its pleiotropic effects including mast cell activation and induction of anaphylaxis have prevented SCF from being adopted for clinical use. In chapter 4, we demonstrated that local delivery of tmSCF protein did not induce mast cell activation while maintaining its ability to revascularize blood flow. We hypothesized that different protein uptake mechanisms may explain the activation differences of SCF and tmSCF.

We found that mast cells use clathrin-mediated endocytosis to uptake SCF while they use caveolin-mediated endocytosis to uptake tmSCF-based treatments. One potential explanation for the differences in uptake may be the size of the therapeutic compound. A previous study demonstrated that cells use clathrin-mediated pathway to take up smaller particles (< 200 nm) while they use caveolin-mediated pathway to take up larger particles (around 500 nm)[208]. Based on our DLS measurements (**Figure 4.3**), tmSCF aggregates when not in a lipid nanocarrier and consequently has a much larger size than soluble SCF. The larger size of tmSCF formulations may drive cells to use preferentially caveolin-mediated endocytosis. Consistent with this concept, our result showed that MC9 mast cells mainly use clathrin-mediated endocytosis to uptake SCF while they use caveolin-mediated endocytosis to uptake tmSCF-based treatments. Another hallmark of clathrin-mediated endocytosis is that it possesses fast uptake kinetics compared to caveolin's slower uptake kinetics[209,210]. Our c-Kit internalization results on mast cells also support this phenomenon. The c-Kit receptor was taken up much faster when mast cells were treated with SCF in comparison to tmSCF-based therapy. Significantly higher phosphorylation of c-Kit was also observed when mast cells were treated with SCF but it is greatly reduced when they were treated with tmSCF-based treatments. These results imply that mast cells use clathrin-mediated endocytosis to uptake SCF, which triggers the activation of the c-Kit/SCF pathway and leads to higher vascular permeability while they use caveolin-mediated endocytosis to uptake tmSCF-based treatments with slow kinetics, suppressing the c-Kit/SCF activation and mast cell activation.

Size of protein treatments may not be the only reason for cells to choose the pathway for endocytosis. Caveolin serves an important role in lipid metabolism. For example, caveolin-1 in adipocytes binds to fatty-acid and supports the formation of lipid droplets (intracellular organelles specialized for lipid storage). Another evidence of linking caveolin and lipid

metabolism is that Cav1-knockout mice are resistant to diet-induced obesity and show decreased adiposity as well as decreased levels of free cholesterol in adipocytes. Previous studies also reported that caveolin is used to endocytose low density lipoproteins[205-207] whose structure may resemble our protein-lipid therapeutics. From these observations, it may be possible that caveolae may have a strong affinity to lipid carriers, leading to a preferential endocytosis of lipid-based therapies.

The size of the drug and lipid may be the main reasons why cells use different uptake mechanisms. However, the relationship of endocytosis and c-Kit downstream signaling is still unclear. It is possible that caveolin-mediated endocytosis does not activate the c-Kit downstream signaling in mast cells. One interesting hypothesis is that caveolin-mediated endocytosis enhances the ubiquitination of c-Kit receptors, stopping the downstream signaling cascade. Previous study on TGF-β receptors revealed that TGF-β receptors enter cells via lipid rafts/caveolae, which facilitates the ubiquitination of TGF-β receptor, leading to the degradation of TGF-β receptors and therefore turnoff of TGF-β signaling[211]. There is an adaptor protein called Src-like-adaptor protein (SLAP), which regulates ubiquitination of c-Kit, thus controlling phosphorylation of c-Kit[212]. Therefore, it is possible that tmSCF-based treatments let c-Kit receptors enter the raft/caveolae, which triggers ubiquitination of c-Kit by SLAP, turning off SCF/c-Kit signaling. Other than SLAP adaptor protein, c-Kit also interacts with several ubiquitin ligases, such as Cbl and SOCS6, or through indirect association of Cbl through Grb2[212]. It should be worth looking into the interaction between these ubiquitin ligases or adaptor proteins for c-Kit and raft/caveolae domain in the future work. Another hypothesis is that caveolin binds to the tyrosine kinase domain of c-Kit, inactivating the phosphorylation. Couet et al. demonstrated that the caveolin scaffold domain of caveolin-1 binds to the tyrosine kinase domain of EGF receptor, suppressing the phosphorylation of EGF receptor[213]. Receptor c-Kit and EGF are both receptor tyrosine kinases, thus it is possible that caveolin binds to c-Kit, inactivating the phosphorylation of tyrosine kinase on c-Kit.

Our results also indicate that we will be able to target certain cell type to enhance protein therapy by choosing a right nanocarrier. Proteoliposomal formations of tmSCF are internalized with faster kinetics and are more active in inducing tube formation in endothelial cells in comparison to free tmSCF or tmSCFNDs. Our group has used proteoliposomal formulations to deliver pro-angiogenic molecules[65,180,181,184-186]. Our trafficking studies performed here support

that there is preferential uptake of proteoliposomal formulations in mature endothelial cells in comparison to the other formulations and may be advantageous for endothelial targeted therapies. In contrast, tmSCFNDs are more active in inducing EPCs *in vitro* and *in vivo*. While MSP-based nanodiscs have been used for performing protein analysis and NMR of purified proteins[214,215], they have had little exploration for use in for protein delivery applications. Our findings indicated that nanodisc formulations of tmSCF enhanced mobilization, colony formation, and homing of EPCs, thus it may be advantageous for EPC targeted therapies.

5.5 CONCLUSION

In this chapter, we further investigated the difference in the endocytosis mechanisms of SCF and tmSCF-based treatments. Our colocalization assay demonstrated that mast cells use clathrin-mediated pathway to uptake SCF while they use caveolin-mediated pathway to uptake tmSCF-based treatments. Size of the protein therapies may be the main factor to drive them to either types of endocytosis. Larger proteins or protein complexes (200 - 500 nm) go through caveolin-mediated endocytosis and smaller proteins (< 200 nm) go through clathrin-mediated endocytosis. SCF-c-Kit complex going through caveolin-mediated endocytosis leads to reduced proliferation and migration of mast cells. Conversely, SCF-c-Kit complex going through clathrin-mediated endocytosis results in increased proliferation and migration of mast cells, leading to anaphylaxis.

We can also target a certain cell type to enhance protein therapy by choosing a right nanocarrier. Proteoliposomal formulations of tmSCF are internalized with faster kinetics and are more active in inducing tube formation in endothelial cells in comparison to free tmSCF or tmSCFNDs. Nanodisc formulations of tmSCF enhanced mobilization, colony formation, and homing ability of EPCs, thus it may be advantageous for EPC targeted therapies.

Chapter 6: Conclusion

6.1 Conclusion

In summary, this study demonstrates the first use of tmSCF as a therapeutic protein for the treatment of peripheral ischemia. Our work supports that there is minimal mast cell activation by tmSCF-based therapies and that the activity can be targeted to specific cell types through the use of different nanocarriers. While both nanodisc and proteoliposome-delivered tmSCF are beneficial in treating ischemia, our work supports that the proteoliposomal tmSCF may act through the stimulation of angiogenesis in endothelial cells and proliferation of bone marrow cells. Conversely, nanodisc delivered tmSCF acts primarily through the mobilization and recruitment of bone marrow cells and stimulation of a $CD34^-$ EPC population. Overall, our work suggests some of the benefits of SCF treatment can be recapitulated using tmSCF therapies and these appear to have improved safety as well as tailorable activity based on the lipid nanocarrier used.

6.2 Future work

6.2.1 Endocytosis mechanism with inhibitors, and its interaction with signaling pathways

Due to the COVID-19 outbreak, I could not finish the inhibitor studies with clathrin or caveolin blockers in chapter 5. Wortmannin is a PI3K inhibitor, indirectly blocking clathrin-mediated endocytosis. Therefore, wortmannin may not be specific to clathrin. Thus, we would like to try Pitstop that is more specific to clathrin. We will also try these inhibitor studies on mast cells and EPCs to examine if we see the similar outcome with the immunostaining studies conducted in the section 5.3.2.

In the discussion in chapter 5, I describe that it may be possible that endocytosis controls the signaling cascades. The relation of endocytosis and signaling is complicated, and it is possible that signaling can control endocytosis mechanism. For example, Src kinases function as downstream mediators of RTKs to increase the rate of de novo clathrin-coated pit formation by phosphorylating the clathrin heavy chain, leading to the assembly of the clathrin triskelion[216]. It

may be possible that kinase downstream of c-Kit signaling may trigger phosphorylation of clahtrin or caveolin, which increases the recruitment of clatrin/caveolin to the surface. It may be interesting to inhibit the kinase activities such as SRC kinase or PI3 kinase and examine the degree of phosphorylation of clathrin or caveolin. These experiments may give us an insight into the link between receptor signaling and induction of endocytosis.

6.2.2 BONE MARROW TRANSPLANTATION

Our study indicated that EPCs mobilize to peripheral blood after subcutaneous injection of tmSCFNDs treatment. To further investigate the mobilization and homing ability of EPCs, we will conduct GFP-expressing bone marrow transplantation. Eight to 10-week-old WT mice will be irradiated with 12.0 Gy of γ-irradiation in 2 divided doses, 2 hours apart, on the day of surgery. Bone marrow cells will be isolated from the femur and tibia of 8 to 10-week-old transgenic mice constitutively producing Green Fluorescent Proteins (GFPs). For bone marrow transplantation, wild-type irradiated mice will be injected with 0.2 ml PBS with or without 2.0×10^5 BM mononuclear cells via tail veins at 2 hours after irradiation. Within 2–3 weeks, control animals should die while transplanted animals will survive and display 99% donor-derived cells in the bone marrow. We will then conduct hind limb ischemia surgery on the BM transplanted mice then treat with our treatments. Peripheral blood and ischemic muscle tissues will be harvested after 1, 3, 4, 7 days of treatments to track the GFP positive BM cells. This will give us an additional confirmation of mobilization and homing ability of EPCs treated by tmSCF-based therapies.

References

1 Economic Costs of Diabetes in the U.S. in 2012. *Diabetes Care* **36**, 1033, doi:10.2337/dc12-2625 (2013).

2 Futrega, K., King, M., Lott, W. B. & Doran, M. R. Treating the whole not the hole: necessary coupling of technologies for diabetic foot ulcer treatment. *Trends in Molecular Medicine* **20**, 137-142, doi:10.1016/j.molmed.2013.12.004 (2014).

3 Frank J. Tursi, C. W., and Mary Yost. Essential Keys To Diagnosing And Treating PAD In Patients With Diabetes. *Podiatry Today* **30**, 12-17 (2017).

4 Norgren, L. *et al.* Inter-Society Consensus for the Management of Peripheral Arterial Disease (TASC II). *Journal of Vascular Surgery* **45**, S5-S67, doi:10.1016/j.jvs.2006.12.037 (2007).

5 Biscetti, F. *et al.* The Role of the Stem Cells Therapy in the Peripheral Artery Disease. *Int J Mol Sci* **20**, 2233, doi:10.3390/ijms20092233 (2019).

6 Raval, Z. & Losordo, D. W. Cell therapy of peripheral arterial disease: from experimental findings to clinical trials. *Circulation research* **112**, 1288-1302, doi:10.1161/CIRCRESAHA.113.300565 (2013).

7 Nikol, S. *et al.* Therapeutic Angiogenesis With Intramuscular NV1FGF Improves Amputation-free Survival in Patients With Critical Limb Ischemia. *Molecular Therapy* **16**, 972-978, doi:https://doi.org/10.1038/mt.2008.33 (2008).

8 Morishita, R. *et al.* Phase I/IIa Clinical Trial of Therapeutic Angiogenesis Using Hepatocyte Growth Factor Gene Transfer to Treat Critical Limb Ischemia. *Arteriosclerosis, Thrombosis, and Vascular Biology* **31**, 713-720, doi:10.1161/ATVBAHA.110.219550 (2011).

9 Kusumanto, Y. H. *et al.* Treatment with Intramuscular Vascular Endothelial Growth Factor Gene Compared with Placebo for Patients with Diabetes Mellitus and Critical Limb Ischemia: A Double-Blind Randomized Trial. *Human Gene Therapy* **17**, 683-691, doi:10.1089/hum.2006.17.683 (2006).

10 Shigematsu, H. *et al.* Randomized, double-blind, placebo-controlled clinical trial of hepatocyte growth factor plasmid for critical limb ischemia. *Gene Therapy* **17**, 1152-1161, doi:10.1038/gt.2010.51 (2010).

11 Lederman, R. J. *et al.* Therapeutic angiogenesis with recombinant fibroblast growth factor-2 for intermittent claudication (the TRAFFIC study): a randomised trial. *The Lancet* **359**, 2053-2058, doi:https://doi.org/10.1016/S0140-6736(02)08937-7 (2002).

12 Simons, M. *et al.* Pharmacological Treatment of Coronary Artery Disease With Recombinant Fibroblast Growth Factor-2. *Circulation* **105**, 788-793, doi:10.1161/hc0802.104407 (2002).

13 Henry Timothy, D. *et al.* The VIVA Trial. *Circulation* **107**, 1359-1365, doi:10.1161/01.CIR.0000061911.47710.8A (2003).

14 Broudy, V. C. Stem Cell Factor and Hematopoiesis. *Blood* **90**, 1345-1364, doi:10.1182/blood.V90.4.1345 (1997).

15 Dehbashi, M., Kamali, E. & Vallian, S. Comparative genomics of human stem cell factor (SCF). *Mol Biol Res Commun* **6**, 1-11 (2017).

16 Matsui, J., Wakabayashi, T., Asada, M., Yoshimatsu, K. & Okada, M. Stem Cell Factor/c-kit Signaling Promotes the Survival, Migration, and Capillary Tube Formation

of Human Umbilical Vein Endothelial Cells. **279**, 18600-18607, doi:10.1074/jbc.m311643200 (2004).

17 Zhao, L. R., Piao, C. S., Murikinati, S. R. & Gonzalez-Toledo, M. E. The role of stem cell factor and granulocyte-colony stimulating factor in treatment of stroke. *Recent Pat CNS Drug Discov* **8**, 2-12, doi:10.2174/1574889811308010002 (2013).

18 Yaniz-Galende, E. *et al.* Stem cell factor gene transfer promotes cardiac repair after myocardial infarction via in situ recruitment and expansion of c-kit+ cells. *Circulation research* **111**, 1434-1445, doi:10.1161/CIRCRESAHA.111.263830 (2012).

19 Ping, S. *et al.* Stem cell factor and granulocyte colony-stimulating factor promote brain repair and improve cognitive function through VEGF-A in a mouse model of CADASIL. *Neurobiology of Disease* **132**, 104561, doi:https://doi.org/10.1016/j.nbd.2019.104561 (2019).

20 Bath, P. M. W., Sprigg, N. & England, T. Colony stimulating factors (including erythropoietin, granulocyte colony stimulating factor and analogues) for stroke. *Cochrane Database of Systematic Reviews*, doi:10.1002/14651858.CD005207.pub4 (2013).

21 Stiff, P. *et al.* A randomized phase 2 study of PBPC mobilization by stem cell factor and filgrastim in heavily pretreated patients with Hodgkin's disease or non-Hodgkin's lymphoma. *Bone Marrow Transplantation* **26**, 471-481, doi:10.1038/sj.bmt.1702531 (2000).

22 Weaver, A. *et al.* Randomized comparison of progenitor-cell mobilization using chemotherapy, stem-cell factor, and filgrastim or chemotherapy plus filgrastim alone in patients with ovarian cancer. *Journal of Clinical Oncology* **16**, 2601-2612, doi:10.1200/JCO.1998.16.8.2601 (1998).

23 Costa, J. J. *et al.* Recombinant human stem cell factor (kit ligand) promotes human mast cell and melanocyte hyperplasia and functional activation in vivo. *J Exp Med* **183**, 2681-2686, doi:10.1084/jem.183.6.2681 (1996).

24 Johnsen, H. E. *et al.* Priming with r-metHuSCF and filgrastim or chemotherapy and filgrastim in patients with malignant lymphomas: a randomized phase II pilot study of mobilization and engraftment. *Bone Marrow Transplantation* **46**, 44-51, doi:10.1038/bmt.2010.84 (2011).

25 Costa, J. J. The therapeutic use of hematopoietic growth factors. *Journal of Allergy and Clinical Immunology* **101**, 1-6, doi:10.1016/S0091-6749(98)70185-X (1998).

26 Driessen, R. L., Johnston, H. M. & Nilsson, S. K. Membrane-bound stem cell factor is a key regulator in the initial lodgment of stem cells within the endosteal marrow region. *Experimental Hematology* **31**, 1284-1291, doi:https://doi.org/10.1016/j.exphem.2003.08.015 (2003).

27 Miyazawa, K. *et al.* Membrane-bound Steel factor induces more persistent tyrosine kinase activation and longer life span of c-kit gene-encoded protein than its soluble form. *Blood* **85**, 641-649, doi:10.1182/blood.V85.3.641.bloodjournal853641 (1995).

28 Friel, J. *et al.* Hierarchy of Stroma-derived Factors in Supporting Growth of Stroma-dependent Hemopoietic Cells: Membrane-bound SCF is Sufficient to Confer Stroma Competence to Epithelial Cells. *Growth Factors* **20**, 35-51, doi:10.1080/08977190290022211 (2002).

29 Liang, J. *et al.* The C-Kit Receptor-Mediated Signal Transduction and Tumor-Related Diseases. *International Journal of Biological Sciences* **9**, 435-443, doi:10.7150/ijbs.6087 (2013).
30 Diagnosis and Classification of Diabetes Mellitus. *Diabetes Care* **37**, S81, doi:10.2337/dc14-S081 (2014).
31 Rajendran, P. *et al.* The vascular endothelium and human diseases. *International journal of biological sciences* **9**, 1057-1069, doi:10.7150/ijbs.7502 (2013).
32 Avogaro, A., Albiero, M., Menegazzo, L., de Kreutzenberg, S. & Fadini, G. P. Endothelial Dysfunction in Diabetes. *The role of reparatory mechanisms* **34**, S285-S290, doi:10.2337/dc11-s239 %J Diabetes Care (2011).
33 Thiruvoipati, T., Kielhorn, C. E. & Armstrong, E. J. Peripheral artery disease in patients with diabetes: Epidemiology, mechanisms, and outcomes. *World journal of diabetes* **6**, 961-969, doi:10.4239/wjd.v6.i7.961 (2015).
34 Brem, H. & Tomic-Canic, M. Cellular and molecular basis of wound healing in diabetes. *The Journal of clinical investigation* **117**, 1219-1222, doi:10.1172/JCI32169 (2007).
35 Rice, J. B. *et al.* Burden of diabetic foot ulcers for medicare and private insurers. *Diabetes Care* **37**, 651-658, doi:10.2337/dc13-2176 (2014).
36 Das, S. & Baker, A. B. Biomaterials and Nanotherapeutics for Enhancing Skin Wound Healing. *Frontiers in bioengineering and biotechnology* **4**, 82-82, doi:10.3389/fbioe.2016.00082 (2016).
37 Das, S. & Baker, A. B. Biomaterials and Nanotherapeutics for Enhancing Skin Wound Healing. *Front Bioeng Biotechnol* **4**, 82, doi:10.3389/fbioe.2016.00082 (2016).
38 Treat-Jacobson, D. <https://www.heart.org/-/media/files/health-topics/peripheral-artery-disease/pad-webinars/webinar-3-exercise-in-pad-slides.pdf?la=en&hash=6541C4273EA61CCF8E6D7C58725DA08502C5684A> (
39 Dawson, D. L. *et al.* A comparison of cilostazol and pentoxifylline for treating intermittent claudication. *The American Journal of Medicine* **109**, 523-530, doi:https://doi.org/10.1016/S0002-9343(00)00569-6 (2000).
40 Hirsch Alan, T. *et al.* ACC/AHA 2005 Practice Guidelines for the Management of Patients With Peripheral Arterial Disease (Lower Extremity, Renal, Mesenteric, and Abdominal Aortic). *Circulation* **113**, e463-e654, doi:10.1161/CIRCULATIONAHA.106.174526 (2006).
41 Treatment Strategies for Patients With Peripheral Artery Disease (PAD). *Agency for Healthcare Research and Quality* (2013). <https://effectivehealthcare.ahrq.gov/products/peripheral-artery-disease-treatment/research-protocol>.
42 Ramcharitar, S., Patterson, M. S., van Geuns, R. J., van Meighem, C. & Serruys, P. W. Technology Insight: magnetic navigation in coronary interventions. *Nature Clinical Practice Cardiovascular Medicine* **5**, 148-156, doi:10.1038/ncpcardio1095 (2008).
43 Cancer research product guide **edition 3** (2015).
44 Heil, M., Eitenmüller, I., Schmitz-Rixen, T., & Schaper, W. Arteriogenesis versus angiogenesis: similarities and differences. Journal of cellular and molecular medicine. *Journal of cellular and molecular medicine* **10**, 45-55 (2006).
45 Kurzrock, R. *Holland-Frei Cancer Medicine*. (BC Decker, 2003).
46 Bozzuto, G. & Molinari, A. Liposomes as nanomedical devices. *Int J Nanomedicine* **10**, 975-999, doi:10.2147/IJN.S68861 (2015).

47 *DOPC* <https://echelon-inc.com/product/dopc-181-181/> (
48 Du, Z., Munye, M. M., Tagalakis, A. D., Manunta, M. D. I. & Hart, S. L. The Role of the Helper Lipid on the DNA Transfection Efficiency of Lipopolyplex Formulations. *Scientific Reports* **4**, 7107, doi:10.1038/srep07107 (2014).
49 *Sphingomylein and related sphingophospholipids*, <https://www.lipidhome.co.uk/lipids/sphingo/sph/index.htm> (
50 *What are the advantages/disadvantages of including cholesterol in my liposomes?*, <https://avantilipids.com/tech-support/faqs/cholesterol-advantages-disadvantages> (
51 McLean, M. A., Gregory, M. C. & Sligar, S. G. Nanodiscs: A Controlled Bilayer Surface for the Study of Membrane Proteins. *Annu Rev Biophys*, 10.1146/annurev-biophys-070816-033620, doi:10.1146/annurev-biophys-070816-033620 (2018).
52 Rouck, J. E., Krapf, J. E., Roy, J., Huff, H. C. & Das, A. Recent advances in nanodisc technology for membrane protein studies (2012-2017). *FEBS Lett* **591**, 2057-2088, doi:10.1002/1873-3468.12706 (2017).
53 Asahara, T. *et al.* Isolation of Putative Progenitor Endothelial Cells for Angiogenesis. *Science* **275**, 964, doi:10.1126/science.275.5302.964 (1997).
54 Chopra, H., Hung, M. K., Kwong, D. L., Zhang, C. F. & Pow, E. H. N. Insights into Endothelial Progenitor Cells: Origin, Classification, Potentials, and Prospects. *Stem Cells Int* **2018**, 9847015-9847015, doi:10.1155/2018/9847015 (2018).
55 Lertkiatmongkol, P., Liao, D., Mei, H., Hu, Y. & Newman, P. J. Endothelial functions of platelet/endothelial cell adhesion molecule-1 (CD31). *Curr Opin Hematol* **23**, 253-259, doi:10.1097/MOH.0000000000000239 (2016).
56 Qin, M. *et al.* An effective ex-vivo approach for inducing endothelial progenitor cells from umbilical cord blood CD34+ cells. *Stem Cell Research & Therapy* **8**, 25, doi:10.1186/s13287-017-0482-9 (2017).
57 Shin, J.-W. *et al.* Isolation of endothelial progenitor cells from cord blood and induction of differentiation by ex vivo expansion. *Yonsei Med J* **46**, 260-267, doi:10.3349/ymj.2005.46.2.260 (2005).
58 Takahashi, T. *et al.* Ischemia- and cytokine-induced mobilization of bone marrow-derived endothelial progenitor cells for neovascularization. *Nature Medicine* **5**, 434-438, doi:10.1038/7434 (1999).
59 Kaksonen, M. & Roux, A. Mechanisms of clathrin-mediated endocytosis. *Nature Reviews Molecular Cell Biology* **19**, 313-326, doi:10.1038/nrm.2017.132 (2018).
60 Kiss, A. L. & Botos, E. Endocytosis via caveolae: alternative pathway with distinct cellular compartments to avoid lysosomal degradation? *J Cell Mol Med* **13**, 1228-1237, doi:10.1111/j.1582-4934.2009.00754.x (2009).
61 Bastiani, M. & Parton, R. G. Caveolae at a glance. *Journal of Cell Science* **123**, 3831, doi:10.1242/jcs.070102 (2010).
62 Lorena Lobos-González, L. A., Gonzalo Fernández, Carlos Sanhueza and Andrew F.G Quest. Caveolin-1 in Melanoma Progression. *Advances in Malignant Melanoma*, 187-214 (2010).
63 National Diabetes Statistics Report. (Centers for Disease Control and Prevention, Atlanta, GA, 2017).
64 Barrientos, S., Brem, H., Stojadinovic, O. & Tomic-Canic, M. Clinical application of growth factors and cytokines in wound healing. *Wound repair and regeneration : official*

publication of the Wound Healing Society [and] the European Tissue Repair Society **22**, 569-578, doi:10.1111/wrr.12205 (2014).

65 Monteforte, A. J. *et al.* Glypican-1 nanoliposomes for potentiating growth factor activity in therapeutic angiogenesis. *Biomaterials* **94**, 45-56, doi:10.1016/j.biomaterials.2016.03.048 (2016).

66 Takematsu, E. *et al.* Genome wide analysis of gene expression changes in skin from patients with type 2 diabetes. *PLoS One* **15**, e0225267, doi:10.1371/journal.pone.0225267 (2020).

67 Hebbar, P. *et al.* Genetic risk variants for metabolic traits in Arab populations. *Scientific reports* **7**, 40988-40988, doi:10.1038/srep40988 (2017).

68 Bettahi, I. *et al.* Genome-wide transcriptional analysis of differentially expressed genes in diabetic, healing corneal epithelial cells: hyperglycemia-suppressed TGFβ3 expression contributes to the delay of epithelial wound healing in diabetic corneas. *Diabetes* **63**, 715-727, doi:10.2337/db13-1260 (2014).

69 Yan, J. *et al.* Diabetes impairs wound healing by Dnmt1-dependent dysregulation of hematopoietic stem cells differentiation towards macrophages. *Nature Communications* **9**, 33, doi:10.1038/s41467-017-02425-z (2018).

70 Chen, Y.-T., Liao, J.-W., Tsai, Y.-C. & Tsai, F.-J. Inhibition of DNA methyltransferase 1 increases nuclear receptor subfamily 4 group A member 1 expression and decreases blood glucose in type 2 diabetes. *Oncotarget* **7**, 39162-39170, doi:10.18632/oncotarget.10043 (2016).

71 Thimmarayappa, J. *et al.* Inhibition of growth hormone receptor gene expression by saturated fatty acids: Role of Kruppel-like zinc finger factor, ZBP-89. *Mol Endocrinol* **20**, 2747-2760, doi:10.1210/me.2006-0128 (2006).

72 Zhao, X. *et al.* Inhibition of CaMKIV relieves streptozotocin-induced diabetic neuropathic pain through regulation of HMGB1. *Bmc Anesthesiol* **16**, doi:ARTN 27 10.1186/s12871-016-0191-4 (2016).

73 Zhao, X. *et al.* Inhibition of CaMKIV relieves streptozotocin-induced diabetic neuropathic pain through regulation of HMGB1. *Bmc Anesthesiol* **16**, 27, doi:10.1186/s12871-016-0191-4 (2016).

74 Iacobazzi, V. *et al.* Transcription of the mitochondrial citrate carrier gene: Identification of a silencer and its binding protein ZNF224. *Biochem Bioph Res Co* **386**, 186-191, doi:10.1016/j.bbrc.2009.06.003 (2009).

75 Kaplan, R. S., Oliveira, D. L. & Wilson, G. L. Streptozotocin-induced alterations in the levels of functional mitochondrial anion transport proteins. *Arch Biochem Biophys* **280**, 181-191 (1990).

76 Gnoni, G. V. *et al.* Reduced activity and expression of mitochondrial citrate carrier in streptozotocin-induced diabetic rats. *Endocrinology* **151**, 1551-1559, doi:10.1210/en.2009-1352 (2010).

77 Meng, Z.-X., Wang, L., Xiao, Y. & Lin, J. D. The Baf60c/Deptor Pathway Links Skeletal Muscle Inflammation to Glucose Homeostasis in Obesity. **63**, 1533-1545, doi:10.2337/db13-1061 %J Diabetes (2014).

78 Meng, W. *et al.* A Genome-wide Association Study Provides Evidence of Sex-specific Involvement of Chr1p35.1 (ZSCAN20-TLR12P) and Chr8p23.1 (HMGB1P46) With Diabetic Neuropathic Pain. *EBioMedicine* **2**, 1386-1393, doi:https://doi.org/10.1016/j.ebiom.2015.08.001 (2015).

79 Suryavanshi, S. V., Jadhav, S. M. & McConnell, B. K. Polymorphisms/Mutations in A-Kinase Anchoring Proteins (AKAPs): Role in the Cardiovascular System. *Journal of cardiovascular development and disease* **5**, 7, doi:10.3390/jcdd5010007 (2018).
80 Wang, X. *et al.* Histone deacetylase 4 selectively contributes to podocyte injury in diabetic nephropathy. *Kidney International* **86**, 712-725, doi:https://doi.org/10.1038/ki.2014.111 (2014).
81 Ung, C. *et al.* Whole exome sequencing identification of novel candidate genes in patients with proliferative diabetic retinopathy. *Vision Research* **139**, 168-176, doi:https://doi.org/10.1016/j.visres.2017.03.007 (2017).
82 Anderson, A. A. *et al.* Pancreatic islet expression profiling in diabetes-prone C57BLKS/J mice reveals transcriptional differences contributed by DBA loci, including Plagl1 and Nnt. *PathoGenetics* **2**, 1-1, doi:10.1186/1755-8417-2-1 (2009).
83 Berry, G. J., Frielle, C., Brucklacher, R. M., Salzberg, A. C. & Waldner, H. Identifying type 1 diabetes candidate genes by DNA microarray analysis of islet-specific CD4 + T cells. *Genomics data* **5**, 184-188, doi:10.1016/j.gdata.2015.05.041 (2015).
84 Baldari, S. *et al.* Hyperglycemia triggers HIPK2 protein degradation. *Oncotarget* **8**, 1190-1203, doi:10.18632/oncotarget.13595 (2016).
85 Small, E. M., Vokes, S. A., Garriock, R. J., Li, D. & Krieg, P. A. Developmental expression of the Xenopus Nkx2-1 and Nkx2-4 genes. *Mech Dev* **96**, 259-262 (2000).
86 Lazzaro, D., Price, M., Defelice, M. & Dilauro, R. The Transcription Factor-Ttf-1 Is Expressed at the Onset of Thyroid and Lung Morphogenesis and in Restricted Regions of the Fetal Brain. *Development* **113**, 1093-& (1991).
87 Malt, E. A., Juhasz, K., Malt, U. F. & Naumann, T. A Role for the Transcription Factor Nk2 Homeobox 1 in Schizophrenia: Convergent Evidence from Animal and Human Studies. *Frontiers in behavioral neuroscience* **10**, 59, doi:10.3389/fnbeh.2016.00059 (2016).
88 Coon, E. A., Ahlskog, J., Patterson, M. C., Niu, Z. & Milone, M. Expanding phenotypic spectrum of nkx2-1–related disorders—mitochondrial and immunologic dysfunction. *JAMA Neurology* **73**, 237-238, doi:10.1001/jamaneurol.2015.2976 (2016).
89 Sivitz, W. I. & Yorek, M. A. Mitochondrial dysfunction in diabetes: from molecular mechanisms to functional significance and therapeutic opportunities. *Antioxidants & redox signaling* **12**, 537-577, doi:10.1089/ars.2009.2531 (2010).
90 Magli, A. *et al.* Time-dependent Pax3-mediated chromatin remodeling and cooperation with Six4 and Tead2 specify the skeletal myogenic lineage in developing mesoderm. *PLoS Biol* **17**, e3000153, doi:10.1371/journal.pbio.3000153 (2019).
91 Chakroun, I. *et al.* Genome-wide association between Six4, MyoD, and the histone demethylase Utx during myogenesis. *FASEB J* **29**, 4738-4755, doi:10.1096/fj.15-277053 (2015).
92 Konishi, Y., Ikeda, K., Iwakura, Y. & Kawakami, K. Six1 and Six4 promote survival of sensory neurons during early trigeminal gangliogenesis. *Brain Res* **1116**, 93-102, doi:10.1016/j.brainres.2006.07.103 (2006).
93 Said, G. Diabetic neuropathy--a review. *Nat Clin Pract Neurol* **3**, 331-340, doi:10.1038/ncpneuro0504 (2007).
94 D'Souza, D. M., Al-Sajee, D. & Hawke, T. J. Diabetic myopathy: impact of diabetes mellitus on skeletal muscle progenitor cells. *Front Physiol* **4**, 379, doi:10.3389/fphys.2013.00379 (2013).

95 Andersen, H., Schmitz, O. & Nielsen, S. Decreased isometric muscle strength after acute hyperglycaemia in Type 1 diabetic patients. *Diabet Med* **22**, 1401-1407, doi:10.1111/j.1464-5491.2005.01649.x (2005).
96 Xu, J. *et al.* Sequence analysis and structure prediction of ABHD16A and the roles of the ABHD family members in human disease. *Open biology* **8**, 180017, doi:10.1098/rsob.180017 (2018).
97 Hsieh, Y.-Y. *et al.* Human lymphocyte antigen B-associated transcript 2, 3, and 5 polymorphisms and haplotypes are associated with susceptibility of Kawasaki disease and coronary artery aneurysm. **24**, 262-268, doi:doi:10.1002/jcla.20409 (2010).
98 Gaultier, A., Hollister, M., Reynolds, I., Hsieh, E.-h. & Gonias, S. L. LRP1 regulates remodeling of the extracellular matrix by fibroblasts. *Matrix biology : journal of the International Society for Matrix Biology* **29**, 22-30, doi:10.1016/j.matbio.2009.08.003 (2010).
99 Nasarre, L. *et al.* Low density lipoprotein receptor–related protein 1 is upregulated in epicardial fat from type 2 diabetes mellitus patients and correlates with glucose and triglyceride plasma levels. *Acta Diabetologica* **51**, 23-30, doi:10.1007/s00592-012-0436-8 (2014).
100 Park, S. Y. & Kim, I. S. Engulfment signals and the phagocytic machinery for apoptotic cell clearance. *Exp Mol Med* **49**, e331, doi:10.1038/emm.2017.52 (2017).
101 Kiss, R. S. *et al.* The lipoprotein receptor-related protein-1 (LRP) adapter protein GULP mediates trafficking of the LRP ligand prosaposin, leading to sphingolipid and free cholesterol accumulation in late endosomes and impaired efflux. *J Biol Chem* **281**, 12081-12092, doi:10.1074/jbc.M600621200 (2006).
102 Wang, T., Baron, M. & Trump, D. An overview of Notch3 function in vascular smooth muscle cells. *Prog Biophys Mol Biol* **96**, 499-509, doi:10.1016/j.pbiomolbio.2007.07.006 (2008).
103 Yuan, X. & Dong, Z. The Association Between the Genetic Variants of the NOTCH3 Gene and Ischemic Stroke Risk. *Medical science monitor : international medical journal of experimental and clinical research* **22**, 3910-3914, doi:10.12659/MSM.896297 (2016).
104 Ozbayer, C. *et al.* The rs1043994 and rs3815188 genetic variations of the NOTCH3 gene and risk of type 2 diabetes mellitus. *Biotechnol Biotec Eq* **31**, 563-567, doi:10.1080/13102818.2017.1294034 (2017).
105 Roy, S. *et al.* Characterization of a preclinical model of chronic ischemic wound. *Physiol Genomics* **37**, 211-224, doi:10.1152/physiolgenomics.90362.2008 (2009).
106 Wong, G. H., Elwell, J. H., Oberley, L. W. & Goeddel, D. V. Manganous superoxide dismutase is essential for cellular resistance to cytotoxicity of tumor necrosis factor. *Cell* **58**, 923-931 (1989).
107 Wang, Y., Branicky, R., Noe, A. & Hekimi, S. Superoxide dismutases: Dual roles in controlling ROS damage and regulating ROS signaling. *J Cell Biol* **217**, 1915-1928, doi:10.1083/jcb.201708007 (2018).
108 Bellot, G. L. *et al.* MnSOD is implicated in accelerated wound healing upon Negative Pressure Wound Therapy (NPWT): A case in point for MnSOD mimetics as adjuvants for wound management. *Redox Biol* **20**, 307-320, doi:10.1016/j.redox.2018.10.014 (2019).

109 Fujiwara, T. *et al.* Extracellular superoxide dismutase deficiency impairs wound healing in advanced age by reducing neovascularization and fibroblast function. *Exp Dermatol* **25**, 206-211, doi:10.1111/exd.12909 (2016).
110 Lawi, Z. K. K. Investigation of SOD2 Gene Polymorphism in the Patients with Type Two Diabetes Disease in Babylon Province. *Journal of Global Pharma Thechnology* **10**, 70-75 (2018).
111 Tian, C., Fang, S., Du, X. & Jia, C. Association of the C47T polymorphism in SOD2 with diabetes mellitus and diabetic microvascular complications: a meta-analysis. *Diabetologia* **54**, 803-811, doi:10.1007/s00125-010-2004-5 (2011).
112 Chen, Y., Frost, S. & Byrne, J. A. Dropping in on the lipid droplet- tumor protein D52 (TPD52) as a new regulator and resident protein. *Adipocyte* **5**, 326-332, doi:10.1080/21623945.2016.1148835 (2016).
113 Montgomery, M. K. & Turner, N. Mitochondrial dysfunction and insulin resistance: an update. *Endocr Connect* **4**, R1-R15, doi:10.1530/EC-14-0092 (2015).
114 Sethumadhavan, S. *et al.* Mitochondrial DNA variant for complex I reveals a role in diabetic cardiac remodeling. *The Journal of biological chemistry* **287**, 22174-22182, doi:10.1074/jbc.M111.327866 (2012).
115 Sinyov, V. V. *et al.* The heteroplasmy level of some mutations in gene MT-CYB among women with asymptomatic atherosclerosis. *Russ J Genet+* **52**, 847-852, doi:10.1134/S1022795416080123 (2016).
116 Van Vranken, J. G. *et al.* SDHAF4 promotes mitochondrial succinate dehydrogenase activity and prevents neurodegeneration. *Cell metabolism* **20**, 241-252, doi:10.1016/j.cmet.2014.05.012 (2014).
117 Nilsson, E. *et al.* Altered DNA Methylation and Differential Expression of Genes Influencing Metabolism and Inflammation in Adipose Tissue From Subjects With Type 2 Diabetes. **63**, 2962-2976, doi:10.2337/db13-1459 %J Diabetes (2014).
118 Xie, X. *et al.* Proteomics analyses of subcutaneous adipocytes reveal novel abnormalities in human insulin resistance. *Obesity (Silver Spring, Md.)* **24**, 1506-1514, doi:10.1002/oby.21528 (2016).
119 Rovira-Llopis, S. *et al.* Mitochondrial dynamics in type 2 diabetes: Pathophysiological implications. *Redox Biology* **11**, 637-645, doi:https://doi.org/10.1016/j.redox.2017.01.013 (2017).
120 Kulkarni, S. S. *et al.* Mfn1 Deficiency in the Liver Protects Against Diet-Induced Insulin Resistance and Enhances the Hypoglycemic Effect of Metformin. **65**, 3552-3560, doi:10.2337/db15-1725 %J Diabetes (2016).
121 Popov, K. M. (National Institutes of Health, University of Alabama Birmingham, 2010).
122 Pink, R. C. *et al.* Pseudogenes: pseudo-functional or key regulators in health and disease? *RNA* **17**, 792-798, doi:10.1261/rna.2658311 (2011).
123 Ansseau, E. *et al.* Homologous Transcription Factors DUX4 and DUX4c Associate with Cytoplasmic Proteins during Muscle Differentiation. *PloS one* **11**, e0146893-e0146893, doi:10.1371/journal.pone.0146893 (2016).
124 Bosnakovski, D., Daughters, R. S., Xu, Z., Slack, J. M. W. & Kyba, M. Biphasic myopathic phenotype of mouse DUX, an ORF within conserved FSHD-related repeats. *PloS one* **4**, e7003-e7003, doi:10.1371/journal.pone.0007003 (2009).

125 Bosnakovski, D. *et al.* Low level DUX4 expression disrupts myogenesis through deregulation of myogenic gene expression. *Sci Rep* **8**, 16957, doi:10.1038/s41598-018-35150-8 (2018).
126 Vanderplanck, C. *et al.* Overexpression of the double homeodomain protein DUX4c interferes with myofibrillogenesis and induces clustering of myonuclei. *Skelet Muscle* **8**, 2, doi:10.1186/s13395-017-0148-4 (2018).
127 Ansseau, E. *et al.* Homologous Transcription Factors DUX4 and DUX4c Associate with Cytoplasmic Proteins during Muscle Differentiation. *PLoS One* **11**, e0146893, doi:10.1371/journal.pone.0146893 (2016).
128 Liu, Y. *et al.* A genetic variant in long non-coding RNA HULC contributes to risk of HBV-related hepatocellular carcinoma in a Chinese population. *PloS one* **7**, e35145-e35145, doi:10.1371/journal.pone.0035145 (2012).
129 Batista, P. J. & Chang, H. Y. Long noncoding RNAs: cellular address codes in development and disease. *Cell* **152**, 1298-1307, doi:10.1016/j.cell.2013.02.012 (2013).
130 Schonrock, N., Harvey, R. P. & Mattick, J. S. Long Noncoding RNAs in Cardiac Development and Pathophysiology. **111**, 1349-1362, doi:doi:10.1161/CIRCRESAHA.112.268953 (2012).
131 Tan, L., Yu, J.-T., Hu, N. & Tan, L. Non-coding RNAs in Alzheimer's Disease. *Molecular Neurobiology* **47**, 382-393, doi:10.1007/s12035-012-8359-5 (2013).
132 Faghihi, M. A. *et al.* Expression of a noncoding RNA is elevated in Alzheimer's disease and drives rapid feed-forward regulation of beta-secretase. *Nature medicine* **14**, 723-730, doi:10.1038/nm1784 (2008).
133 Wang, T.-H. *et al.* Long noncoding RNA CPS1-IT1 suppresses the metastasis of hepatocellular carcinoma by regulating HIF-1α activity and inhibiting epithelial-mesenchymal transition. *Oncotarget* **7**, 43588-43603, doi:10.18632/oncotarget.9635 (2016).
134 Vial, I. N. *et al.* HIF-1α dysfunction in diabetes AU - Thangarajah, Hariharan. *Cell Cycle* **9**, 75-79, doi:10.4161/cc.9.1.10371 (2010).
135 Shi, C. & Wang, M. LINC01118 Modulates Paclitaxel Resistance of Epithelial Ovarian Cancer by Regulating miR-134/ABCC1. *Medical science monitor : international medical journal of experimental and clinical research* **24**, 8831-8839, doi:10.12659/MSM.910932 (2018).
136 Shi, X., Guo, X., Li, X., Wang, M. & Qin, R. Loss of Linc01060 induces pancreatic cancer progression through vinculin-mediated focal adhesion turnover. *Cancer Lett* **433**, 76-85, doi:10.1016/j.canlet.2018.06.015 (2018).
137 Ling, C., Groop, L., Guerra, S. D. & Lupi, R. Calpain-10 expression is elevated in pancreatic islets from patients with type 2 diabetes. *PloS one* **4**, e6558-e6558, doi:10.1371/journal.pone.0006558 (2009).
138 Wight, M. & Werner, A. The functions of natural antisense transcripts. *Essays in biochemistry* **54**, 91-101, doi:10.1042/bse0540091 (2013).
139 Gu, Y. *et al.* Differential gene expression profiling of the sciatic nerve in type 1 and type 2 diabetic mice. *Biomedical reports* **9**, 291-304, doi:10.3892/br.2018.1135 (2018).
140 Blackburn, K., Bustamante-Marin, X., Yin, W., Goshe, M. B. & Ostrowski, L. E. Quantitative Proteomic Analysis of Human Airway Cilia Identifies Previously Uncharacterized Proteins of High Abundance. *J Proteome Res* **16**, 1579-1592, doi:10.1021/acs.jproteome.6b00972 (2017).

141 Gupta, M. *et al.* TSPAN5, ERICH3 and selective serotonin reuptake inhibitors in major depressive disorder: pharmacometabolomics-informed pharmacogenomics. *Mol Psychiatry* **21**, 1717-1725, doi:10.1038/mp.2016.6 (2016).
142 Mangelsdorf, D. J. *et al.* The nuclear receptor superfamily: the second decade. *Cell* **83**, 835-839 (1995).
143 Corton, J. C., Anderson, S. P. & Stauber, A. Central Role of Peroxisome Proliferator–Activated Receptors in the Actions of Peroxisome Proliferators. **40**, 491-518, doi:10.1146/annurev.pharmtox.40.1.491 (2000).
144 Guan, F. *et al.* Two-stage association study to identify the genetic susceptibility of a novel common variant of rs2075290 in ZPR1 to type 2 diabetes. *Scientific reports* **6**, 29586-29586, doi:10.1038/srep29586 (2016).
145 Yoshihito Nogusa, N. Y., Naoki Sumiyoshi, Keiko Takeda, Norihisa Kato Expression of zinc finger protein ZPR1 mRNA in brain is up-regulated in mice fed a high-fat diet. *International journal of molecular medicine* **17(3)**, 491-496 (2006).
146 Hansen, J. S. *et al.* Type 2 diabetes alters metabolic and transcriptional signatures of glucose and amino acid metabolism during exercise and recovery. *Diabetologia* **58**, 1845-1854, doi:10.1007/s00125-015-3584-x (2015).
147 Berry, G. J., Frielle, C., Brucklacher, R. M., Salzberg, A. C. & Waldner, H. Identifying type 1 diabetes candidate genes by DNA microarray analysis of islet-specific CD4 + T cells. *Genom Data* **5**, 184-188, doi:10.1016/j.gdata.2015.05.041 (2015).
148 Bettahi, I. *et al.* Genome-Wide Transcriptional Analysis of Differentially Expressed Genes in Diabetic, Healing Corneal Epithelial Cells: Hyperglycemia-Suppressed TGFβ3 Expression Contributes to the Delay of Epithelial Wound Healing in Diabetic Corneas. **63**, 715-727, doi:10.2337/db13-1260 %J Diabetes (2014).
149 Hien, T. T. *et al.* Elevated Glucose Levels Promote Contractile and Cytoskeletal Gene Expression in Vascular Smooth Muscle via Rho/Protein Kinase C and Actin Polymerization. *The Journal of biological chemistry* **291**, 3552-3568, doi:10.1074/jbc.M115.654384 (2016).
150 Cai, Y. & Zeng, C. GW29-e1533 MYO1F exacerbates atherogenesis and can be as a novel candidate biomarker for patients with obstructive coronary artery disease or advanced atherosclerosis. **72**, C74, doi:10.1016/j.jacc.2018.08.419 %J Journal of the American College of Cardiology (2018).
151 Karthik, D., Ilavenil, S., Kaleeswaran, B., Sunil, S. & Ravikumar, S. Proteomic Analysis of Plasma Proteins in Diabetic Rats by 2D Electrophoresis and MALDI-TOF-MS. *Applied Biochemistry and Biotechnology* **166**, 1507-1519, doi:10.1007/s12010-012-9544-8 (2012).
152 Weijers, R. N. Lipid composition of cell membranes and its relevance in type 2 diabetes mellitus. *Curr Diabetes Rev* **8**, 390-400 (2012).
153 Gottfried, I., Ehrlich, M. & Ashery, U. The Sla2p/HIP1/HIP1R family: similar structure, similar function in endocytosis? **38**, 187-191, doi:10.1042/BST0380187 %J Biochemical Society Transactions (2010).
154 Berchtold, L. A. *et al.* Huntingtin-interacting protein 14 is a type 1 diabetes candidate protein regulating insulin secretion and β-cell apoptosis. **108**, E681-E688, doi:10.1073/pnas.1104384108 %J Proceedings of the National Academy of Sciences (2011).
155 in *Type 2 Diabetes Mellitus_Pancreas_GSE2470* (Harmonizome).

156 Rodríguez-Fraticelli, A. E. *et al.* Developmental regulation of apical endocytosis controls epithelial patterning in vertebrate tubular organs. *Nature cell biology* **17**, 241-250, doi:10.1038/ncb3106 (2015).
157 Le Guelte, A. & Macara, I. G. Plasmolipin--a new player in endocytosis and epithelial development. *The EMBO journal* **34**, 1147-1148, doi:10.15252/embj.201591448 (2015).
158 Shu, B. & Yang, R. H. Notch1 Signaling Regulates Wound Healing via Changing the Characteristics of Epidermal Stem Cells. *Journal of Stem Cell Research & Therapy* **2016**, doi:10.4172/2157-7633.1000348 (2016).
159 Khalfaoui, T. *et al.* Laminin receptor 37/67LR regulates adhesion and proliferation of normal human intestinal epithelial cells. *PLoS One* **8**, e74337, doi:10.1371/journal.pone.0074337 (2013).
160 Miragliotta, V., Lussier, J. G. & Theoret, C. L. Laminin receptor 1 is differentially expressed in thoracic and limb wounds in the horse. *Vet Dermatol* **20**, 27-34, doi:10.1111/j.1365-3164.2008.00718.x (2009).
161 Longmate, W. M. *et al.* Suppression of integrin alpha3beta1 by alpha9beta1 in the epidermis controls the paracrine resolution of wound angiogenesis. *J Cell Biol* **216**, 1473-1488, doi:10.1083/jcb.201510042 (2017).
162 Margadant, C. *et al.* Integrin alpha3beta1 inhibits directional migration and wound re-epithelialization in the skin. *J Cell Sci* **122**, 278-288, doi:10.1242/jcs.029108 (2009).
163 Reynolds, L. E. *et al.* alpha3beta1 integrin-controlled Smad7 regulates reepithelialization during wound healing in mice. *J Clin Invest* **118**, 965-974, doi:10.1172/JCI33538 (2008).
164 Weis, S. M. & Cheresh, D. A. alphaV integrins in angiogenesis and cancer. *Cold Spring Harb Perspect Med* **1**, a006478, doi:10.1101/cshperspect.a006478 (2011).
165 Longmate, W. M. & Dipersio, C. M. Integrin Regulation of Epidermal Functions in Wounds. *Adv Wound Care (New Rochelle)* **3**, 229-246, doi:10.1089/wound.2013.0516 (2014).
166 Gragnano, F. *et al.* The Role of von Willebrand Factor in Vascular Inflammation: From Pathogenesis to Targeted Therapy. *Mediators Inflamm* **2017**, 5620314, doi:10.1155/2017/5620314 (2017).
167 Frankel, D. S. *et al.* Von Willebrand factor, type 2 diabetes mellitus, and risk of cardiovascular disease: the framingham offspring study. *Circulation* **118**, 2533-2539, doi:10.1161/CIRCULATIONAHA.108.792986 (2008).
168 Seligman, B. G., Biolo, A., Polanczyk, C. A., Gross, J. L. & Clausell, N. Increased plasma levels of endothelin 1 and von Willebrand factor in patients with type 2 diabetes and dyslipidemia. **23**, 1395-1400, doi:10.2337/diacare.23.9.1395 %J Diabetes Care (2000).
169 Mannucci, P. M. von Willebrand Factor. **18**, 1359-1362, doi:doi:10.1161/01.ATV.18.9.1359 (1998).
170 Tajhya, R. B. *et al.* Functional KCa1.1 channels are crucial for regulating the proliferation, migration and differentiation of human primary skeletal myoblasts. *Cell Death Dis* **7**, e2426, doi:10.1038/cddis.2016.324 (2016).
171 Tanner, M. R. *et al.* KCa1.1 and Kv1.3 channels regulate the interactions between fibroblast-like synoviocytes and T lymphocytes during rheumatoid arthritis. *Arthritis Res Ther* **21**, 6, doi:10.1186/s13075-018-1783-9 (2019).
172 Tanner, M. R., Pennington, M. W., Laragione, T., Gulko, P. S. & Beeton, C. KCa1.1 channels regulate beta1-integrin function and cell adhesion in rheumatoid arthritis

fibroblast-like synoviocytes. *FASEB J* **31**, 3309-3320, doi:10.1096/fj.201601097R (2017).
173 Takagi, N. *et al.* IL-17A promotes neutrophilic inflammation and disturbs acute wound healing in skin. *Exp Dermatol* **26**, 137-144, doi:10.1111/exd.13115 (2017).
174 Lambert, S., Swindell, W. R., Tsoi, L. C., Stoll, S. W. & Elder, J. T. Dual Role of Act1 in Keratinocyte Differentiation and Host Defense: TRAF3IP2 Silencing Alters Keratinocyte Differentiation and Inhibits IL-17 Responses. *J Invest Dermatol* **137**, 1501-1511, doi:10.1016/j.jid.2016.12.032 (2017).
175 Carrier, Y. *et al.* Inter-regulation of Th17 cytokines and the IL-36 cytokines in vitro and in vivo: implications in psoriasis pathogenesis. *J Invest Dermatol* **131**, 2428-2437, doi:10.1038/jid.2011.234 (2011).
176 Jiang, Z. *et al.* IL-36gamma Induced by the TLR3-SLUG-VDR Axis Promotes Wound Healing via REG3A. *J Invest Dermatol* **137**, 2620-2629, doi:10.1016/j.jid.2017.07.820 (2017).
177 Wu, C., Chen, X., Shu, J. & Lee, C. T. Whole-genome expression analyses of type 2 diabetes in human skin reveal altered immune function and burden of infection. *Oncotarget* **8**, 34601-34609, doi:10.18632/oncotarget.16118 (2017).
178 Ramirez, H. A. *et al.* Comparative Genomic, MicroRNA, and Tissue Analyses Reveal Subtle Differences between Non-Diabetic and Diabetic Foot Skin. *PLoS One* **10**, e0137133, doi:10.1371/journal.pone.0137133 (2015).
179 Theocharidis, G., Bhasin, S. S., Kounas, K., Bhasin, M. K. & Veves, A. Single Cell RNA-Seq Analyses of Healthy Lower Extremity Skin and Diabetic Foot Ulcers Uncover Distinct Immune Landscape of Diabetic Wound Healing. *Diabetes* **67**, 647-P, doi:10.2337/db18-647-P (2018).
180 Das, S. *et al.* Syndesome Therapeutics for Enhancing Diabetic Wound Healing. *Adv Healthc Mater* **5**, 2248-2260, doi:10.1002/adhm.201600285 (2016).
181 Jang, E., Albadawi, H., Watkins, M. T., Edelman, E. R. & Baker, A. B. Syndecan-4 proteoliposomes enhance fibroblast growth factor-2 (FGF-2)-induced proliferation, migration, and neovascularization of ischemic muscle. *Proc Natl Acad Sci U S A* **109**, 1679-1684, doi:10.1073/pnas.1117885109 (2012).
182 Schiekofer, S., Galasso, G., Sato, K., Kraus, B. J. & Walsh, K. Impaired revascularization in a mouse model of type 2 diabetes is associated with dysregulation of a complex angiogenic-regulatory network. *Arterioscler Thromb Vasc Biol* **25**, 1603-1609, doi:10.1161/01.ATV.0000171994.89106.ca (2005).
183 Takematsu, E. *et al.* Genome wide analysis of gene expression changes in skin from patients with type 2 diabetes. *PLoS One* **15**, e0225267, doi:10.1371/journal.pone.0225267 (2020).
184 Das, S., Majid, M. & Baker, A. B. Syndecan-4 enhances PDGF-BB activity in diabetic wound healing. *Acta Biomater* **42**, 56-65, doi:10.1016/j.actbio.2016.07.001 (2016).
185 Das, S. *et al.* Syndecan-4 Enhances Therapeutic Angiogenesis after Hind Limb Ischemia in Mice with Type 2 Diabetes. *Adv Healthc Mater* **5**, 1008-1013, doi:10.1002/adhm.201500993 (2016).
186 Das, S., Singh, G. & Baker, A. B. Overcoming disease-induced growth factor resistance in therapeutic angiogenesis using recombinant co-receptors delivered by a liposomal system. *Biomaterials* **35**, 196-205, doi:10.1016/j.biomaterials.2013.09.105 (2014).

187 Rodrigues, M. *et al.* Progenitor cell dysfunctions underlie some diabetic complications. *Am J Pathol* **185**, 2607-2618, doi:10.1016/j.ajpath.2015.05.003 (2015).
188 Kang, L. *et al.* Decreased mobilization of endothelial progenitor cells contributes to impaired neovascularization in diabetes. *Clinical and Experimental Pharmacology and Physiology* **36**, e47-e56, doi:10.1111/j.1440-1681.2009.05219.x (2009).
189 Das, S. *et al.* Syndesome Therapeutics for Enhancing Diabetic Wound Healing. *Adv Healthc Mater* **5**, 2248-2260, doi:10.1002/adhm.201600285 (2016).
190 Taylor, A. M., Galli, S. J. & Coleman, J. W. Stem-cell factor, the kit ligand, induces direct degranulation of rat peritoneal mast cells in vitro and in vivo: dependence of the in vitro effect on period of culture and comparisons of stem-cell factor with other mast cell-activating agents. *Immunology* **86**, 427-433 (1995).
191 Da Silva, C. A., Reber, L. & Frossard, N. Stem cell factor expression, mast cells and inflammation in asthma. *Fundamental & Clinical Pharmacology* **20**, 21-39, doi:10.1111/j.1472-8206.2005.00390.x (2006).
192 Friedrich Erik, B., Walenta, K., Scharlau, J., Nickenig, G. & Werner, N. CD34−/CD133+/VEGFR-2+ Endothelial Progenitor Cell Subpopulation With Potent Vasoregenerative Capacities. *Circulation Research* **98**, e20-e25, doi:10.1161/01.RES.0000205765.28940.93 (2006).
193 Mihail Hristov, A. Z., Elisa A Liehn, Christian Weber. Regulation of endothelial progenitor cell homing after arterial injury. *Thrombosis and haemostasis* **98 2**, 274-277 (2007).
194 Li, X. *et al.* Administration of signalling molecules dictates stem cell homing for in situ regeneration. *J Cell Mol Med* **21**, 3162-3177, doi:10.1111/jcmm.13286 (2017).
195 Fitridge, R., Pena, G. & Mills, J. L. The patient presenting with chronic limb-threatening ischaemia. Does diabetes influence presentation, limb outcomes and survival? *Diabetes Metab Res Rev*, e3242, doi:10.1002/dmrr.3242 (2019).
196 Takahara, M. *et al.* Diabetes mellitus and other cardiovascular risk factors in lower-extremity peripheral artery disease versus coronary artery disease: an analysis of 1,121,359 cases from the nationwide databases. *Cardiovasc Diabetol* **18**, 155, doi:10.1186/s12933-019-0955-5 (2019).
197 Susumu Yamazaki, N. N., Asuka Honjo, Mutsuko Hara, Keiko Maeda, Chiharu Nishiyama, Jiro Kitaura, Yoshikazu Ohtsuka, Ko Okumura, Hideoki Ogawa and Toshiaki Shimizu. The Transcription Factor Ehf Is Involved in TGF-β–Induced Suppression of FcεRI and c-Kit Expression and FcεRI-Mediated Activation in Mast Cells. *The journal of immunology* **195**, 3427-3435, doi:https://doi.org/10.4049/jimmunol.1402856 (2015).
198 Yang, J. *et al.* CD34+ cells represent highly functional endothelial progenitor cells in murine bone marrow. *PLoS One* **6**, e20219-e20219, doi:10.1371/journal.pone.0020219 (2011).
199 Ekmekcioglu, S., Kurzrock, R. & Grimm, E. A. in *The Molecular Basis of Cancer (Fourth Edition)* (eds John Mendelsohn *et al.*) 789-808.e784 (Content Repository Only!, 2015).
200 Cruse, G. *et al.* The CD20 homologue MS4A4 directs trafficking of KIT toward clathrin-independent endocytosis pathways and thus regulates receptor signaling and recycling. *Mol Biol Cell* **26**, 1711-1727, doi:10.1091/mbc.E14-07-1221 (2015).
201 Goh, L. K. & Sorkin, A. Endocytosis of receptor tyrosine kinases. *Cold Spring Harb Perspect Biol* **5**, a017459-a017459, doi:10.1101/cshperspect.a017459 (2013).

202 Cruse, G. *et al.* The CD20 homologue MS4A4 directs trafficking of KIT toward clathrin-independent endocytosis pathways and thus regulates receptor signaling and recycling. *Mol Biol Cell* **26**, 1711-1727, doi:10.1091/mbc.E14-07-1221 (2015).
203 Lartigue, J. d. *The SCF/KIT Pathway's Roles: Interest in Therapeutic Targets Is Growing*, <https://www.onclive.com/publications/oncology-live/2011/august-2011/the-scfkit-pathways-roles-interest-in-therapeutic-targets-is-growing> (2011).
204 Morales, J. K., Falanga, Y. T., Depcrynski, A., Fernando, J. & Ryan, J. J. Mast cell homeostasis and the JAK–STAT pathway. *Genes & Immunity* **11**, 599-608, doi:10.1038/gene.2010.35 (2010).
205 Bai, X.-L. *et al.* Cavin-1 regulates caveolae-mediated LDL transcytosis: crosstalk in an AMPK/eNOS/ NF-κB/Sp1 loop. **8** (2017).
206 Gerbod-Giannone, M.-C. *et al.* Involvement of caveolin-1 and CD36 in native LDL endocytosis by endothelial cells. *Biochimica et Biophysica Acta (BBA) - General Subjects* **1863**, 830-838, doi:https://doi.org/10.1016/j.bbagen.2019.01.005 (2019).
207 Ramírez Cristina, M. *et al.* Caveolin-1 Regulates Atherogenesis by Attenuating Low-Density Lipoprotein Transcytosis and Vascular Inflammation Independently of Endothelial Nitric Oxide Synthase Activation. *Circulation* **140**, 225-239, doi:10.1161/CIRCULATIONAHA.118.038571 (2019).
208 Rejman, J., Oberle, V., Zuhorn, I. S. & Hoekstra, D. Size-dependent internalization of particles via the pathways of clathrin- and caveolae-mediated endocytosis. *Biochem J* **377**, 159-169, doi:10.1042/BJ20031253 (2004).
209 Henley, J. R., Krueger, E. W., Oswald, B. J. & McNiven, M. A. Dynamin-mediated internalization of caveolae. *J Cell Biol* **141**, 85-99, doi:10.1083/jcb.141.1.85 (1998).
210 Tran, D., Carpentier, J. L., Sawano, F., Gorden, P. & Orci, L. Ligands internalized through coated or noncoated invaginations follow a common intracellular pathway. *Proc Natl Acad Sci U S A* **84**, 7957-7961, doi:10.1073/pnas.84.22.7957 (1987).
211 Chen, Y.-G. Endocytic regulation of TGF-β signaling. *Cell Research* **19**, 58-70, doi:10.1038/cr.2008.315 (2009).
212 Kazi, J. U., Agarwal, S., Sun, J., Bracco, E. & Rönnstrand, L. Src-like-adaptor protein (SLAP) differentially regulates normal and oncogenic c-Kit signaling. *Journal of Cell Science* **127**, 653, doi:10.1242/jcs.140590 (2014).
213 Couet, J., Sargiacomo, M. & Lisanti, M. P. Interaction of a Receptor Tyrosine Kinase, EGF-R, with Caveolins: CAVEOLIN BINDING NEGATIVELY REGULATES TYROSINE AND SERINE/THREONINE KINASE ACTIVITIES. **272**, 30429-30438, doi:10.1074/jbc.272.48.30429 (1997).
214 Reid, D. J. *et al.* Engineering Nanodisc Scaffold Proteins for Native Mass Spectrometry. *Anal Chem* **89**, 11189-11192, doi:10.1021/acs.analchem.7b03569 (2017).
215 Grinkova, Y. V., Denisov, I. G. & Sligar, S. G. Engineering extended membrane scaffold proteins for self-assembly of soluble nanoscale lipid bilayers. *Protein Eng Des Sel* **23**, 843-848, doi:10.1093/protein/gzq060 (2010).
216 Sorkin, A. & von Zastrow, M. Endocytosis and signalling: intertwining molecular networks. *Nat Rev Mol Cell Biol* **10**, 609-622, doi:10.1038/nrm2748 (2009).